





NOVEMBER | 2025





# Modeling the Impact of Wildfire-Related Air Pollution on Mortality

**AUTHORS** Eve Titon

Flora Auter Tinhinane Talbi Marie Ganon **SPONSORS** 

Mortality and Longevity Strategic

Research Program

Catastrophe and Climate Strategic

Research Program

Sun Life Assurance Company of

Canada

Reinsurance Group of America







#### Caveat and Disclaimer

The opinions expressed and conclusions reached by the authors are their own and do not represent any official position or opinion of the Society of Actuaries Research Institute, Society of Actuaries, its members, or any sponsors of this research. The Society of Actuaries Research Institute makes no representation or warranty to the accuracy of the information.

# **CONTENTS**

Executive S	ummary	5
Section 1: I	ntroduction	6
Section 2: F	listorical Trends Analysis	8
2.1	Risk Description: Direct vs. Indirect Mortality	
2.2	Mortality Databases	11
	2.2.1 Identification of Mortality Databases	11
	2.2.2 Comparison of CDC and GBD Death Rates for "Respiratory Diseases and Infections"	12
	2.2.3 GBD Death Rates for the Air Pollution Risk Factor	13
2.3	Wildfires and Air Pollution Data	16
	2.3.1 Wildfire Data	17
	2.3.2 Air Pollution Data	19
2.4	Link Between Air Pollution and Mortality	21
Section 3: N	Nodeling Approaches	26
3.1	Short-Term Mortality Modeling	26
3.2	Long-Term Mortality Modeling	
3.3	Consideration of Climatic Interactions	27
3.4	Modeling Frameworks Used in This Study	27
3.5	Limitations of the State-Level Approach	28
Section 4: S	tochastic Modeling Approach: Climate Lee-Carter Model	29
4.1	Principle	29
4.2	Model Specification	30
4.3	Results	31
	4.3.1 Climate Index by States	
	4.3.2 Calibration for Alaska	32
	4.3.3 Results	
	4.3.4 Calibration for California	36
4.4	Analysis	38
	4.4.1 Model Calibration Observations	
	4.4.2 Limitations of State-Level Modeling	38
	4.4.3 Projection Considerations	38
Section 5: D	erivation of Prevalence Scenarios	40
Section 6: A	irQ+ Methodology: Computing the Attributable Risk	42
6.1	Health Impact Function (HIF)	42
	6.1.1 Linking Exposure and Health Outcome	42
	6.1.2 Attributable Risk	43
	6.1.3 Estimating Attributable Cases	43
	6.1.4 Risk Quantification	43
6.2	Advantages and Limitations of the HIF Approach	44
6.3	Results	45
	6.3.1 Projected Impact of Ozone on Mortality (Aged 65+)	45
	6.3.2 Projected Impact of PM <sub>2.5</sub> on Mortality (Aged 65+)	46
	$6.3.3$ Projected Impact of PM $_{2.5}$ Levels on Mortality Among the Elderly (Aged $65+$ ) in California,	
	2021 Baseline Scenario and Temperature Variations	47
	6.3.4 Challenges in Assessing Air Pollution's Impact on Mortality	48
Saction 7: C	onclusion	40

Section 8:	Acknowledgments	51
Appendix A	A: Comparison Between CDC and GBD Death Rates	52
A.1	CDC Rates	52
A.2	2 GBD Rates	55
A.3	Comparison of CDC and GBD by State	60
Appendix I	B: Evolution of Air Pollution Variables	62
Appendix (	C: GBD Death Rates by Risk Factor Methodology	71
Appendix I	D: A Stepwise Description of the Clustering Process	72
About The	Society of Actuaries Research Institute	74

# **Executive Summary**

This report examines the impact of wildfires and broader air pollution on mortality, with an emphasis on modeling approaches relevant to life insurers.

Although wildfires can cause immediate fatalities—such as caused by burns and smoke inhalation—their more substantial mortality impact arises from increased air pollution. Smoke from wildfires raises concentrations of harmful pollutants, especially fine particulate matter (PM<sub>2.5</sub> and PM<sub>10</sub>), which contribute to chronic health conditions and long-term excess mortality not always directly linked to wildfire events.

Capturing this indirect, delayed relationship between pollution and mortality is the primary modeling challenge. This report addresses that challenge through three modeling approaches, each suited to different actuarial applications and time horizons:

## 1. Stochastic Mortality Framework

An adaptation of the Lee-Carter model incorporates climate variables to estimate short- to medium-term impacts. This method is most effective where strong empirical relationships exist between pollution indicators and mortality and is compatible with insurers' existing stochastic frameworks.

# 2. Prevalence Scenario Approach

Mortality is projected based on expected increases in disease prevalence attributable to pollution. This intuitive method aligns with morbidity modeling practices but depends on reliable disease prevalence data and Global Burden of Disease mortality estimates, which are derived from statistical modeling rather than direct counts.

# 3. WHO AirQ+ Methodology

This epidemiological model uses concentration-response functions (CRFs) to estimate deaths attributable to pollutants such as PM<sub>2.5</sub> and ozone. Although well suited for scenario testing, it requires careful calibration and may not fully reflect local conditions because of assumptions embedded in the CRFs.

Across all approaches, several limitations are identified:

- Data granularity: Accurate modeling requires geographically and temporally detailed mortality
  data
- Historical data gaps: Long-term pollutant exposure modeling is limited by sparse historical
  measurement data. It is challenging to obtain a comprehensive historical record of reliable air
  pollution data, due to either an insufficient number of monitoring stations or inadequate
  frequency of data collection, particularly for older years.
- *Population dynamics:* Calibration on historical data may not reflect future changes in vulnerability or exposure.
- Spatial averaging: State-level data may obscure local pollution hotspots and topographic effects.
- Interaction effects: Existing models do not capture combined impacts of pollution and other climate stressors, such as heatwaves or behavioral adaptations.

Despite these challenges, the models provide valuable tools for actuaries assessing environmental risks. They can inform stress testing, pricing adjustments, and the quantification of climate-related mortality shocks. For example, region-specific pollution risk factors could support the development of mortality zoning or adjusted pricing for wildfire-prone areas.

# Section 1: Introduction

Climate change presents a growing concern for life and health insurance companies. A wide range of climate-related factors—including heatwaves, cold spells, vector-borne diseases, and extreme precipitation—have been the subject of modeling studies. Air pollution is no exception, particularly as it is increasingly exacerbated by wildfires. Climate change contributes to more frequent and severe wildfires, which, in turn, intensify air pollution and extend its impact across regions and over time.

In addition to the direct physical effects of wildfires, the spread of smoke has introduced broader and longer-lasting public health risks. These secondary effects—such as prolonged exposure to harmful pollutants—represent a significant challenge for insurers seeking to understand and manage long-term mortality trends.

This report serves as an educational resource for actuaries and other professionals assessing the insured risks associated with wildfires, pollution, and air quality. It is intended to support current and future evaluations of how these environmental hazards affect mortality and impact the operations of life insurance companies.

The primary focus of this project is to better understand the relationship between wildfires—particularly wildfire-related air pollution—and mortality. This report outlines a structured framework for modeling the effects of climate change on air quality and associated mortality outcomes. Specifically, it offers the following:

- A review of mortality and climate-related data sources required for modeling.
- A descriptive analysis of historical air pollution and wildfire trends.
- An explanation of how air pollution affects health and contributes to mortality.
- Illustrative modeling approaches applicable to both short- and long-term impacts.

It is important to note that many available datasets—including both mortality and pollution data—are aggregated at the state level.¹ Although this resolution allows for consistent national analysis, it can obscure local variations in pollution exposure, especially in areas with complex topography or where wildfire smoke disperses unevenly. As a result, some models presented in this report may underrepresent localized risks or overgeneralize the impact across broader regions. Where possible, the report highlights these limitations and discusses opportunities for refinement through more granular or regionally tailored data. Although the focus is on U.S. mortality, the methodologies discussed are generalizable and could be applied to other geographies with appropriate local data.

The report structure is as follows:

- Section 2 describes the nature of wildfire-related mortality and the data required for modeling this risk
- Section 3 presents a review of existing literature and modeling approaches, including a discussion of the methods chosen for this study.
- Section 4 introduces a stochastic mortality model that integrates climate variables, with results shown for selected states.
- Section 5 outlines an approach for projecting long-term mortality using disease prevalence scenarios.

<sup>&</sup>lt;sup>1</sup> "State" will always refer to a state in the United States.

- Section 6 details the World Health Organization's methodology for estimating mortality attributable to air pollution using the AirQ+ tool.
- Section 7 summarizes key findings, modeling challenges, and considerations for future applications.

Appendixes and footnote references are included to provide supporting data and methodological detail.

# Section 2: Historical Trends Analysis

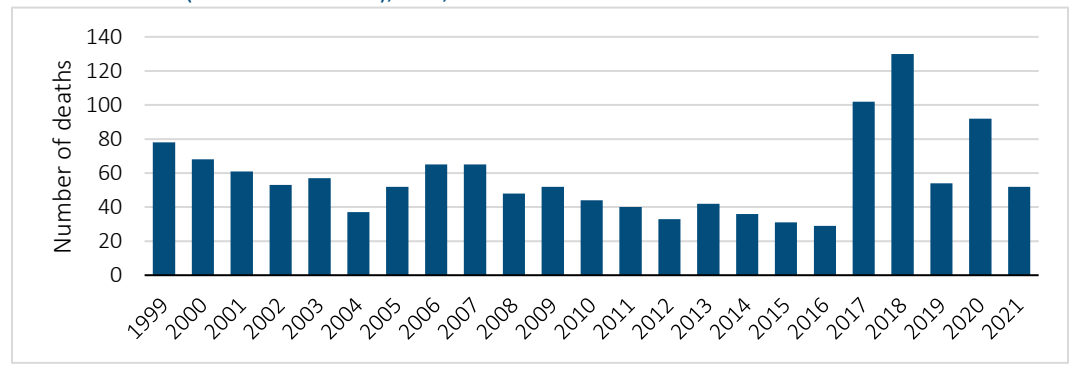
This section is dedicated to exploring the complexity of air pollution risk and to analyzing historical trends of mortality due to air pollution.

# 2.1 RISK DESCRIPTION: DIRECT VS. INDIRECT MORTALITY

Mortality related to wildfires can be categorized into two main types: *direct mortality* and *indirect mortality*.

Direct mortality results from immediate exposure to wildfire events, including fatalities due to burns and the inhalation of toxic fumes such as chemicals and combustion by-products. These are classified under ICD-10 code X01 "Exposure to uncontrolled fire, not in building or structure." Although direct mortality is relatively rare, a notable increase has occurred since 2017 (see Figure 1).

Figure 1
NUMBER OF DEATHS DUE TO EXPOSURE TO UNCONTROLLED FIRE, NOT IN A BUILDING OR STRUCTURE (ICD-10 CODE X01), U.S., 1999–2021



Data sources: CDC WONDER—Underlying Cause of Death, 2018–2021, Single Race Request; Underlying Cause of Death, 1999–2020 Request

In contrast, indirect mortality occurs because of elevated levels of wildfire-related air pollution. Smoke from wildfires contains a complex mixture of harmful pollutants that impact public health, including the following:<sup>3</sup>

- Carbon monoxide (CO).
- Nitrogen dioxide (NO<sub>2</sub>).
- Ozone  $(O_3)$ .
- Particulate matter (PM<sub>2.5</sub> and PM<sub>10</sub>, depending on the diameter).<sup>4</sup>
- Sulfur dioxide (SO<sub>2</sub>).

<sup>&</sup>lt;sup>2</sup> https://icd.who.int/browse10/2019/en#/X01. Other causes of death may be included in this code, but it is assumed that they are negligible compared with the number of deaths due to wildfires.

<sup>&</sup>lt;sup>3</sup> A. Keswani et al., "Health and Clinical Impacts of Air Pollution and Linkages with Climate Change," *NEJM Evidence* 1, no. 7 (2022), https://doi.org/10.1056/EVIDra2200068.

<sup>&</sup>lt;sup>4</sup> Particulate matter with a diameter of 2.5 microns or less (PM<sub>2.5</sub>) and particular matter with a diameter of 10 microns or less (PM<sub>10</sub>).

Wildfires have accounted for up to 40% of total annual PM<sub>2.5</sub> emissions in recent years.<sup>5</sup> These pollutants exacerbate the prevalence and severity of numerous chronic conditions, leading to increased mortality over the medium and long term. Health impacts include the following:

- Cardiovascular diseases: Long-term PM<sub>2.5</sub> exposure is associated with hypertension, <sup>6</sup> heart failure, and arrhythmias. <sup>7</sup> Short-term spikes in NO<sub>2</sub>, SO<sub>2</sub>, and PM<sub>2.5</sub> also correlate with increased mortality and heart failure hospitalizations. <sup>8</sup>
- Respiratory diseases: Air pollution is linked to asthma development, especially in children, and
  worsens chronic conditions such as COPD and lung cancer. Results from a Dutch birth cohort
  reveal that children highly exposed to PM<sub>10</sub> and NO<sub>2</sub> are more likely to develop asthma before the
  age of 20.9 Other respiratory conditions are amplified by long-term exposure to particulate
  matter, such as lung cancers.<sup>10</sup>
- *Diabetes:* Chronic exposure to particulate matter and NO<sub>2</sub> has been shown to aggravate diabetes. <sup>11</sup>
- *Kidney disease*: Exposure to PM, NO<sub>2</sub>, and CO is associated with increased incidence of chronic and end-stage renal disease. <sup>12</sup>
- Gastrointestinal and autoimmune diseases: Pollution has been linked to elevated risk.<sup>13</sup>
- Neurological and psychiatric disorders: Short- and long-term exposure to particulate matter is
  correlated with increased risk of stroke, dementia, and Parkinson's disease.<sup>14</sup> Being chronically
  highly exposed to PM<sub>2.5</sub> increases the probability of anxiety and depression. The risk of suicide
  depends on exposure to PM<sub>10</sub>, even in the short term.<sup>15</sup>
- Cancer: The risk of cancer mortality is increased with air pollution. Every 10  $\mu$ g/m³ increase in PM<sub>2.5</sub> exposure is associated with a 22% increase in cancer mortality.
- Dermatological and ophthalmological conditions: Pollution-related ozone depletion can lead to increased UV exposure, heightening the risk of skin cancers and eye diseases such as cataracts. <sup>16</sup>

<sup>5</sup> https://www.epa.gov/system/files/documents/2024-02/pm-naaqs-wildland-fire-air-quality-fact-sheet-final.pdf.

<sup>&</sup>lt;sup>6</sup> B. Y. Yang et al., "Global Association Between Ambient Air Pollution and Blood Pressure: A Systematic Review and Meta-analysis," *Environmental Polluution* 235 (2018): 576–588, https://doi.org/10.1016/j.envpol.2018.01.001.

<sup>&</sup>lt;sup>7</sup> C. A. Pope III et al., "Cardiovascular Mortality and Long-Term Exposure to Particulate Air Pollution: Epidemiological Evidence of General Pathophysiological Pathways of Disease," *Circulation* 109 (2004): 71–77, https://doi.org/10.1161/01.CIR.0000108927.80044.7F.

<sup>&</sup>lt;sup>8</sup> A. S. Shah et al., "Global Association of Air Pollution and Heart Failure: A Systematic Review and Meta-analysis," *Lancet* 382 (2013): 1039–1048, https://doi.org/10.1016/S0140-6736(13)60898-3.

<sup>&</sup>lt;sup>9</sup> U. Gehring et al., "Air Pollution and the Development of Asthma from Birth Until Young Adulthood," *European Respiratory Journal* 56 (2020): 2000147, https://doi.org/10.1183/13993003.00147-2020.

<sup>&</sup>lt;sup>10</sup> M. C. Turner et al., "Long-Term Ambient Fine Particulate Matter Air Pollution and Lung Cancer in a Large Cohort of Never-Smokers," *American Journal of Respiratory Critical Care Medicine* 184 (2011): 1374–1381, https://doi.org/10.1164/rccm.201106-10110C.

<sup>&</sup>lt;sup>11</sup> According to the Global Burden of Disease study, in the United Kingdom in 2019, about 8.2% of the deaths caused by diabetes were attributable to air pollution, whereas it represented 14.1% of deaths in 1990, <a href="https://vizhub.healthdata.org/gbd-results/">https://vizhub.healthdata.org/gbd-results/</a>

<sup>&</sup>lt;sup>12</sup> B. Bowe et al., "Associations of Ambient Coarse Particulate Matter, Nitrogen Dioxide, and Carbon Monoxide with the Risk of Kidney Disease: A Cohort Study," *Lancet Planet Health* 1 (2017): e267–e276, https://doi.org/10.1016/S2542-5196(17)30117-1.

<sup>&</sup>lt;sup>13</sup> G. Nagel et al., "Air Pollution and Incidence of Cancers of the Stomach and the Upper Aerodigestive Tract in the European Study of Cohorts for Air Pollution Effects (ESCAPE)," *International Journal of Cancer* 143 (2018): 1632–1643, https://doi.org/10.1002/ijc.31564.

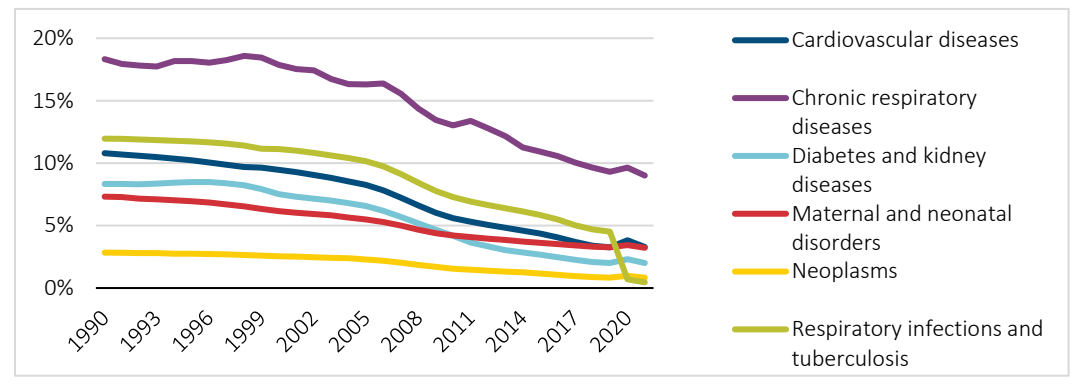
<sup>14</sup> P. Fu et al., "The Association Between PM<sub>2.5</sub> Exposure and Neurological Disorders: A Systematic Review and Meta-Analysis," *Science of the Total Environment* 655 (2019): 1240–1248, https://doi.org/10.1016/j.scitotenv.2018.11.218.

<sup>&</sup>lt;sup>15</sup> I. Braithwaite et al., "Air Pollution (Particulate Matter) Exposure and Associations with Depression, Anxiety, Bipolar, Psychosis and Suicide Risk: A Systematic Review and Meta-Analysis," *Environmental Health Perspectives* 127, no. 12 (2019): 126002, https://doi.org/10.1289/EHP4595.

<sup>16</sup> World Health Organization, "Radiation: The Known Health Effects of Ultraviolet Radiation" (Geneva: World Health Organization, 2024), https://www.who.int/news-room/questions-and-answers/item/radiation-the-known-health-effects-of-ultraviolet-radiation.

The Global Burden of Disease (GBD) database estimates mortality attributable to air pollution by quantifying the relationship between pollutant exposure and relative risk (see Appendix C). After extrapolating exposure data, the GBD estimates the number of attributable deaths (see Figure 2).17

Figure 2
PROPORTION OF DEATHS ATTRIBUTABLE TO AIR POLLUTION, BY GIVEN CAUSE OF DEATH, 1990–2021



Data source: Global Burden of Disease Study

In 2021 air pollution was estimated to contribute to 9% of chronic respiratory disease deaths, 2% of diabetes deaths and more than 3% of cardiovascular deaths.

Although the proportion of attributable deaths has declined since 2000, reflecting overall improvements in air quality (see Appendix B), the absolute number of deaths remains significant (Figure 3).

<sup>&</sup>lt;sup>17</sup> C. J. L. Murray et al., "Global Burden of 87 Risk Factors in 204 Countries and Territories, 1990–2019: A Systematic Analysis for the Global Burden of Disease Study 2019, *Lancet* 396, no. 10258 (2019): 1223–1249, https://doi.org/10.1016/S0140-6736(20)30752-2.

35,000 30,000 25,000 20,000 15,000 10,000 5,000 0 Cardiovascular Chronic Diabetes and Maternal and Neoplasms Respiratory diseases respiratory kidney diseases neonatal infections and disorders tuberculosis diseases

Figure 3
NUMBER OF DEATHS ATTRIBUTED TO THE AIR POLLUTION RISK FACTOR, U.S., 2021

Data source: Global Burden of Disease Study

#### 2.2 MORTALITY DATABASES

#### 2.2.1 IDENTIFICATION OF MORTALITY DATABASES

Analyzing mortality trends attributable to air pollution—particularly from wildfires—requires detailed and geographically specific data. Both the cause of death and geographic location must be captured in the underlying data to establish a meaningful link between climatic conditions and mortality.

In this study, air pollution is considered in aggregate, irrespective of the pollution source. The objective is to understand how increased frequency and intensity of wildfires contribute to deteriorating air quality, thereby elevating pollution-related mortality. Importantly, it is the cumulative exposure to pollutants—whether from wildfires or other sources—that contributes to adverse health outcomes.

Two key data sources are used for mortality information:

Centers for Disease Control and Prevention (CDC): This source provides mortality rates by cause of
death and by state. Data are derived from death certificates, which include one underlying cause
of death, up to 20 contributing causes, and demographic variables such as age, sex, and place of
death. Metrics include the number of deaths, crude and age-adjusted mortality rates, and 95%
confidence intervals, organized by ICD-10 code, state of residence, and age group. However, these
data do not identify which deaths are specifically attributable to air pollution.

To utilize the CDC data for this study, a literature review was conducted to identify diseases that are either caused or exacerbated by air pollution. From this, a set of relevant ICD-10 codes was compiled. Although this allows for analysis of mortality trends by cause, it does not provide a means to isolate the proportion of these deaths directly attributable to air pollution.

• Global Burden of Disease (GBD) Study: The GBD database complements the CDC data by providing mortality rates by cause of death and risk factor, including air pollution. It offers estimates of mortality rates by year, age group, and state, as well as death rates specifically attributed to the "air pollution" risk factor. These estimates are derived using exposure-response relationships documented in the scientific literature (see Appendix C). GBD data enable an approximation of the portion of deaths due to air pollution, distinguishing it from mortality attributable to other causes or disease progression.

A comparison of the CDC and GBD mortality rates was conducted to validate the consistency of these datasets for use in modeling (see Appendix A). The objective was to assess whether the databases yield comparable mortality patterns for diseases impacted by air pollution.

# 2.2.2 COMPARISON OF CDC AND GBD DEATH RATES FOR "RESPIRATORY DISEASES AND INFECTIONS"

To assess the alignment between the CDC and GBD mortality databases, a comparative analysis was conducted for respiratory diseases that are likely to be affected by air pollution. Table 1 outlines the mapping of ICD-10 codes between the two data sources.

Table 1
MAPPING OF CDC/GBD CAUSE-OF-DEATH CATEGORIES USED FOR DATABASES COMPARISON

CDC	GBD
Asthma	Asthma
<ul> <li>Solid and liquid lung disease</li> </ul>	Tuberculosis
<ul> <li>Other chronic obstructive pulmonary diseases</li> </ul>	Chronic obstructive pulmonary disease
<ul> <li>Pneumoconiosis and chemical effects</li> </ul>	Pneumoconiosis
Other respiratory diseases mainly affecting the	Interstitial lung disease and pulmonary sarcoidosis
interstitium	Other chronic respiratory diseases
Other diseases of the respiratory system	

Mortality rates were evaluated by age group, focusing on the 20–54 and 55+ cohorts. Data for individuals under age 20 were excluded because of insufficient mortality counts across relevant ICD-10 codes. Additionally, the CDC dataset contains many missing values. The chosen age groups provide a balance between broad coverage and specific insights, enhancing the statistical reliability of the findings.

The age groups selected for analysis in this comparison reflect insurance industry practice and align with differential susceptibility to air pollution: (1) adults aged 20–54 may face occupational and lifestyle exposure risks and (2) individuals aged 55+ are more vulnerable to pollution-related health outcomes because of age-related comorbidities and chronic disease prevalence.

Although the 75+ age group may show more pronounced mortality effects, the 55+ category was emphasized to highlight the earlier onset of vulnerability, an important consideration for life insurers assessing future risk.

As shown in Appendix A, the mortality rates for respiratory causes are generally consistent in level between the CDC and GBD databases. Although one finds discrepancies for specific states, the overall trends and magnitudes align sufficiently.

Differences between the two databases are largely attributable to their methodological approaches. The CDC relies primarily on raw death certificate data, which can vary in quality and completeness across states and over time. The GBD database integrates multiple sources—such as epidemiological studies, <sup>18</sup> health surveys and statistical models—to adjust for underreporting and to smooth temporal fluctuations. As a result, GBD estimates tend to be more stable and suitable for trend analysis. The methodologies employed

<sup>&</sup>lt;sup>18</sup> Institute for Health Metrics and Evaluation, *Protocol for the Global Burden of Diseases, Injuries, and Risk Factors Study (GBD)*, version 3 (Seattle: Institute for Health Metrics and Evaluation, 2018), <a href="https://www.healthdata.org/sites/default/files/frijes/Projects/GBD/GBD\_Protocol.pdf">https://www.healthdata.org/sites/default/files/frijes/Projects/GBD/GBD\_Protocol.pdf</a>.

in the GBD study are tailored for global applicability, which means some parameter values in the GBD models might not accurately reflect the conditions of specific countries.<sup>19</sup>

In summary, although methodological differences exist, the CDC and GBD data sources provide complementary insights. GBD data offer advantages in estimating mortality attributable to air pollution and are therefore used in subsequent modeling.

## 2.2.3 GBD DEATH RATES FOR THE AIR POLLUTION RISK FACTOR

For the remainder of this study, the Global Burden of Disease (GBD)<sup>20</sup> database is used as the primary source for mortality rates attributable to air pollution—specifically fine particulate matter and ambient ozone. The rationale for selecting GBD over CDC data includes the following:

- Broader historical coverage across years and age groups.
- Consistency in mortality levels relative to CDC data (as shown in Section 2.2.2).
- Availability of risk factor—specific death rates, which estimate the proportion of deaths directly attributed to air pollution exposure.

To explore geographic variation in mortality due to air pollution, a clustering analysis was conducted. This methodology is described in detail in Appendix D. The analysis employed an ascending hierarchical classification (AHC) using GBD mortality data from 1990 to 2019. The metrics "average mortality rate across the period" and "maximum mortality rate observed" from the full historic dataset were used as inputs. These metrics were calculated for each state and stratified by age group.

A dendrogram was used to determine the appropriate number of clusters, followed by a principal components analysis (PCA) to identify which variables most strongly differentiate the clusters.

The resulting classification is illustrated in Figure 4, a U.S. map shaded by cluster assignment.

<sup>&</sup>lt;sup>19</sup> Y. Wu et al., "Injury Death Estimates from GBD 2015 and CDC WONDER," *International Journal of Environmental Research and Public Health* 15, no. 1 (2018): 87, https://doi.org/10.3390/ijerph15010087.

<sup>&</sup>lt;sup>20</sup> https://vizhub.healthdata.org/gbd-results/.

Powered by Bing © GeoNames, Microsoft, Tomforn

Figure 4
CLUSTERING PROCESS: CLUSTERED MAP OF THE U.S. AND FOCUS AROUND DISTRICT OF COLUMBIA

Data source: Global Burden of Disease Study

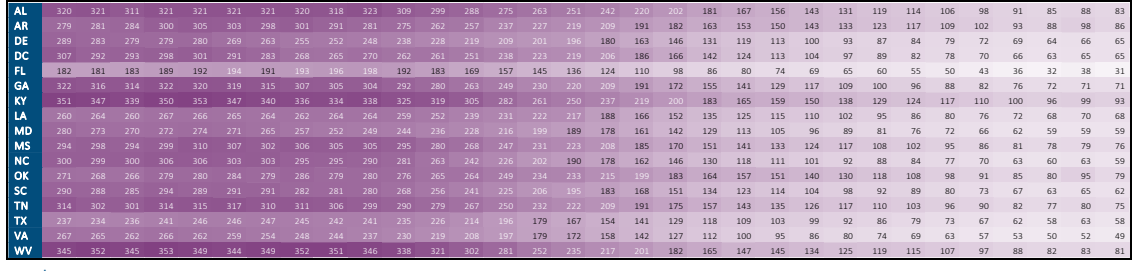
- Cluster 1 (purple): States with elevated air pollution mortality among the two oldest age groups.
- Cluster 2 (dark blue): States with consistently low air pollution mortality.
- Cluster 3 (light blue): The District of Columbia, characterized by unusually high pollution-related mortality in younger ages.

Further insight is provided by heat maps. Figure 5 displays air pollution—attributed mortality rates (per 100,000 population) by state and by year for individuals aged 55+, the most affected age group. States such as Kentucky, West Virginia, Georgia, and Alabama (all in the South) exhibit the highest mortality rates attributable to air pollution over the historical data period.

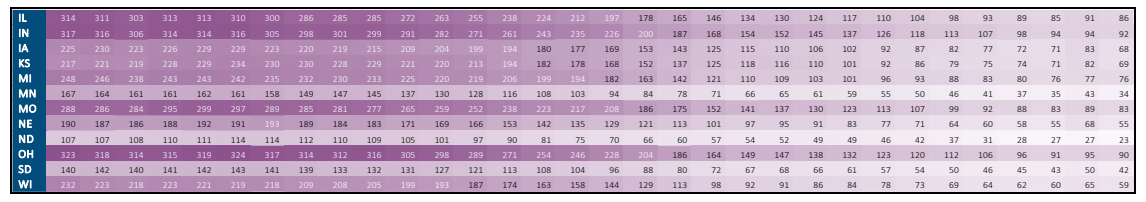
Figure 5
HEAT MAP OF MORTALITY RATES BY STATE (DEATHS PER 100,000 POPULATION) FOR THE RISK FACTOR "AIR POLLUTION": 55+ AGE GROUP

State	1990	1991	1992	1993	1994	1995	1996	1997	1998	1999	2000	2001	2002	2003	2004	2005	2006	2007	2008	2009	2010	2011	2012	2013	2014	2015	2016	2017	2018	2019	2020	2021
СТ								191	188	183	181	175	171	160	152	145	138	121	108	94	83	78	73	69	63	61	58	54	51	49	55	47
ME	114	109	104	102	101	99	96	97	97	93	91	87	87	81	76	72	66	59	52	45	39	35	32	30	27	23	19	15	15	14	17	13
MA	186	182	185	186	186	183	179	173	171	166	162	159	155	148	138	130	121	110	96	86	75	70	63	58	53	49	43	39	36	33	41	30
NH	148	142	138	140	140	141	137	135	133	126	122	119	114	106	103	99	91	82	74	64	57	54	48	43	39	35	30	26	25	23	30	21
NJ																184	170	150	135	118	107	102	92	85	78	73	69	64	60	56	62	54
NY														192	179	167	152	137	121	107	95	90	83	77	71	67	63	57	53	50	58	50
PA																			175	155	138	134	123	116	107	103	97	90	81	77	81	75
RI														183	175	170	159	143	128	111	99	92	84	78	72	67	59	54	49	47	56	43
VT	147	146	147	142	142	139	133	132	127	123	120	114	112	105	99	94	86	77	69	62	55	51	47	42	37	34	28	24	22	20	26	20

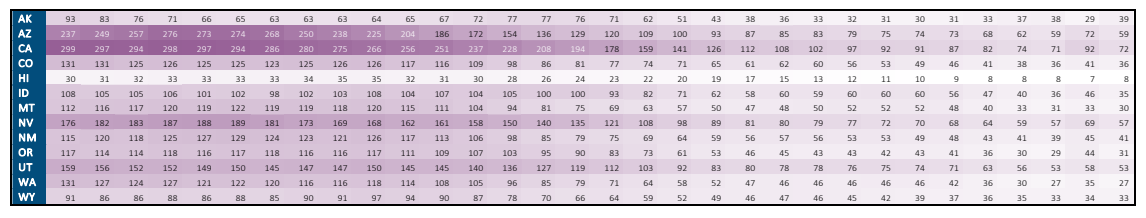
## South



## Midwest



#### West



Data source: Global Burden of Disease Study Rates: Deaths per 100,000 population

Figure 6 presents the percentage change of those mortality rates over time. Air pollution—related mortality has declined across most states since 1990. These declines mirror reductions in fine particulate matter concentrations (see Appendix B) because of efforts to reduce particle emissions, such as automobile exhaust improvement and the Clean Air Act.

A sharp increase in mortality appears in 2020, as noted by the darker purple coloring, coinciding with the onset of the COVID-19 pandemic. Although pollution levels temporarily declined because of reduced economic activity,  $^{21}$  long-term exposure to PM<sub>2.5</sub> and NO<sub>2</sub> has been linked to increased vulnerability to

<sup>&</sup>lt;sup>21</sup> L. Saha et al., "The Impact of the COVID-19 Lockdown on Global Air Quality: A Review," *Environmental Sustainability* 5, no. 1 (2022): 5–23, https://doi.org/10.1007/s42398-021-00213-6.

COVID- $19^{22}$  and higher associated mortality. PM<sub>2.5</sub>, fine inhalable particulate matter, is more likely to travel into and deposit on the surface of the deeper parts of the lungs.

Figure 6
HEAT MAP OF MORTALITY RATES EVOLUTION FOR THE RISK FACTOR "AIR POLLUTION": 55+ AGE GROUP

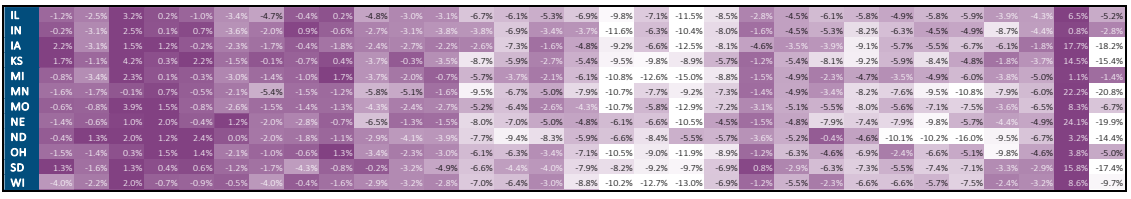
State	1991	1992	1993	1994	1995	1996	1997	1998	1999	2000	2001	2002	2003	2004	2005	2006	2007	2008	2009	2010	2011	2012	2013	2014	2015	2016	2017	2018	2019	2020	2021
СТ													-6.3%	-4.6%	-4.7%	-5.1%	-12.2%	-11.0%	-13.0%	-11.6%	-5.2%	-7.2%	-5.9%	-7.7%		-5.6%	-5.7%	-6.5%	-3.9%	11.8%	-14.2%
ME	-4.8%	-4.6%				-3.0%		0.2%	-4.6%				-7.1%	-5.5%	-5.5%	-8.9%	-10.7%	-11.2%	-13.6%	-13.6%	-9.4%	-9.1%	-6.1%	-11.4%	-13.5%	-19.0%	-17.7%		-7.3%	27.1%	-28.3%
MA													-4.7%	-6.7%	-5.7%	-6.9%	-9.2%	-12.5%	-10.2%	-13.5%	-5.8%	-10.7%	-7.5%	-8.1%	-8.1%	-11.8%	-9.9%	-8.1%	-6.5%	21.8%	-26.5%
NH					0.9%			-1.0%	-5.8%				-6.8%		-3.6%	-8.5%	-9.4%	-10.4%	-12.7%	-11.6%	-5.5%	-10.9%	-9.2%	-9.7%	-11.7%	-12.7%	-14.1%	-3.5%	-9.5%	33.0%	-29.6%
NJ					0.5%			-3.8%	1.9%				-6.8%	-6.7%	-6.1%	-7.3%	-12.1%	-10.0%	-12.1%	-9.3%	-5.2%	-10.1%	-7.3%	-8.7%	-6.4%	-5.5%	-6.7%	-6.2%	-6.1%	9.2%	-12.6%
NY								-2.3%	1.3%				-6.8%	-6.4%	-6.7%	-9.0%	-10.0%	-11.4%	-11.8%	-11.5%	-5.2%	-7.8%	-6.7%	-7.6%	-5.7%	-6.3%	-9.2%	-7.1%	-5.3%	15.4%	-13.8%
PA								-4.2%	2.4%				-5.8%	-5.5%	-3.9%	-8.5%	-10.0%	-9.6%	-11.6%	-11.1%		-8.3%	-5.8%	-7.3%		-6.6%	-7.2%	-9.5%	-4.8%	4.9%	-7.1%
RI							1.1%						-5.6%	-4.5%	-2.8%	-6.3%	-10.1%	-10.7%	-12.6%	-11.0%	-7.1%	-8.3%	-8.1%	-7.9%	-6.4%	-12.4%	-7.2%	-9.6%	-3.8%	17.6%	-23.2%
VT							-1.0%						-5.8%	-5.6%	-5.6%	-8.3%	-10.8%	-9.8%	-10.6%	-11.2%	-7.5%	-7.8%	-9.6%	-11.6%	-10.3%	-16.0%	-16.2%	-6.6%	-7.4%	27.5%	-24.2%

## South

Northeast



## Midwest



## West



Data source: Global Burden of Disease Study Rate evolution: % change in mortality rates by year

Because air pollution was not the proximate cause of excess mortality in 2020–2021, those years are excluded from the mortality modeling to avoid distortion.

# 2.3 WILDFIRES AND AIR POLLUTION DATA

Wildfire-related air pollution comprises a complex mixture of gases and fine particulate matter produced during the combustion of organic materials. These pollutants can travel hundreds to thousands of

<sup>&</sup>lt;sup>22</sup> I. Hernandez Carballo et al., "The Impact of Air Pollution on COVID-19 Incidence, Severity, and Mortality: A Systematic Review of Studies in Europe and North America," *Environmental Research* 215, part 1 (2022): 114155, <a href="https://doi.org/10.1016/j.envres.2022.114155">https://doi.org/10.1016/j.envres.2022.114155</a>.

kilometers, affecting air quality well beyond the origin of the wildfire. This dispersion makes it challenging to isolate the health and mortality impacts of wildfire-related pollution at a local or even state level.

To assess the influence of wildfires on air quality and mortality, two primary types of climate data are used: (1) wildfire activity data (e.g., number of fires, area burned) and (2) air pollution data (e.g., concentrations of specific pollutants).

## 2.3.1 WILDFIRE DATA

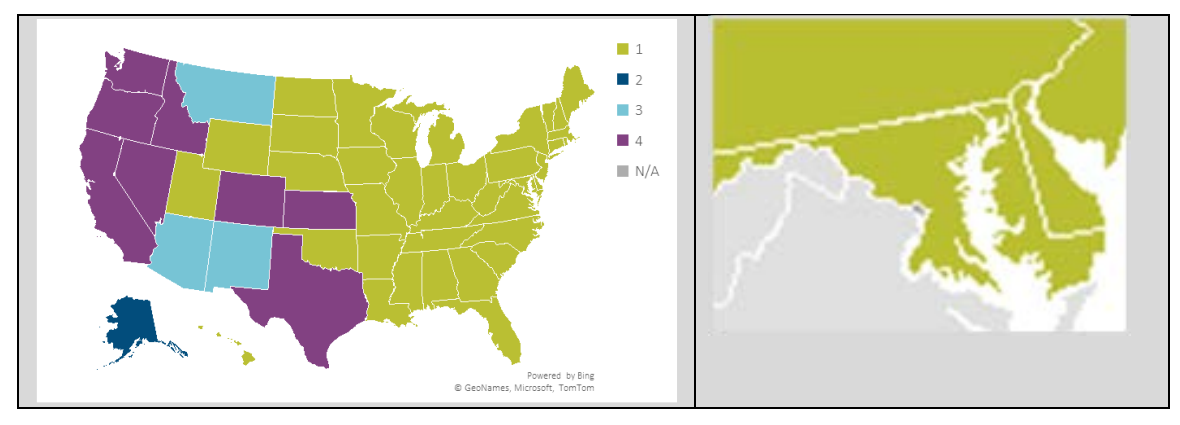
Wildfire activity data were sourced from the National Interagency Fire Center (NIFC) Open Data repository, which provides annual wildfire counts and area burned by state from 1992 to 2023.<sup>23</sup> To normalize the data by geography, the burned area was also expressed as a percentage of each state's total land area.<sup>24</sup>

To analyze wildfire exposure patterns, an ascending hierarchical clustering was conducted based on the following variables:

- Average and maximum number of wildfires.
- Average and maximum total area burned.
- Average and maximum proportion of state area burned.

Four clusters were identified, as outlined in Figure 7. A PCA (as explained in Appendix D) was conducted to identify the primary features of each cluster.

Figure 7
CLUSTERING PROCESS: CLUSTERED MAP OF U.S. STATES AND FOCUS AROUND DISTRICT OF COLUMBIA



Data source: National Interagency Fire Center Open Data

This analysis identified four distinct clusters of states, shown in Figure 7:

- Cluster 1 (green): States with low wildfire risk.
- Cluster 2 (dark blue): Alaska, uniquely characterized by a sizable proportion of land burned.
- Cluster 3 (light blue): States with large absolute areas burned relative to their size.

<sup>&</sup>lt;sup>23</sup> https://data-nifc.opendata.arcgis.com/datasets/nifc::inform-fire-occurrence-data-records/about.

<sup>&</sup>lt;sup>24</sup> https://worldpopulationreview.com/state-rankings/states-by-area.

• **Cluster 4 (purple)**: States frequently exposed to wildfires, with high total burn areas but small proportional impact because of larger landmass (e.g., California).

Since no wildfire data were available for the District of Columbia, it does not belong to any cluster.

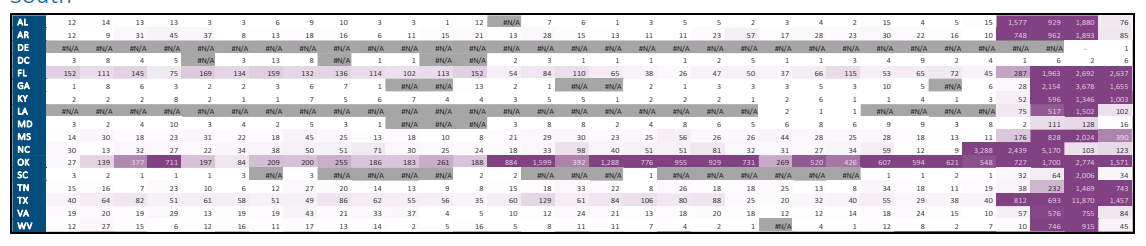
Figure 8a

# NUMBER OF WILDFIRES BY STATE, FROM 1992 TO 2023

# Northeast

_																																
State	1992	1993	1994	1995	1996	1997	1998	1999	2000	2001	2002	2003	2004	2005	2006	2007	2008	2009	2010	2011	2012	2013	2014	2015	2016	2017	2018	2019	2020	2021	2022	2023
СТ	#N/A	1	#N/A	#N/A	#N/A	#N/A	#N/A	πN/A	mN/A	#N/A	1	#N/A	#N/A	#N/A	#N/A	2	1	#N/A	#N/A	mN/A	293	537	#N/A									
ME	1	8	7	6	#N/A	10	2	1	1	11	6	3	5	2	#N/A	1	#N/A	1	3	4	2	2	4	5	22	7	3	3	1,157			496
MA	7	4	1	14	4	10	1	7	2	4	1	#N/A	4	3	1	1	1	1	2	#N/A	3	4	1	4	5	2	πN/A	mN/A	5	1,105	1,199	1,106
NH	#N/A	1	#N/A	#N/A	#N/A	1	#N/A	πN/A	#N/A	mN/A	43	74	73	101																		
NJ	2	4	3	3	4	1	3	7	2	6	1	1	#N/A	4	3	2	6	3	5	3	5	1	1	1	2	1	5	6	12	959	12	24
NY	65	70	3	65	27	46	35	62	30	40	35	1	6	7	20	19	34	7	51	43	26	25	28	34	26	17	3	7	19		1,170	10
PA	14	15	10	9	3	5	4	13	2	13	11	1	2	5	1	5	5	3	6	#N/A	10	3	3	5	2	5	2	9	31	1,263	1,058	50
RI	#N/A	πN/A	mN/A	#N/A	an/A	#N/A	#N/A	#N/A	#N/A	πN/A	#N/A	#N/A	mN/A	92	#N/A	56																
VT	#N/A	πN/A	mv/A	#N/A	πN/A	πN/A	mN/A	4	99	83	67																					

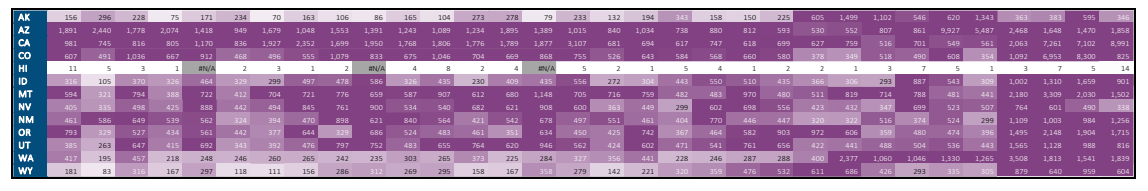
# South



# Midwest



# West



Data source: National Interagency Fire Center Open Data

Figure 8b
AREA BURNED BY STATE, FROM 1992 TO 2023



#### South



#### Midwest



#### West



Data source: National Interagency Fire Center Open Data

Figures 8a and 8b present the evolution of wildfire metrics across states, showing an increase in wildfire frequency (Figure 8a) and scale (Figure 8b) beginning around 2017. Alaska, Idaho, Washington, and Oregon exhibit the most extensively burned areas, and states such as California, Arizona, and Colorado report high wildfire counts.

The two variables shown in Figure 8 are correlated, especially in the eastern states. However, it is important to note that the number of wildfires alone is not a reliable indicator of impact severity, as large individual fires may have a disproportionate effect compared to numerous smaller events.

# 2.3.2 AIR POLLUTION DATA

Air pollution metrics were obtained from the Copernicus Atmospheric Monitoring Service (CAMS), a well-regarded source in climate research. CAMS provides monthly pollutant concentration data at a 70 km  $\times$  70 km grid resolution.<sup>25</sup> The following four pollutant indicators were selected for this study:

- OMAOD550: Organic matter aerosol optical depth at 550 nm.<sup>26</sup>
- BCAOD550: Black carbon aerosol optical depth at 550 nm.

<sup>25</sup> https://ads.atmosphere.copernicus.eu/cdsapp#!/dataset/cams-global-reanalysis-eac4-monthly?tab=form.

<sup>&</sup>lt;sup>26</sup> A nanometer (nm) is one billionth of a meter, one millionth of a millimeter, or one thousandth of a micrometer.

- $PM_{2.5}$ : Fine particulate matter (<2.5 µm diameter).<sup>27</sup>
- *PM*<sub>10</sub>: Coarse particulate matter (<10 μm diameter).

These indicators capture the primary wildfire-related pollutants:

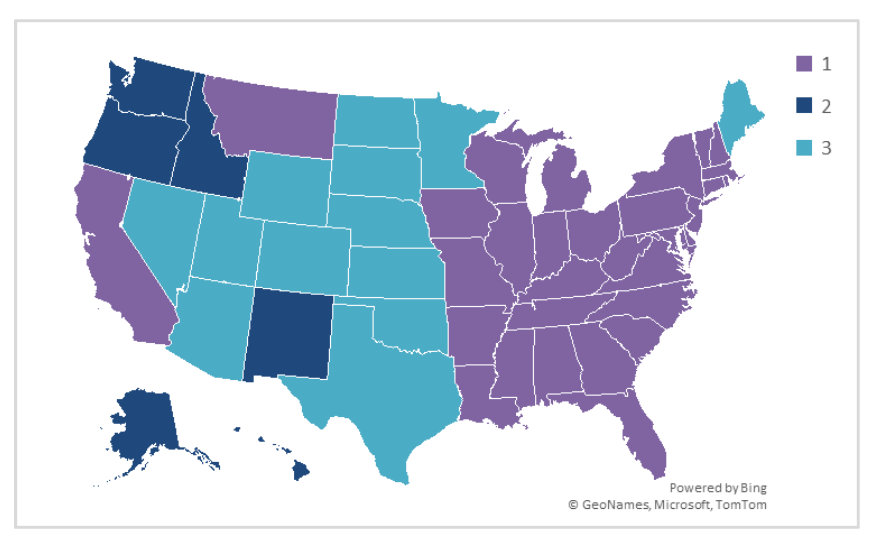
- Particulate organic matter (OM): This comes from the incomplete combustion of vegetation and includes many organic compounds associated with carbonaceous matter.
- Black carbon (BC): A major by-product of wildfires, it consists of very fine and highly lightabsorbing particles.
- *PM<sub>2.5</sub> and PM<sub>10</sub>:* Widely recognized as significant health risk factors because of their ability to penetrate the respiratory system.

Pollutant concentrations were interpolated by state, month, and year. Three annual indicators were computed for each pollutant: annual mean, annual maximum, and mean of the top six monthly values.

An ascending hierarchical clustering was performed using the following variables (Figure 9):

- PM<sub>2.5</sub> and PM<sub>10</sub> mean and maximum values in 2022.
- Changes in mean and maximum concentrations from 2003 to 2022.

Figure 9
CLUSTERING PROCESS: CLUSTERED MAP OF U.S. STATES



Data source: Copernicus Atmospheric Monitoring System

Then, as previously, a PCA was enabled to identify the major features of each cluster. This analysis yielded three distinct state groupings, displayed in Figure 9:

- Cluster 1 (purple): States with persistently high pollution throughout the year.
- Cluster 2 (dark blue): States with high annual peaks in particulate matter pollution.

-

 $<sup>^{27}</sup>$  A micrometer (µm) is one millionth of a meter.

• Cluster 3 (light blue): States with low pollution levels and relatively minor variation over time.

## 2.4 LINK BETWEEN AIR POLLUTION AND MORTALITY

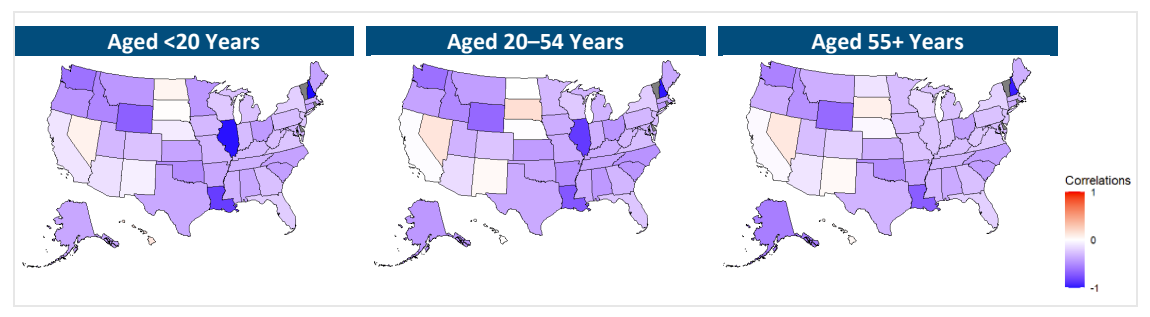
The previous sections outlined historical data sources and trends related to mortality, wildfire activity, and pollutant concentrations. This section now synthesizes those datasets to explore how pollution—particularly from fine particulate matter—correlates with mortality at the state level, offering key insights into which variables are most relevant for modeling.

To assess the association between air pollution and mortality, correlations were calculated between state-level mortality rates attributed to air pollution and wildfire activity (measured by the number of wildfires and area burned). The Pearson correlation coefficient was used for this analysis.

Figures 10 and 11 show that correlations between air pollution-related mortality and wildfire metrics are generally weak or negative across most states and age groups. Specifically, Figure 10 shows that correlations between mortality and wildfire count are minimal across all age categories, and in Figure 11, similarly, correlations between mortality and area burned are largely insignificant or negative.

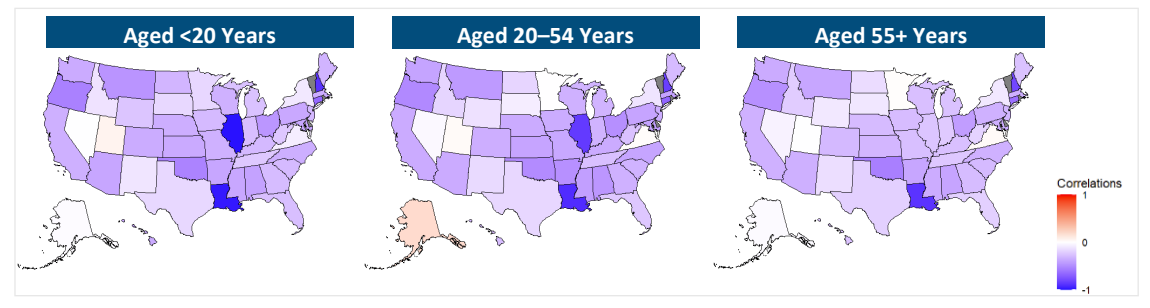
Figure 10

CORRELATION BETWEEN MORTALITY RATES BY STATE DUE TO AIR POLLUTION AND THE NUMBER OF WILDFIRES



Data sources: National Interagency Fire Center Open Data, Copernicus Atmospheric Monitoring System

Figure 11
CORRELATION BETWEEN MORTALITY RATES DUE TO AIR POLLUTION AND THE AREA BURNT



Data sources: National Interagency Fire Center Open Data, Copernicus Atmospheric Monitoring System

These results suggest that wildfire frequency and burned area, although indicative of wildfire activity, are not reliable proxies for modeling air pollution-related mortality. This is likely because of the long-range transport of pollutants, which can affect regions far from the fire source, as well as the temporal disconnect between wildfire events and their health consequences.

In contrast, strong positive correlations were observed between mortality attributed to air pollution and pollutant concentration levels, particularly  $PM_{2.5}$  and  $PM_{10}$ . These relationships are more pronounced in older age groups, reflecting increased vulnerability due to chronic health conditions. Note that the prominence of air pollutants is not directly due solely from wildfires and can be attributed to other behavioral and environmental factors.

The clustering analyses presented earlier (Section 2.3.2) help contextualize these correlations:

- States which consistently experience low pollution levels and low air pollution-related mortality—such as Idaho, North Dakota, and South Dakota—show minimal correlations, consistent with their classification as low-risk.
- States where both pollution levels and pollution-attributed mortality are elevated—such as Alabama, California, and Connecticut—show stronger correlations, especially for mean pollutant values rather than peak concentrations.

These findings are illustrated in Figure 12 with correlations for the <20 age group (2003–2019), Figure 13 with correlations for the 20–54 age group (2003–2019), and Figure 14 with correlations for the 55+ age group (2003–2019). In these figures, positive correlations of greater than 0.8 are highlighted purple.

The results emphasize that fine particulate matter ( $PM_{2.5}$  and  $PM_{10}$ ) concentrations are the most relevant predictors of air pollution-related mortality, particularly in older populations. These pollutants offer more reliable inputs for mortality modeling than wildfire metrics alone, reinforcing the need for pollutant-level granularity in climate-mortality risk frameworks.

Figure 12
CORRELATIONS BETWEEN MORTALITY RATES BY STATE DUE TO AIR POLLUTION AND POLLUTANT VARIABLES, POPULATION AGED <20 YEARS (2003–2019)

									Mean_	Mean_	Mean_	Mean_
	Max_	Max_	Max_	Max_	Mean_	Mean_	Mean_	Mean_	Top6_	Top6_	Top6_	Top6_
State	BCA	OMA	PM10	PM2	BCA	OMA	PM10	PM2	BCA	OMA	PM10	PM2
СТ	0.2	8.0	0.9	0.9	0.8	0.9	1.0	1.0	0.7	0.9	0.9	0.9
ME	0.0	0.5	0.7	0.7	0.2	0.6	0.7	0.7	0.1	0.6	0.7	0.7
MA	0.1	0.7	0.9	0.9	0.6	0.9	1.0	1.0	0.5	0.9	1.0	1.0
NH	0.0	0.6	0.9	0.9	0.4	0.8	0.9	0.9	0.3	0.8	0.9	0.9
NJ	0.3	0.9	1.0	1.0	0.8	0.9	1.0	1.0	0.7	0.9	1.0	1.0
NY	0.0	0.6	0.9	0.9	0.5	0.8	1.0	1.0	0.3	0.8	1.0	1.0
PA	0.0	0.8	1.0	1.0	0.6	0.9	0.9	0.9	0.4	0.8	1.0	1.0
RI	0.2	8.0	0.9	0.9	0.7	0.9	1.0	1.0	0.6	0.9	1.0	1.0
VT	0.0	0.6	0.9	0.9	0.3	0.8	0.9	0.9	0.2	0.8	1.0	1.0
outh												
AL	0.6	0.8	0.9	0.8	0.6	0.9	0.9	0.9	0.6	0.8	0.9	0.9
AR	0.3	0.7	0.8	0.7	0.2	0.7	0.9	0.9	0.2	0.6	0.9	0.9
DE	0.2	0.8	1.0	1.0	0.7	0.9	1.0	1.0	0.5	0.9	1.0	1.0
DC	0.3	0.9	1.0	1.0	0.8	0.9	1.0	1.0	0.6	0.9	1.0	1.0
FL	0.3	0.4	0.5	0.5	0.5	0.7	0.9	0.9	0.4	0.6	8.0	0.8
GA	0.3	0.6	0.5	0.5	0.3	0.7	0.8	0.8	0.3	0.7	0.7	0.7
KY	0.0	0.7	0.9	0.9	0.4	0.8	1.0	1.0	0.4	0.8	1.0	0.9
LA	0.5	0.6	0.6	0.4	0.4	0.8	0.9	0.9	0.4	0.8	0.9	0.9
MD	0.2	0.9	1.0	1.0	0.7	0.9	1.0	1.0	0.6	0.9	1.0	1.0
MS	0.5	0.7	0.8	0.7	0.4	0.8	0.9	0.9	0.3	8.0	0.9	0.9
МО	-0.2	0.5	0.8	0.8	0.0	0.6	0.9	0.9	0.0	0.6	0.9	0.8
NC	0.4	0.7	0.6	0.6	0.5	0.8	1.0	1.0	0.4	8.0	0.9	0.9
ok	-0.1	0.2	0.4	0.3	0.0	0.5	0.8	8.0	0.0	0.5	0.7	0.7
SC	0.3	0.7	0.9	0.9	0.4	8.0	1.0	1.0	0.4	0.7	0.9	0.9
TN	0.3	8.0	0.9	0.9	0.3	0.8	1.0	1.0	0.3	8.0	1.0	0.9
VA	0.3	0.9	0.9	0.9	0.6	0.9	1.0	1.0	0.5	0.9	1.0	1.0
wv	0.1	0.8	0.9	0.9	0.5	0.9	1.0	1.0	0.4	0.8	1.0	1.0
1idwes <sup>-</sup>	t											
IL	-0.4	0.2	0.9	0.9	0.0	0.6	1.0	0.9	-0.1	0.6	0.9	0.9
IN	-0.3	0.4	0.9	0.9	0.2	0.7	1.0	1.0	0.0	0.7	0.9	0.9
IA	-0.6	-0.1	0.7	0.7	-0.4	0.1	0.8	0.8	-0.4	0.2	0.8	0.8
KS	-0.5	-0.3	0.1	0.1	-0.2	0.2	0.7	0.7	-0.3	0.2	0.6	0.6
MI	-0.4	-0.1	0.8	0.8	-0.1	0.5	0.9	0.9	-0.2	0.4	0.9	0.9
MN	-0.3	-0.2	0.2	0.2	-0.2	0.0	0.4	0.4	-0.3	0.0	0.5	0.4
NE	-0.5	-0.5	0.1	0.0	-0.5	-0.3	0.2	0.2	-0.4	-0.2	0.4	0.3
ND	-0.5	-0.4	-0.3	-0.3	-0.3	-0.1	0.1	0.0	-0.4	-0.2	-0.1	-0.1
ОН	-0.2	0.7	0.9	0.9	0.4	0.8	1.0	1.0	0.2	8.0	1.0	1.0
SD	-0.6	-0.5	-0.1	-0.1	-0.4	-0.3	0.0	0.0	-0.4	-0.3	0.0	0.0
WI	-0.4	-0.2	0.6	0.6	-0.2	0.3	0.9	0.9	-0.3	0.2	8.0	0.8
/est												
AK	0.4	0.3	0.3	0.3	0.3	0.3	0.4	0.4	0.3	0.3	0.4	0.4
ΑZ	0.4	0.5	0.0	0.1	0.4	0.2	0.6	0.6	0.5	0.3	0.4	0.4
CA	-0.1	-0.1	0.0	0.0	0.2	0.2	0.6	0.6	0.1	0.1	0.3	0.3
со	-0.3	-0.2	-0.1	-0.2	-0.2	-0.1	0.3	0.3	-0.2	-0.1	0.1	0.1
HI	0.5	0.3	-0.7	-0.7	0.6	-0.1	-0.6	-0.6	0.4	0.0	-0.6	-0.6
ID	-0.4	-0.4	0.0	0.0	-0.3	-0.3	0.0	0.0	-0.3	-0.2	0.0	0.0
МТ	-0.5	-0.4	0.0	0.0	-0.4	-0.2	0.0	0.0	-0.4	-0.2	0.0	0.0
NV	-0.2	-0.3	-0.1	-0.1	-0.1	-0.3	0.0	0.0	-0.1	-0.2	0.1	0.1
NM	0.0	0.2	0.0	0.0	0.2	0.2	0.3	0.3	0.2	0.2	0.2	0.2
OR	-0.5	-0.4	-0.3	-0.3	-0.4	-0.4	-0.1	-0.1	-0.4	-0.3	-0.2	-0.2
TX	0.4	0.4	0.4	0.3	0.1	0.5	0.9	0.8	0.1	0.5	0.7	0.7
UT	-0.1	-0.2	0.1	0.1	0.0	-0.1	0.4	0.4	0.1	0.1	0.1	0.1
WA	-0.5	-0.5	-0.2	-0.2	-0.4	-0.3	0.1	0.1	-0.4	-0.3	0.0	0.0
										-0.1		

Data sources: Global Burden of Disease Study, Copernicus Atmospheric Monitoring System

Figure 13
CORRELATIONS BETWEEN MORTALITY RATES DUE TO AIR POLLUTION AND POLLUTANT VARIABLES,
POPULATION AGED 20–54 YEARS (2003–2019)

									Mean_	Mean_	Mean_	Mean
	Max_	Max_	Max_	Max_	Mean_	Mean_	Mean_	Mean_	Top6_	Top6_	Top6_	Top6_
State	BCA	OMA	PM10	PM2	BCA	OMA	PM10	PM2	BCA	OMA	PM10	PM2
СТ	0.2	0.7	1.0	1.0	0.7	0.9	1.0	1.0	0.6	0.9	1.0	1.0
ME	0.1	0.6	0.8	0.8	0.3	0.7	0.8	0.9	0.2	0.7	0.9	0.9
MA	0.1	0.7	0.9	0.9	0.6	0.9	1.0	1.0	0.5	0.9	1.0	1.0
NH	0.0	0.6	0.9	0.9	0.4	0.8	0.9	0.9	0.3	0.8	0.9	0.9
NJ	0.3	0.8	1.0	1.0	0.8	0.9	1.0	1.0	0.7	0.9	1.0	1.0
NY	0.0	0.7	0.9	0.9	0.4	0.8	1.0	1.0	0.3	0.8	1.0	1.0
PA	0.0	0.8	1.0	1.0	0.6	0.9	1.0	1.0	0.4	0.8	1.0	1.0
RI	0.2	0.7	0.9	0.9	0.7	0.9	1.0	1.0	0.6	0.9	1.0	1.0
VT	-0.1	0.6	0.9	0.9	0.4	0.8	0.9	0.9	0.2	0.8	0.9	0.9
outh												
AL	0.6	0.8	0.9	0.8	0.6	0.8	0.9	0.9	0.5	0.8	0.9	0.9
AR	0.4	0.6	0.7	0.7	0.3	0.7	0.9	0.8	0.2	0.7	0.8	0.8
DE	0.2	0.8	1.0	1.0	0.7	0.9	1.0	1.0	0.6	0.9	1.0	1.0
DC	0.2	0.8	1.0	1.0	0.7	0.9	1.0	1.0	0.5	0.9	1.0	1.0
FL	0.3	0.5	0.5	0.5	0.5	0.7	0.9	0.9	0.5	0.7	0.8	0.8
GA	0.3	0.6	0.5	0.6	0.4	0.8	0.9	0.9	0.4	0.7	0.8	0.8
KY	0.0	0.7	0.9	0.8	0.5	0.9	1.0	0.9	0.4	0.8	0.9	0.9
LA	0.5	0.6	0.6	0.4	0.4	0.8	0.9	0.9	0.4	0.8	0.9	0.8
MD	0.2	0.8	1.0	1.0	0.6	0.9	1.0	1.0	0.5	0.9	1.0	1.0
MS	0.5	0.7	0.8	0.8	0.5	0.8	0.9	0.9	0.4	0.8	0.9	0.9
мо	-0.2	0.4	0.8	0.7	0.1	0.6	0.9	0.9	0.0	0.6	0.8	0.8
NC	0.4	0.8	0.6	0.6	0.5	0.8	1.0	1.0	0.5	0.8	0.9	0.9
ок	-0.1	0.1	0.4	0.3	0.1	0.6	0.8	0.8	0.1	0.5	0.7	0.6
sc	0.3	0.7	0.9	0.9	0.5	0.8	1.0	1.0	0.5	0.8	1.0	1.0
TN	0.3	0.8	0.9	0.8	0.5	0.8	1.0	1.0	0.4	0.8	0.9	0.9
VA	0.3	0.8	0.9	0.9	0.6	0.9	1.0	1.0	0.5	0.9	1.0	1.0
wv	0.1	0.8	0.9	0.9	0.6	0.9	1.0	1.0	0.5	0.9	1.0	1.0
idwe	st											
IL	-0.4	0.2	0.9	0.9	0.0	0.7	1.0	1.0	-0.1	0.6	0.9	0.9
IN	-0.3	0.4	0.9	0.9	0.3	0.8	1.0	1.0	0.1	0.7	0.9	0.9
IA	-0.6	-0.2	0.8	0.8	-0.4	0.2	0.8	0.8	-0.4	0.2	0.8	0.8
KS	-0.4	-0.3	0.1	0.1	-0.2	0.2	0.7	0.7	-0.3	0.2	0.6	0.5
MI	-0.4	-0.1	0.8	0.8	-0.1	0.5	0.9	0.9	-0.2	0.4	0.9	0.9
MN	-0.5	-0.3	0.3	0.2	-0.4	0.0	0.6	0.6	-0.5	-0.1	0.6	0.6
NE	-0.5	-0.5	0.1	0.1	-0.4	-0.2	0.3	0.3	-0.4	-0.2	0.5	0.4
ND	-0.5	-0.4	-0.3	-0.3	-0.4	-0.2	0.1	0.1	-0.4	-0.2	0.0	0.0
ОН	-0.2	0.6	0.9	0.9	0.4	0.8	1.0	1.0	0.2	0.8	1.0	1.0
SD	-0.5	-0.5	-0.1	-0.2	-0.4	-0.4	-0.1	-0.1	-0.4	-0.3	-0.1	-0.1
WI	-0.4	-0.2	0.6	0.6	-0.2	0.3	0.9	0.9	-0.3	0.2	0.8	0.8

West

AK	0.5	0.4	0.4	0.4	0.4	0.4	0.4	0.4	0.4	0.4	0.4	0.4
AZ	0.4	0.5	0.1	0.1	0.4	0.3	0.6	0.6	0.5	0.4	0.5	0.5
CA	-0.1	-0.2	0.0	0.0	0.2	0.2	0.6	0.6	0.1	0.0	0.2	0.2
со	-0.2	-0.1	-0.1	-0.1	-0.1	-0.1	0.4	0.4	-0.2	-0.1	0.1	0.1
HI	0.5	0.3	-0.6	-0.6	0.6	-0.1	-0.6	-0.6	0.5	0.0	-0.6	-0.6
ID	-0.4	-0.4	0.0	0.0	-0.3	-0.3	0.0	0.0	-0.3	-0.3	0.0	0.0
MT	-0.4	-0.3	0.1	0.1	-0.3	-0.2	0.1	0.1	-0.3	-0.2	0.1	0.1
NV	-0.2	-0.3	-0.1	-0.1	-0.2	-0.4	0.0	0.0	-0.2	-0.4	0.0	0.0
NM	0.0	0.1	0.0	0.0	0.1	0.1	0.2	0.3	0.1	0.2	0.2	0.2
OR	-0.5	-0.5	-0.3	-0.4	-0.4	-0.4	-0.1	-0.1	-0.4	-0.4	-0.2	-0.2
TX	0.4	0.4	0.4	0.3	0.2	0.5	0.9	0.8	0.2	0.5	0.7	0.7
UT	-0.1	-0.2	0.1	0.1	0.0	-0.1	0.4	0.4	0.1	0.1	0.1	0.1
WA	-0.5	-0.5	-0.2	-0.2	-0.4	-0.3	0.1	0.1	-0.5	-0.4	0.0	0.0
WY	-0.4	-0.4	0.0	0.0	-0.2	-0.2	0.1	0.0	-0.2	-0.2	0.0	0.0

Data sources: Global Burden of Disease Study, Copernicus Atmospheric Monitoring System

Figure 14

CORRELATIONS BETWEEN MORTALITY RATES DUE TO AIR POLLUTION AND POLLUTANT VARIABLES,
POPULATION AGED 55+ YEARS (2003–2019)

	Max_	Max_	Max_	Max_	Mean_	Mean_	Mean_	Mean_	Mean_ Top6_	Mean_ Top6_	Mean_ Top6_	Mean Top6_
State	BCA	OMA	PM10	PM2	BCA	OMA	PM10	PM2	ВСА	OMA	PM10	PM2
СТ	0.2	0.8	1.0	1.0	0.7	0.9	1.0	1.0	0.6	0.9	1.0	1.0
ME	0.1	0.6	0.8	0.8	0.3	0.7	0.9	0.9	0.2	0.8	0.9	0.9
MA	0.1	0.7	0.9	0.9	0.6	0.9	1.0	1.0	0.5	0.9	1.0	1.0
NH	0.1	0.7	0.9	0.9	0.4	0.8	1.0	1.0	0.3	0.8	1.0	1.0
NJ	0.3	0.8	1.0	1.0	0.8	0.9	1.0	1.0	0.6	0.9	1.0	1.0
NY	0.0	0.7	0.9	0.9	0.4	0.8	1.0	1.0	0.3	0.8	1.0	1.0
PA	0.0	0.8	1.0	1.0	0.5	0.9	1.0	1.0	0.4	0.9	1.0	1.0
RI	0.2	0.7	0.9	0.9	0.7	0.9	1.0	1.0	0.6	0.9	1.0	1.0
VT	-0.1	0.6	0.9	0.9	0.3	0.8	1.0	1.0	0.2	0.8	1.0	1.0
uth												
AL	0.5	0.7	0.9	0.8	0.5	0.8	1.0	0.9	0.5	0.8	1.0	0.9
AR	0.4	0.7	0.8	0.7	0.3	0.7	0.9	0.9	0.2	0.7	0.9	0.8
DE	0.2	0.8	1.0	1.0	0.6	0.9	1.0	1.0	0.5	0.9	1.0	1.0
DC	0.3	0.8	1.0	1.0	0.7	0.9	1.0	1.0	0.6	0.9	1.0	1.0
FL	0.3	0.4	0.5	0.5	0.5	0.7	0.9	0.9	0.4	0.7	0.8	0.8
GA	0.3	0.6	0.5	0.5	0.4	0.8	0.9	0.9	0.4	0.7	0.8	0.8
KY	0.0	0.7	0.9	0.9	0.4	0.8	1.0	1.0	0.3	0.8	1.0	1.0
LA	0.5	0.6	0.6	0.4	0.4	0.8	0.9	0.9	0.4	0.8	0.9	0.9
MD	0.2	0.8	1.0	1.0	0.6	0.9	1.0	1.0	0.5	0.9	1.0	1.0
MS	0.5	0.7	0.8	0.7	0.4	0.8	0.9	0.9	0.3	0.8	0.9	0.9
NC	0.4	0.7	0.6	0.6	0.5	0.8	1.0	1.0	0.5	0.8	0.9	0.9
OK	-0.1	0.1	0.5	0.3	0.1	0.6	0.8	0.8	0.0	0.5	0.7	0.7
SC	0.3	0.7	0.9	0.9	0.5	0.8	1.0	1.0	0.4	0.7	1.0	1.0
TN	0.3	0.8	0.9	0.9	0.4	0.8	1.0	1.0	0.4	0.8	1.0	0.9
TX	0.4	0.4	0.4	0.3	0.2	0.5	0.9	0.8	0.2	0.5	0.7	0.7
VA WV	0.3 0.1	0.8	0.9 0.9	0.9 0.9	0.6 0.5	0.9	1.0 1.0	1.0 1.0	0.5 0.4	0.8	1.0 1.0	1.0
dwe:		0.0	0.5	0.5	0.5	0.5	1.0	1.0	0.4	0.8	1.0	1.0
IL	-0.4	0.2	0.9	0.9	0.0	0.6	1.0	1.0	-0.1	0.6	0.9	0.9
IN	-0.3	0.4	0.9	0.9	0.2	0.8	1.0	1.0	0.1	0.7	1.0	0.9
IA	-0.6	-0.1	0.8	0.7	-0.4	0.2	0.9	0.8	-0.4	0.2	0.8	0.8
KS	-0.5	-0.3	0.1	0.1	-0.3	0.2	0.7	0.7	-0.3	0.2	0.6	0.6
MI	-0.3	-0.1	0.8	0.8	-0.1	0.5	0.9	0.9	-0.2	0.4	0.9	0.9
MN	-0.4	-0.3	0.3	0.2	-0.4	0.0	0.7	0.7	-0.4	-0.1	0.7	0.7
мо	-0.2	0.5	0.8	0.8	0.1	0.6	0.9	0.9	0.0	0.6	0.9	0.8
NE	-0.5	-0.5	0.1	0.0	-0.4	-0.3	0.3	0.3	-0.4	-0.2	0.4	0.4
ND	-0.5	-0.4	-0.3	-0.3	-0.5	-0.3	0.1	0.1	-0.5	-0.3	0.0	-0.
ОН	-0.2	0.7	0.9	0.9	0.4	0.8	1.0	1.0	0.2	0.8	1.0	1.0
SD	-0.5	-0.5	-0.1	-0.1	-0.4	-0.4	-0.1	-0.1	-0.4	-0.4	-0.1	-0.
WI	-0.3	-0.1	0.6	0.6	-0.2	0.3	0.9	0.9	-0.2	0.3	0.9	0.9

# West

AK	0.5	0.4	0.4	0.4	0.4	0.4	0.4	0.4	0.4	0.4	0.4	0.4
AZ	0.3	0.5	0.1	0.1	0.4	0.2	0.6	0.6	0.5	0.3	0.5	0.5
CA	-0.1	-0.2	0.0	0.0	0.1	0.2	0.6	0.6	0.0	0.0	0.3	0.3
со	-0.2	-0.1	0.0	-0.1	-0.2	-0.1	0.4	0.4	-0.2	-0.1	0.2	0.2
HI	0.5	0.3	-0.6	-0.6	0.6	-0.1	-0.6	-0.6	0.5	0.0	-0.6	-0.6
ID	-0.4	-0.4	0.0	0.0	-0.3	-0.3	0.0	0.0	-0.3	-0.3	0.0	0.0
MT	-0.4	-0.2	0.1	0.1	-0.3	-0.2	0.2	0.1	-0.3	-0.1	0.1	0.1
NV	-0.2	-0.3	-0.1	-0.1	-0.3	-0.4	-0.1	-0.1	-0.3	-0.4	-0.1	-0.1
NM	0.0	0.0	0.0	-0.1	0.0	0.1	0.2	0.2	0.1	0.1	0.1	0.1
OR	-0.5	-0.5	-0.3	-0.3	-0.4	-0.4	-0.1	-0.1	-0.4	-0.4	-0.2	-0.2
UT	-0.1	-0.2	0.1	0.1	-0.1	-0.2	0.4	0.4	0.0	0.0	0.1	0.1
WA	-0.4	-0.4	-0.2	-0.2	-0.4	-0.3	0.2	0.2	-0.4	-0.3	0.0	0.0
WY	-0.3	-0.4	0.0	0.0	-0.3	-0.2	0.0	0.0	-0.2	-0.2	0.0	0.0

Data sources: Global Burden of Disease Study, Copernicus Atmospheric Monitoring System

# Section 3: Modeling Approaches

Having examined historical patterns of wildfires, air pollution, and their association with mortality, the report now turns to the modeling frameworks that can quantify these effects. This section introduces the types of models used in the literature and provides context for selecting the three specific approaches explored in detail in the following sections.

Modeling the impact of wildfire-related air pollution on mortality can be approached from two perspectives:

- Short-term effects, such as acute increases in mortality following specific wildfire events, and
- Long-term effects, which capture the cumulative health burden from sustained or repeated exposure to air pollution.

A range of models has been used in the literature to assess these effects. This section presents representative examples of short- and long-term modeling strategies, including both statistical and epidemiological approaches.

## 3.1 SHORT-TERM MORTALITY MODELING

Short-term models typically assess the immediate health impacts following spikes in air pollution due to wildfire events. Two representative studies are the following:

- Chen et al. <sup>28</sup> employed *quasi-Poisson regression models* at the city level to estimate the relationship between daily PM<sub>2.5</sub> concentrations from wildfire-related air pollution and daily mortality counts (cardiovascular, respiratory, and all-cause). Their model included lagged effects (up to seven days), average temperature, and relative humidity. City-level estimates were then pooled using a random-effects metaregression to generate broader regional or national risk estimates.
- Johnston et al.<sup>29</sup> estimated *annual mortality* attributable to wildfire-related air pollution using a spatial model with  $2^{\circ} \times 2.5^{\circ}$  resolution. Mortality estimates were weighted by the number of days  $PM_{2.5}$  concentrations fell within specific ranges and adjusted by a relative risk factor based on a literature-derived concentration-response relationship for  $PM_{10}$ , subsequently scaled to  $PM_{2.5}$ .

# 3.2 LONG-TERM MORTALITY MODELING

Long-term models assess the cumulative health impact of prolonged or repeated exposure to wildfire-related air pollution. Key approaches include the following:

• Grant and Runkle<sup>30</sup> conducted a review of 17 studies that project future wildfire-related air pollution impacts on U.S. mortality. Many<sup>31,32</sup> rely on:

 $<sup>^{28}</sup>$  G. Chen et al., "Mortality Risk Attributable to Wildfire-Related PM<sub>2</sub>·5 Pollution: A Global Time Series Study in 749 Locations," *Lancet Planet Health* 5, no. 9 (2021): e579–e587, https://doi.org/10.1016/S2542-5196(21)00200-X.

<sup>&</sup>lt;sup>29</sup> F. H. Johnston et al., "Estimated Global Mortality Attributable to Smoke from Landscape Fires," *Environmental Health Perspectives* 120, no. 5 (2012): 695–701, https://doi.org/10.1289/ehp.1104422.

<sup>&</sup>lt;sup>30</sup> E. Grant and J. D. Runkle, "Long-Term Health Outcomes of Wildfire Exposure: A Scoping Review," *Journal of Climate Change and Health* 6 (2022): 100110, https://doi.org/10.1016/j.joclim.2021.100110.

<sup>&</sup>lt;sup>31</sup> B. Ford et al., "Future Fire Impacts on Smoke Concentrations, Visibility, and Health in the Contiguous United States," *GeoHealth* 2 (2018): 229–247, https://doi.org/10.1029/2018GH000144.

 $<sup>^{32}</sup>$  J. E. Neumann et al., "Estimating PM<sub>2.5</sub>-Related Premature Mortality and Morbidity Associated with Future Wildfire Emissions in the Western US," Environmental Research Letters 16, no. 3 (2021): 035019, https://doi.org/10.1088/1748-9326/abe82b.

- o Estimation of relative risks for PM<sub>2.5</sub> exposure (e.g., from Ostro et al. <sup>33</sup>) and
- o Application of concentration-response functions (CRFs) to project excess mortality.
- Gao et al.<sup>34</sup> applied *Cox proportional hazards models* to estimate long-term mortality risks associated with wildfire-derived PM<sub>2.5</sub>. Variants of their model incorporated individual-level covariates (e.g., age, sex, education), environmental exposures (e.g., nonwildfire pollution by PM<sub>2.5</sub>), and behavioral risk factors (e.g., smoking, alcohol use).

## 3.3 CONSIDERATION OF CLIMATIC INTERACTIONS

One important limitation of most studies is their treatment of air pollution as an isolated factor. Climatic phenomena often interact. For example:

- Rising temperatures, whether of natural origin or from manufactured causes, <sup>35</sup> can intensify pollutant emissions and chemical reactions that increase secondary pollutant formation (e.g., ozone).
- Heat can worsen pollution dispersion by promoting atmospheric stagnation.
- Conversely, some pollutants (e.g., sulfate aerosols) may have cooling effects, <sup>36</sup> complicating the interaction between pollution and climate change.

These interactions introduce feedback loops that can influence both exposure and health outcomes. However, this complexity is not captured in the current study, which models air pollution impacts on mortality independently of other environmental stressors.

## 3.4 MODELING FRAMEWORKS USED IN THIS STUDY

Based on a review of the literature and internal analyses, three distinct modeling frameworks were selected to illustrate the range of approaches available to practitioners.

- *Climate Lee-Carter Model:* A stochastic modeling approach adapted from the classic Lee-Carter model, which has been effectively applied to heat wave mortality.<sup>37</sup> This framework demonstrates how widely used mortality models can be extended to incorporate the impact of climate variables.
- Prevalence scenario derivation: An intuitive approach that aligns with morbidity modeling
  practices. It involves projecting mortality by applying fixed death rates to disease prevalence
  scenarios influenced by air pollution exposure.
- The AIRQ+ methodology, found in the World Health Organization's AirQ+ tool and directly following the work performed by Ostro.<sup>38</sup> This approach has been retained because it allows the capture of long-term effects of air pollution on mortality. It uses concentration-response functions and baseline mortality rates.

<sup>&</sup>lt;sup>33</sup> B. Ostro, "Outdoor Air Pollution: Assessing the Environmental Burden of Disease at National and Local Levels," *Environmental Burden of Disease* Series No. 5 (Geneva: World Health Organization, 20024), https://iris.who.int/handle/10665/42909.

<sup>&</sup>lt;sup>34</sup> G. Yuan et al., "Association Between Long-Term Exposure to Wildfire-Related PM<sub>2.5</sub> and Mortality: A Longitudinal Analysis of the UK Biobank," *Journal of Hazardous Materials* 457 (2023): 131779, https://doi.org/10.1016/j.jhazmat.2023.131779.

<sup>&</sup>lt;sup>35</sup> World Meteorological Organization, *Air Quality and Climate Bulletin No. 4* (Geneva: World Meteorological Organization, 2024), https://library.wmo.int/records/item/69006-no-4-september-2024.

<sup>&</sup>lt;sup>36</sup> J. Gao et al., "Fast Climate Responses to Emission Reductions in Aerosol and Ozone Precursors in China During 2013–2017," Atmospheric Chemistry and Physics 22, no. 11 (2022): 7131–7142, https://doi.org/10.5194/acp-22-7131-2022.

<sup>&</sup>lt;sup>37</sup> https://www.milliman.com/en/insight/modeling-the-impact-of-climate-risks-on-mortality.

<sup>&</sup>lt;sup>38</sup> See note 34 above.

The three approaches are summarized in Table 2, with their strengths and limitations.

Table 2
SUMMARY OF THE SPECIFICATIONS OF THE STUDIED APPROACHES

Approach	Climate Lee-Carter Model	Derivation of Prevalence Scenarios	AIRQ+ Methodology
Purpose	Stochastic modeling of mortality with a climate index component to capture wildfire related mortality	Estimate mortality via morbidity projections linked to air pollution	Epidemiological approach using CRFs and baseline mortality
Benefits	Integrates climate variables into widely used mortality models	Intuitive; aligns with morbidity modeling practices	Transparent; allows long-term projections
Drawbacks	Requires high-quality mortality and pollution data; suited to short- term impacts (1–3 years)	Dependent on GBD estimates and assumes static death rates	Calibration challenges; subject to temporal and spatial biases

## 3.5 LIMITATIONS OF THE STATE-LEVEL APPROACH

Modeling mortality at the state level may obscure local effects because of topographic features that influence smoke dispersion (e.g., mountain valleys)<sup>39</sup> and long-range transport of smoke, which can affect regions far from fire origins<sup>40</sup> (e.g., U.S. impacts from Canadian wildfires<sup>41</sup> or the transboundary health impact of Arctic wildfire-related air pollution study).<sup>42</sup>

Therefore, wildfire exposure in one state may influence pollution-related mortality in another, complicating attribution.

In the following sections, each of the three selected modeling approaches is explored in greater detail, highlighting implementation methods and calibration considerations.

<sup>&</sup>lt;sup>39</sup> https://airquality.climate.ncsu.edu/2021/06/06/atmospheric-dispersion-and-pollution\_transport/#:~:text=Note%20that%20horizontal%20dispersion%20can,the%20ridges%20that%20define%20it.

<sup>&</sup>lt;sup>40</sup> G. Chen et al., "Mortality Risk Attributable to Wildfire-Related PM<sub>2</sub>·5 Pollution: A Global Time Series Study in 749 Locations," *Lancet Planet Health* 5, no. 9 (2021): e579–e587, https://doi.org/10.1016/S2542-5196(21)00200-X.

<sup>&</sup>lt;sup>41</sup> https://airquality.climate.ncsu.edu/2021/06/06/atmospheric-dispersion-and-pollution-transport/#:~:text=Note%20that%20horizontal%20dispersion%20can,the%20ridges%20that%20define%20it.

<sup>&</sup>lt;sup>42</sup> B. Silver et al., "Large Transboundary Health Impact of Arctic Wildfire-Related Air Pollution," *Communications Earth & Environment* 5 (2024): 199, https://doi.org/10.1038/s43247-024-01361-3.

# Section 4: Stochastic Modeling Approach: Climate Lee-Carter Model

The first modeling framework examined is an adaptation of the classic Lee-Carter model, selected for its compatibility with stochastic mortality modeling commonly used by life insurers. This approach provides a practical entry point for incorporating climate variables into familiar actuarial tools and focuses on estimating short- to medium-term impacts of pollution on mortality.

## 4.1 PRINCIPLE

Mortality can be modeled using classical stochastic frameworks such as the Lee-Carter model, which decomposes mortality rates by age and time components and allows for projections through time series modeling. In this study, the Lee-Carter model is adapted to include a climate-sensitive component of mortality—specifically, the influence of air pollution on mortality.

The key innovation lies in separating mortality into two components: (1) a baseline component that reflects mortality trends unrelated to climate factors and (2) a climate-sensitive component that varies with pollutant exposure levels.

This can be accomplished in two steps:

• Decomposing the age × time mortality matrix into separate age and time components based on a singular value decomposition:

$$\ln(\mu_{x,t}) = \alpha_x + \beta_x \, \kappa_t$$

where x represents age, t represents the age, here in years,  $\mu$  denotes the mortality rate,  $\alpha_x$  the static mortality age structure,  $\beta_x$  the sensitivity of each age to overall time dynamics, and  $\kappa_t$  time pattern of mortality.

• Considering the time parameter  $(\kappa_t)$  as a random series [ARIMA (0,1,0)] to draw future mortality scenarios.

An adaptation of this model to capture the climate-sensitive component of mortality has been proposed:<sup>43</sup>

$$\ln(\mu_{x,t}) = \alpha_x + \beta_x^o \kappa_t^o + \delta_x^C C_t.$$

The purpose of the term  $\beta_x^o \kappa_t^o$  is to capture mortality exclusive of the climate cause (here air pollution mortality). Therefore c is related to the climate cause of mortality and o is related to other causes. The term  $c_t$  represents the climatic indicator for year t, capturing the impact of the studied climate variables on mortality.

Ultimately, the purpose of this approach is to generate mortality scenarios that reflect both observed data and climate-based projections, providing insurers with a flexible framework to assess the potential impacts of air pollution on future mortality experience.

The primary objective of this model is to isolate and quantify the portion of mortality attributable to a specific climatic factor, namely, air pollution. Although the contribution of air pollution to all-cause

<sup>43</sup> https://www.milliman.com/en/insight/modeling-the-impact-of-climate-risks-on-mortality.

mortality is relatively modest, the model is designed to extract this climate-sensitive component without diminishing the overall performance of the traditional Lee-Carter framework.

Once calibrated, the model allows for projections of pollution-attributable mortality under various climate scenarios. This requires input assumptions for key air quality indicators, including average annual and peak monthly concentrations of  $PM_{2.5}$  and  $PM_{10}$ , to capture both baseline and episodic exposure patterns.

By integrating observed mortality data with climate-based projections, this approach provides a flexible framework for insurers to assess the potential long-term impact of air pollution on mortality and incorporate it into forward-looking risk assessments and pricing strategies.

#### 4.2 MODEL SPECIFICATION

The model calibration is performed in two main steps: age-class calibration followed by continuous age calibration. The beginning equation for the calibration process is the following:

$$\ln(\mu_{c_i,t}) = \alpha_{c_i} + \beta_{c_i}^0 \kappa_t^0 + \delta_{c_i} C_t.$$

1. Age-class calibration: In the first step, mortality is segmented by age classes to more precisely estimate the climate-related component. This involves establishing a static age-class structure for overall mortality, constructing a climate index that captures the evolution of mortality attributable to air pollution, and determining the sensitivity of each age class to changes in the climate index.

Estimation of mortality related to climate risk:44

$$\ln(\mu_{c_i,t}) = \alpha_{c_i} + \beta_{c_i}^0 \kappa_t^0 + \delta_{c_i} C_t.$$

- a. Calibration of  $\alpha_{c_i}$  by using a Lee-Carter model on 1990–2018 mortality data (HMD): The  $\alpha_{c_i}$  is three vector parameters for the three age classes.
- b. Calibration of the climate index (a,b): To identify the most relevant climate variables for explaining climate-related mortality rates, a variable selection process is conducted using linear regression. The selection begins with a stepwise Akaike Information Criterion (AIC) procedure, which evaluates all possible combinations of climate variables and retains the model that minimizes the AIC. This approach balances model fit and complexity. Following this, a p-value analysis is performed to assess the statistical significance of each variable. The most significant climate variables—those that best explain the variation in climate-related mortality—are retained for use in the model. Thus, the final climate index  $C_t$  follows the following three-parameter linear equation:

$$C_t = a + b^T X_t$$

where a, b are the linear regression parameters, and  $X_t$  is the vector of climate variables of year t.

<sup>&</sup>lt;sup>44</sup> For some climate risk factors, it might be interesting to consider a "harvesting effect." The harvesting effect refers to the fact that fragile people are primarily affected by an event that causes excess mortality in the general population. Without this event, these people would have died in the days or weeks that follow. The consequence of this harvesting effect is that the event is followed by a period of undermortality.

c. Calibration of  $\delta_{c_i}$ , by minimizing the residuals, which are

$$R_{c_i,t} = \ln(\mu_{c_i,t}) - \alpha_{c_i} - \delta_{c_i}C_t.$$

Continuous age calibration: In the second step, the model is refined to incorporate continuous age variables. This allows for the calibration of remaining parameters related to baseline (non-climate-related) mortality and the continuous age-based structure of overall mortality. All the age-class parameters are converted into single-age parameters, and the equation becomes:

$$\ln(\mu_{x,t}) = \alpha_x + \beta_x^0 \kappa_t^0 + \delta_x C_t.$$

Consider the following residuals (by removing the  $\alpha_x$ ):

$$R_{x,t} = \ln(\mu_{x,t}) - \delta_x C_t.$$

Final calibration consists of applying a Lee-Carter model on the residuals  $R_{x,t}$  to find the  $\alpha_x$ ,  $\beta_x^0$  and  $\kappa_t^0$  parameters.

#### 4.3 RESULTS

#### 4.3.1 CLIMATE INDEX BY STATES

The calibration methodology described above was applied across all states. For each state, a linear regression was conducted between climate-related mortality rates and various climate variables. To ensure model parsimony, only the most statistically significant variables were retained in each case.

Table 3 summarizes the proportion of states achieving specific levels of predictive accuracy, as measured by the  $R^2$ , for models using either two or four explanatory variables. For 60% of states, using the two most significant variables resulted in an  $R^2$  below 80%. Conversely, even with four variables, 34% of states still did not reach an  $R^2$  above 80%.

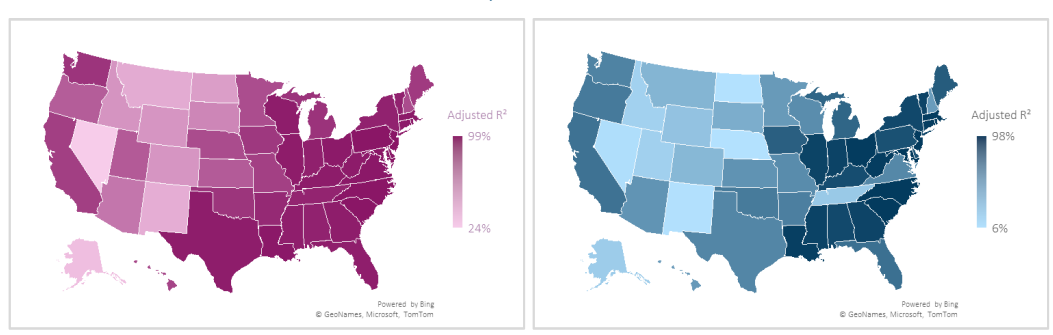
Table 3 CLIMATE INDEX REGRESSION GOODNESS OF FIT: PROPORTION OF STATES FOR WHICH  $\mathbb{R}^2$  IS ABOVE A CERTAIN THRESHOLD

R <sup>2</sup>	Four Variables	Two Variables
>90%	52%	32%
>80%	66%	40%
>60%	80%	54%

In addition, a comparison of the Bayesian Information Criterion was conducted between models using two and four climate variables. In 68% of states, the four-variable model demonstrated a better fit, indicating improved likelihood with acceptable model complexity.

Figure 15 complements Table 3 by illustrating the quality of the climate index regression across states. Darker shades of pink (left figure) or blue (right figure) indicate stronger model performance. Notably, the four-variable specification yields particularly strong predictive results in the eastern United States and California.

Figure 15
ADJUSTED  $R^2$  OF THE CLIMATE INDEX CALIBRATION
LEFT: WITH FOUR EXPLANATORY VARIABLES; RIGHT WITH TWO EXPLANATORY VARIABLES

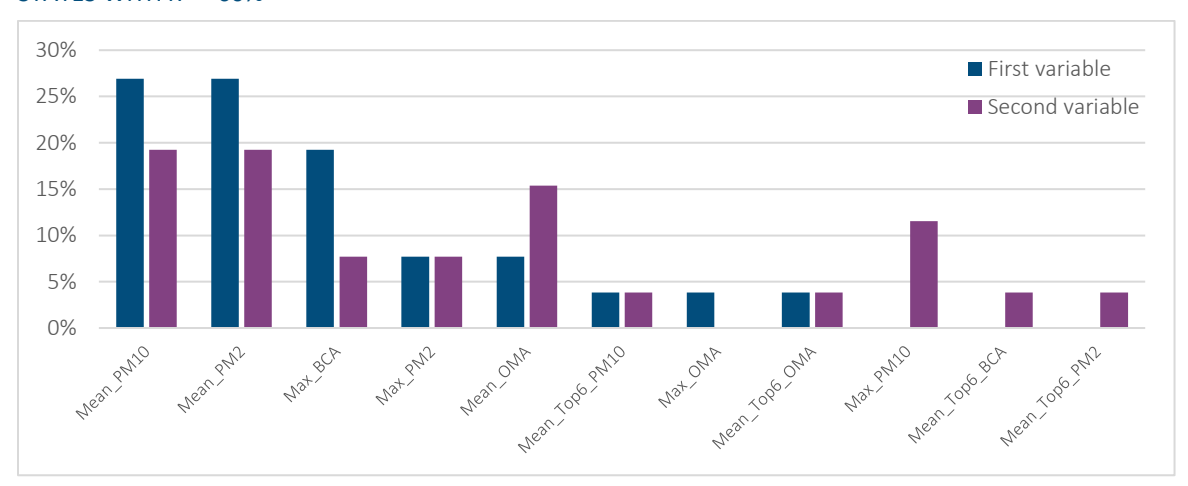


Data sources: Authors' calculations.

For each state, the two most statistically significant climate variables were identified. A national-level analysis was then conducted to determine which variables were most frequently selected across states. As shown in Figure 16, either the average concentration of  $PM_{10}$  (Mean\_ $PM_{10}$ ) or  $PM_{2.5}$  (Mean\_ $PM_2$ ) emerged as the most predictive variable in 27% of states. These two variables are also ranked as the second-most significant in nearly 20% of states.

In contrast, variables representing annual maximum concentrations and the mean of the top six annual values were generally less influential. An exception is the maximum value of black carbon aerosol optical depth at 550 nm (Max BCA), which was the most predictive variable in approximately 20% of states.

Figure 16 VARIABLES RETAINED FOR CLIMATE INDEX CALIBRATION WITH TWO EXPLANATORY VARIABLES STATES WITH  $\it R^2 > 60\%$ 



Note: For example, for 27% of states for which the linear regression results in  $R^2$  higher than 60%, the most significant variable is either the average level of  $PM_{10}$  or the average level of  $PM_{10}$ . The annual maximum level of  $PM_{10}$  appears in only 11.5% of the regressions, and it is never the most significant variable.

# 4.3.2 CALIBRATION FOR ALASKA

Alaska is presented as an illustrative case because of its pronounced peaks in air pollution-related mortality (see Figure 6). The initial calibration of the climate index for Alaska yielded poor results, with an  $R^2$  of only

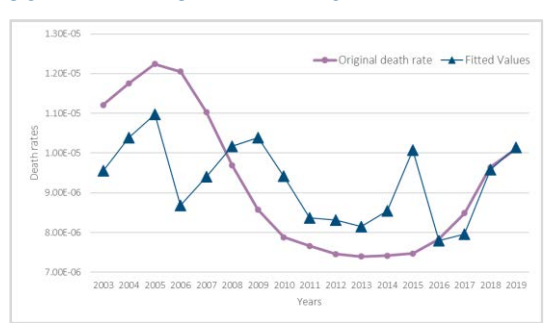
17% using two explanatory variables and 30% using four. As shown in Figure 17, the model struggled to capture observed mortality peaks.

However, model performance improved significantly when lagged climate variables were introduced, suggesting that climate-related mortality in Alaska may be influenced by pollutant exposure sustained over multiple years. Incorporating lagged variables raised the  $R^2$  to 99%, indicating a much stronger fit.

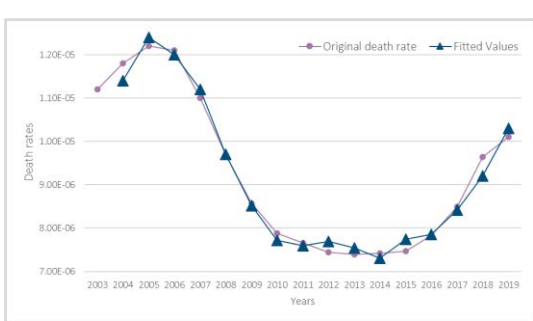
As a result, the following variables were used in the final calibration for Alaska, listed in order of significance:

- Mean\_Top6\_PM<sub>2</sub>,
- Mean PM<sub>2</sub>,
- Mean Top6 PM<sub>10</sub>,
- Mean PM<sub>10</sub>,
- Mean\_Top6\_PM<sub>2</sub>\_lag,
- Mean\_PM<sub>2</sub>\_lag,
- Mean\_Top6\_PM<sub>10</sub>\_lag, and s
- Mean\_PM<sub>10</sub>\_lag.

Figure 17
CLIMATE INDEX CALIBRATION: ALASKA
FOUR EXPLANATORY VARIABLES



# FOUR EXPLANATORY VARIABLES + LAG



Further refinement was applied to the climate index calibration by adjusting the model based on the direction of change in climate-related mortality. During periods of declining mortality, the regression incorporated lagged variables from years 1, 2, and 3, suggesting that three consecutive years of reduced air pollution are associated with improved mortality outcomes. Conversely, during periods of increasing mortality, only current-year data and a one-year lag were used, indicating a more immediate response to rising pollution levels (Figure 18).

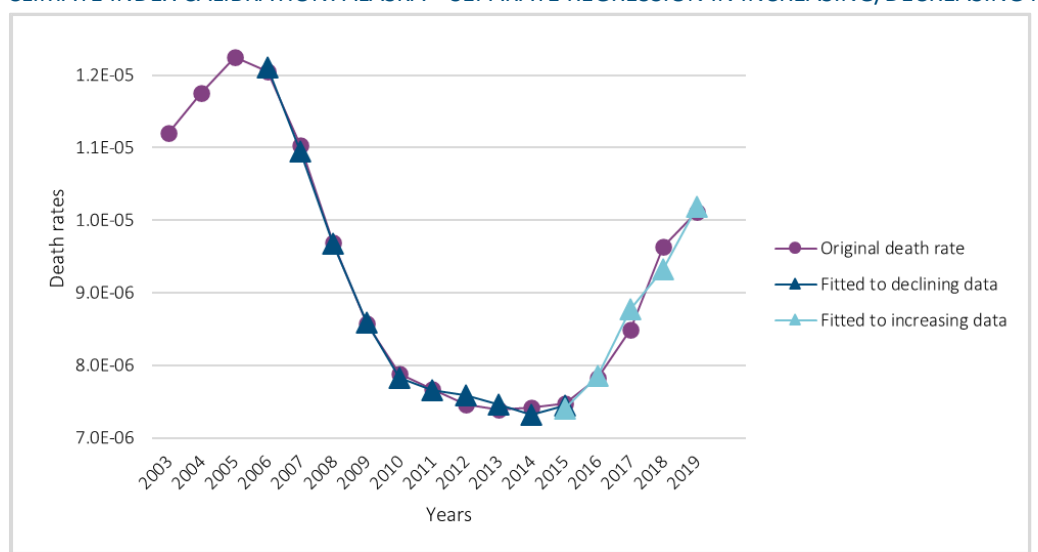


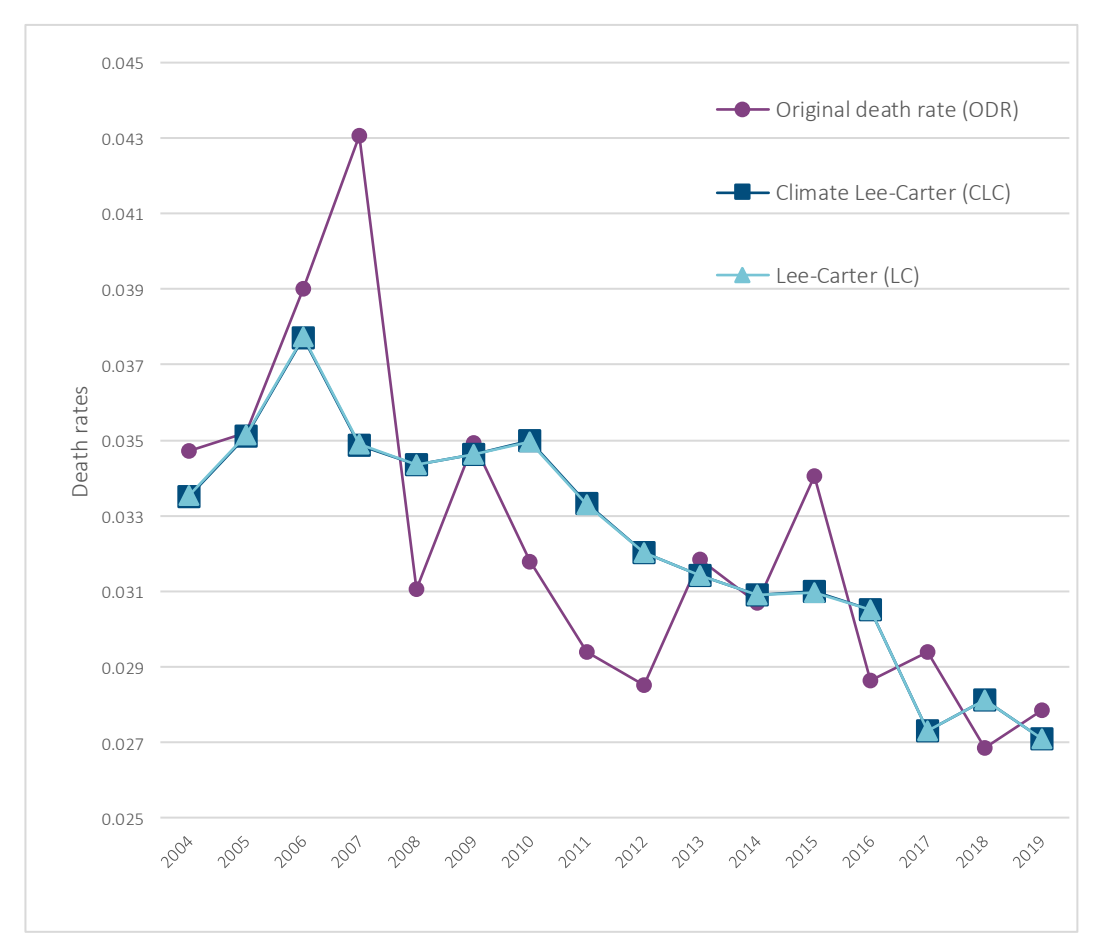
Figure 18
CLIMATE INDEX CALIBRATION: ALASKA—SEPARATE REGRESSION IN INCREASING/DECREASING PARTS

It is important to note that the number of available data points is limited, making it difficult to generalize a regression model calibrated on such a small sample.

# **4.3.3 RESULTS**

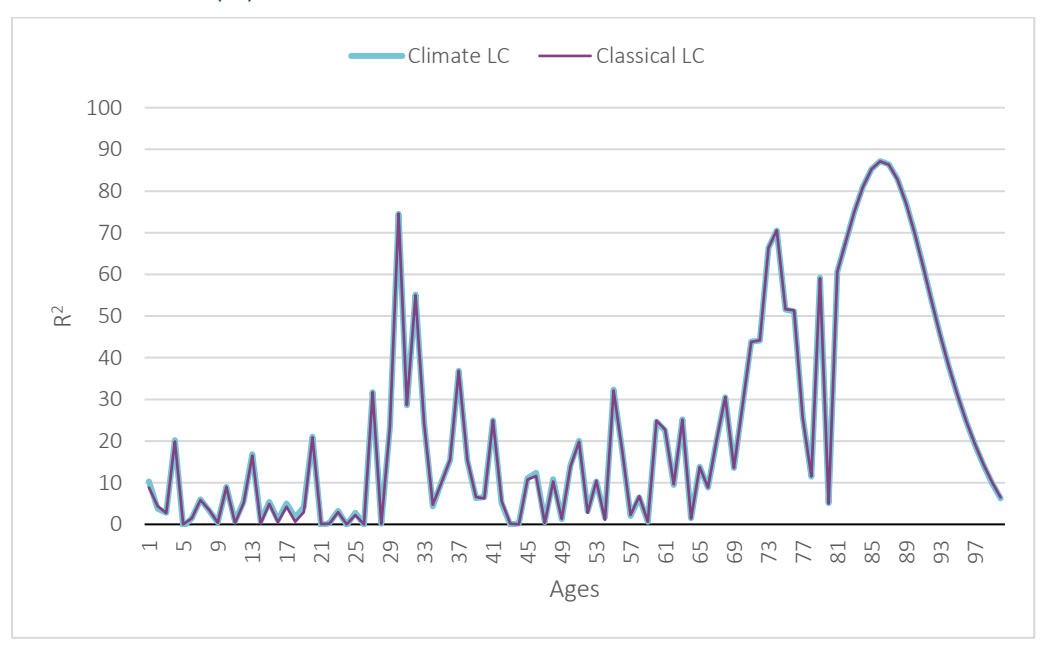
The climatic Lee-Carter model produced results that were very similar to those of the standard Lee-Carter model, as illustrated in Figure 19. This outcome is expected, given that the mortality attributable to air pollution represents a small fraction of total mortality. Although the climatic model does not outperform the traditional model in overall fit, its primary advantage lies in isolating the climate-related mortality component, which can then be projected under various climate scenarios.

Figure 19
CLIMATIC LEE-CARTER MODEL AND CLASSIC LEE-CARTER MODEL FITS ON ALASKA



However, both Lee-Carter models do not appear to be suitable to model mortality in Alaska: The models'  $R^2$  are low for most ages between zero and 70, as well as at very high ages (Figure 20).

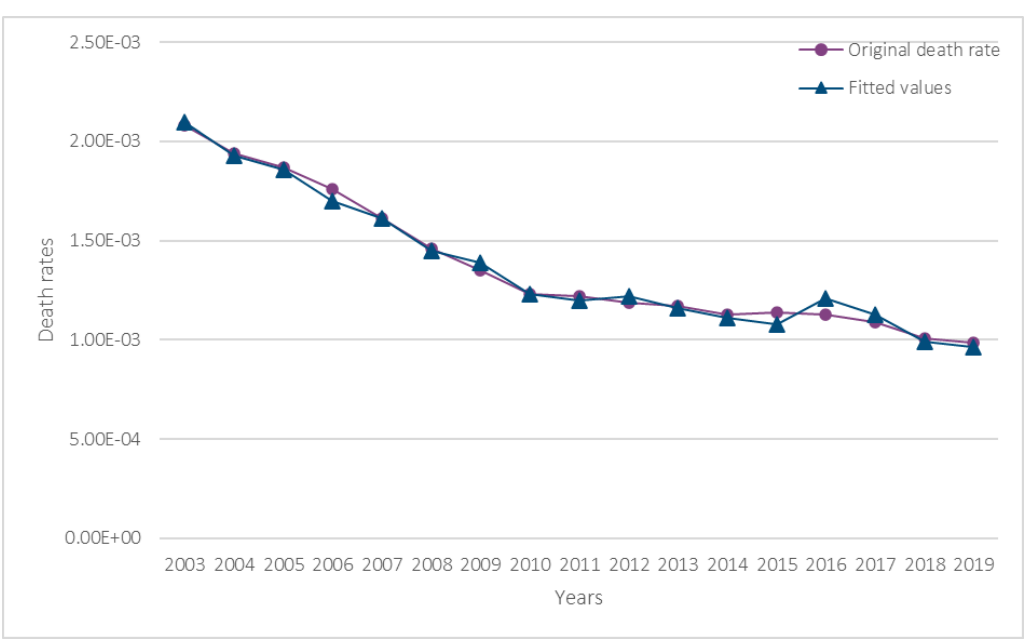
Figure 20 GOODNESS OF FIT (R<sup>2</sup>)



# 4.3.4 CALIBRATION FOR CALIFORNIA

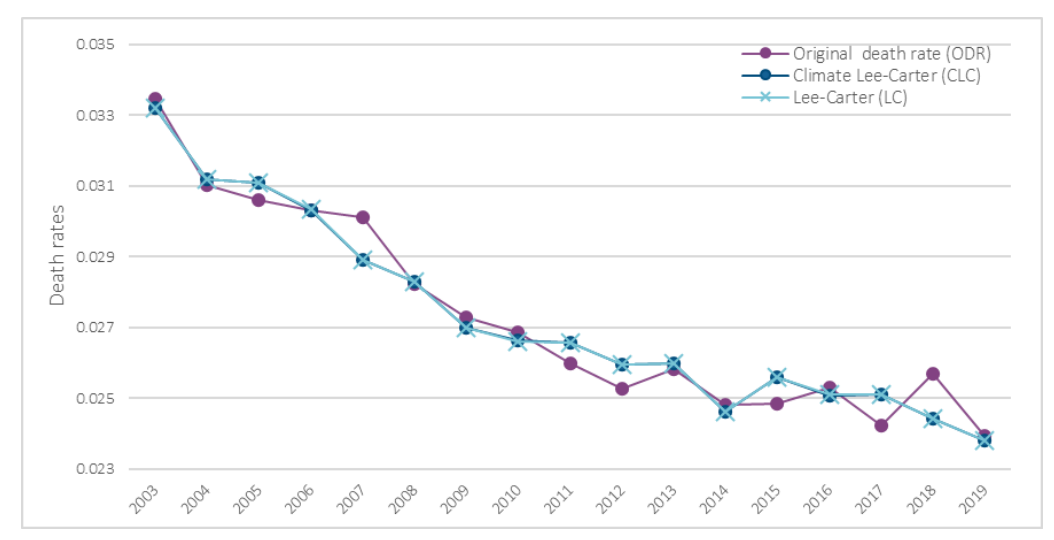
California serves as a contrasting case to Alaska, with a notably smoother calibration process for the climate index (Figure 21). Using six explanatory variables—Mean\_Top6\_OMA, Mean\_PM<sub>10</sub>, Mean\_Top6\_BCA, Mean\_PM<sub>2</sub>, Mean\_Top6\_PM<sub>10</sub>, and Max\_PM<sub>10</sub> (listed in order of statistical significance)—the model achieved an  $R^2$  of 99%, indicating an excellent fit.

Figure 21
CLIMATE INDEX CALIBRATION: CALIFORNIA



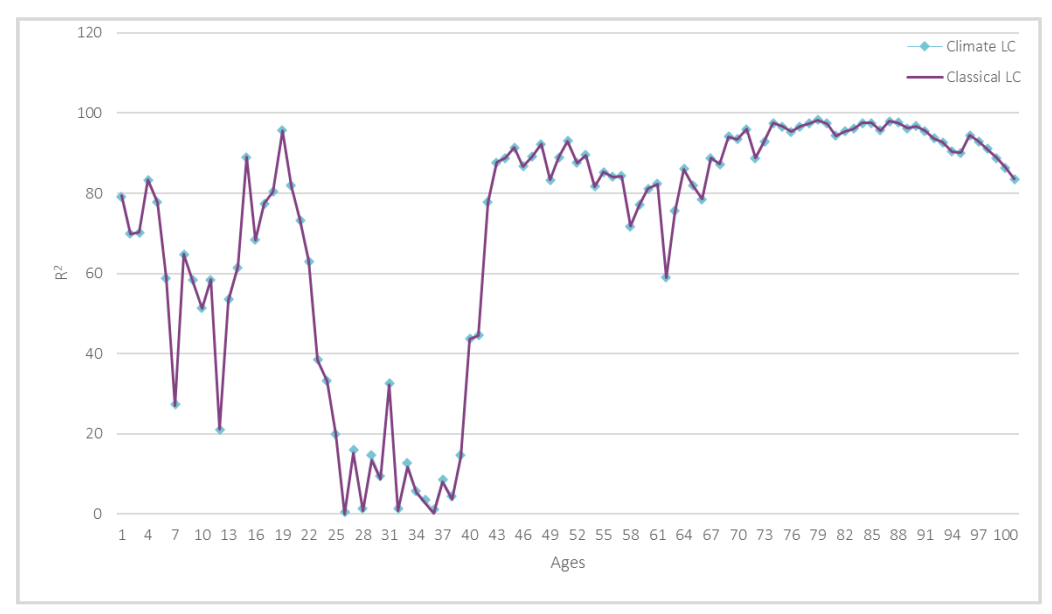
As shown in Figure 21, the climate index accurately reflects the observed mortality trends. The resulting outputs from the climatic Lee-Carter model are nearly indistinguishable from those produced by the classic Lee-Carter model, as illustrated in Figure 22. This is consistent with expectations, given the relatively small share of total mortality attributable to air pollution.

Figure 22
CLIMATIC LEE-CARTER MODEL AND CLASSIC LEE-CARTER MODEL FITS ON CALIFORNIA



However, unlike the Alaska case, the model's overall fit in California is strong across a broad age range, particularly for individuals aged 40 and above. This is demonstrated in Figure 23, which shows high  $R^2$  values across most age segments, confirming the model's robustness in this setting.

Figure 23
CLIMATE LEE-CARTER MODEL AND CLASSIC LEE-CARTER MODEL GOODNESS OF FIT (R2): CALIFORNIA



## 4.4 ANALYSIS

#### 4.4.1 MODEL CALIBRATION OBSERVATIONS

The calibration results vary significantly by state. In some cases, such as California, the Climate Lee-Carter model can be calibrated effectively using a limited number of climate variables, producing a strong fit. In contrast, other states—like Alaska—require more complex modeling. For these states, the climate index may depend not only on current-year pollution levels but also on lagged exposures from previous years. This suggests that cumulative exposure to air pollution over multiple years may play a more critical role in driving mortality outcomes than single-year concentrations.

For example, in Alaska, a meaningful improvement in the model's fit was achieved only after including multiple years of lagged pollution data. Additionally, periods of decreasing mortality appeared to require three consecutive years of low pollution exposure, while increases in mortality could result from as little as one or two years of elevated exposure.

Given these complexities, establishing a standardized, automated calibration approach across all states is not feasible. Each state's pollution and mortality dynamics may require a tailored calibration process.

#### 4.4.2 LIMITATIONS OF STATE-LEVEL MODELING

Modeling at the state level also introduces structural limitations. As discussed in Section 2.1, smoke dispersion patterns can decouple pollution exposure from the location of wildfire events, limiting the precision of state-level attribution. As another example, pollutant concentrations may be disproportionately higher in specific counties even if the state-wide average appears moderate.

#### 4.4.3 PROJECTION CONSIDERATIONS

Although autoregressive models can be used to project future mortality under various climate scenarios, doing so requires detailed forecasts for all climate variables used in the model. These include not only annual average pollutant concentrations (e.g.,  $PM_{2.5}$  and  $PM_{10}$ ) but also measures of peak exposure (e.g., monthly maxima). Constructing such projections is not straightforward, especially for variables that exhibit strong seasonal or episodic behavior.

To address this, decomposition techniques for daily time series may be applied, allowing projected trends to be combined with historical seasonal patterns. <sup>45</sup> However, each climate variable used in the model must be handled individually, reinforcing the value of keeping the number of inputs as low as possible for practical implementation.

The Climate Lee-Carter model can be adapted to quantify and project mortality attributable to climate-sensitive factors such as wildfire-related air pollution. By separating baseline mortality from a climate-driven component, it offers a way to isolate and analyze pollution-linked mortality trends. However, calibration results in this study varied widely by state, reflecting differences in pollution-mortality relationships, data quality, and the most predictive pollutant variables. In some states, a small number of variables produced an excellent fit, while in others, complex lag structures or custom adjustments were

<sup>45</sup> https://www.milliman.com/en/insight/climate-driven-mortality-projections-under-different-scenarios.

needed. Because no single specification worked well everywhere, the model's applicability to mortality from wildfire-related air pollution must be evaluated and calibrated individually for each state.

Because of the challenges of calibration and data availability, projections were not conducted as part of this study. However, if comprehensive climate scenario data—including pollutant projections—were available, the model could be used to estimate the future mortality impact for individual states.

# Section 5: Derivation of Prevalence Scenarios

Although the Climate Lee-Carter model captures short-term effects using time-series mortality data, the next approach considers long-term impacts by linking pollution exposure to chronic disease prevalence. This method aligns with morbidity modeling techniques and enables scenario-based forecasting over longer time horizons.

This method assumes that air pollution contributes to an increase in the prevalence of specific diseases over time, which in turn drives increases in mortality. Implementing this approach requires access to health data that link air pollution exposure to disease incidence. Because different diseases respond to air pollution through distinct biological mechanisms, a separate model would be required for each condition affected. The development of such morbidity models—although outside the scope of this report—would ideally rely on detailed health datasets that can track individuals' disease progression and exposure history.

Assuming that morbidity scenarios are available (i.e., projected prevalence rates for specific diseases), mortality can be estimated by applying known death rates for individuals affected by those diseases. This results in projected mortality figures attributable to air pollution-induced disease prevalence.

Assume the availability of morbidity scenarios: scenarios of prevalence  $(P_{t_0}, P_{t_1}, ..., P_{t_N})$ . One can then capitalize on the data on the death rate due to air pollution, denoted  $Death\ Rates_{pollution}$ , provided by the GBD database:

$$\begin{aligned} \textit{Death Rates}_{pollution, t_0} &= \frac{\textit{Number of deaths}_{airpollution}}{\textit{Total population}_{t_0}} = \frac{\textit{q}_{\textit{Exposed population}} \textit{x} \, \textit{Exposed population}_{t_0}}{\textit{Total population}_{t_0}} \\ &= \textit{q}_{\textit{Exposed population}} \times \textit{P}_{t_0} \end{aligned}$$

with  $P_{t_0} = \frac{Exposed\ population_{t_0}}{Total\ population_{t_0}}$  the initial prevalence at  $t_0$ , and  $q_{Exposed\ population}$  the death rate of the exposed population.

Then  $Death\ Rates_{pollution,t} = q_{Exposed\ population} \times P_t$ , with the assumption that the death rate of the exposed population is constant over time.

The strengths of this approach include its simplicity, transparency, and alignment with morbidity modeling frameworks already familiar to actuaries. It also allows for consistency across mortality and morbidity projections and can support analyses segmented by socioeconomic or demographic characteristics.

However, there are notable limitations:

- The method relies on Global Burden of Disease (GBD) data. As described in Section 2.2.2, GBD mortality estimates provide pollution-attributed mortality rates based on modeled exposure-response functions, which differ from empirical cause-of-death reporting. This introduces a level of uncertainty.
- It assumes that the death rate among the exposed population remains constant over time, which may not hold true given changes in health care, population resilience, or adaptation strategies.
- Developing disease-specific prevalence scenarios is highly resource-intensive. It requires comprehensive health data at a granular geographic level to allow linkage with local air pollution data. This includes detailed claims data or health surveillance records that can capture longitudinal disease trends.

The "prevalence scenario" approach described here can be directly informed by the companion "Wildfire-Related Air Pollution and Morbidity" study. That research uses advanced statistical and machine learning techniques to quantify how PM<sub>2.5</sub> exposure during wildfire season, including lag effects, changes the prevalence of major disease categories (circulatory, respiratory, mental and behavioral, and neoplasms) across different populations and geographies. These empirically derived prevalence changes can serve as the core inputs to the mortality projection formula in this section. By mapping each morbidity category to a corresponding GBD-based mortality rate, the model can estimate state-, age-, or coverage-specific deaths attributable to wildfire-related PM<sub>2.5</sub>. This integration ensures that mortality scenarios reflect both the magnitude and the variation of pollution-driven disease burdens observed in the morbidity analysis, producing projections that are grounded in observed health impacts rather than broad national averages.

In summary, this method offers an accessible and logically consistent way to estimate long-term air pollution-related mortality. Although it may not provide the precision of more complex epidemiological models, it offers a practical starting point, particularly when integrated into broader morbidity-based projection frameworks.

# Section 6: AirQ+ Methodology: Computing the Attributable Risk

To estimate the number of premature deaths and illnesses attributable to air pollution, one widely used tool is the World Health Organization's AirQ+. <sup>46</sup> This tool is based on a health impact function (HIF), which calculates health outcomes based on data such as air pollutant concentrations, population demographics, baseline mortality or morbidity rates, and the concentration-response relationship parameter.

# **6.1 HEALTH IMPACT FUNCTION (HIF)**

The third approach employs the World Health Organization's AirQ+ tool, which estimates mortality attributable to pollution using epidemiological response functions. Unlike the prior models, this method is grounded in public health research and enables risk attribution based on pollutant concentration thresholds and relative risks.

The HIF provides a framework for estimating excess deaths or illnesses linked to exposure to specific pollutants. The method requires four main inputs:

- Air pollutant concentrations, based on either modeled projections or observed environmental data.
- Exposed population data, often broken down by age, gender, and geographic location.
- Baseline mortality or morbidity rates, which represent expected health outcomes in the absence of pollution exposure.
- Concentration-response beta coefficients (or relative risk estimates), which quantify the increase in health risk per unit increase in pollutant concentration and are derived from peer-reviewed epidemiological studies.

These parameters are integrated into the HIF, which uses the following equation to estimate the health impact:

$$\Delta Y = [1 - \exp(-\beta \times \Delta C)] \times Y_0 \times Pop$$

where

- $\Delta Y$  = the estimated number of premature deaths or illnesses.
- $\beta$  = the risk estimate (or beta coefficient) from an epidemiological study.
- $\Delta C$  = the defined change in concentration of the examined air pollutant.
- $Y_0$  = the baseline rate (i.e., incidence) of deaths or illnesses.
- *Pop* = the population exposed to air pollution.

This equation links air pollution exposure directly to health outcomes, providing an estimate of the health burden caused by specific pollutants in a given population.

#### 6.1.1 LINKING EXPOSURE AND HEALTH OUTCOME

The methodology distinguishes between exposed and unexposed populations and between healthy and affected individuals. By comparing the incidence of illness or death between exposed and unexposed

<sup>46</sup> https://www.who.int/tools/airq.

groups, the model estimates *relative risk*—the ratio of risk in the exposed population to that in the unexposed. See Table 4.

Table 4
SCHEMA OF EXPOSED/NON-EXPOSED AND HEALTHY/AFFECTED POPULATION

Illness	Exposi	ure	Total
Illness	Not Exposed	Exposed	Total
Healthy	а	b	a + b
Affected	С	d	c+d
Total	a+c	b+d	n

Note: Among the (b+d) exposed, the risk equals  $R_e=\frac{d}{b+d}$ . Among the (a+c) not exposed, the risk equals  $R_0=\frac{c}{a+c}$ .

The ratio between these two risks will express the risk of the exposed relative to the nonexposed. This ratio, called relative risk, is given as  $RR = \frac{R_e}{R_0}$ 

#### 6.1.2 ATTRIBUTABLE RISK

Using the relative risk, the model calculates the *attributable risk* (or attributable fraction), which represents the proportion of observed health outcomes in the exposed population that can be directly attributed to air pollution. This allows users to estimate the excess disease burden linked specifically to pollutant exposure.

Attributable risk can be expressed by estimating excess risk as  $R_e-R_0$  divided by the risk for those who are exposed to the factor,  $R_e$ :

$$AR = \frac{R_e - R_0}{R_e}$$

This gives the proportion of the excess risk for disease that can be attributed to the exposure for the factor in question. Substituting relative risk in the equation for the attributable risk gives:

$$AR = \frac{RR - 1}{RR}$$

# **6.1.3 ESTIMATING ATTRIBUTABLE CASES**

Once the attributable fraction is determined, it is applied to the exposed population and the baseline mortality or morbidity rate to estimate the number of *attributable cases*, such as premature deaths. This figure represents the health impact of pollution under current or projected environmental conditions:

$$\Delta D = Pop \times y_0 \times AR$$

Here Pop represents the exposed population, and  $y_0$  is the baseline mortality rate, allowing for an estimate of the total number of attributable deaths in the exposed population.

# 6.1.4 RISK QUANTIFICATION

The model uses *concentration-response functions* (CRFs) to quantify the increase in health risk associated with rising pollutant levels. These CRFs are typically derived from peer-reviewed cohorts or time-series studies and reflect the change in risk for a given change in concentration of a pollutant, such as PM<sub>2.5</sub> or ozone.

The risk of mortality in a population due to exposure to air pollution is represented by the CRF, which is based on relative risk (RR) estimates derived from epidemiological studies:

$$RR = \exp(\beta \times \Delta C)$$

where

- $\beta$ : the CRF (i.e., the estimated slope of the log-linear relation between concentration and mortality, often referred to as a beta coefficient from an epidemiologic study that measures the risk of a health effect due to a one-unit change in an air pollutant concentration).
- $\Delta C$ : the change in concentration.

The attributable fraction (AR) can be expressed as:

$$AR = 1 - \exp(-\beta \times \Delta C)$$

Multiplying the AR by the baseline mortality rate  $y_0$  and the population size Pop gives an estimate of excess mortalities due to air pollution:

$$\Delta D = Pop \times y_0 \times [1 - \exp(-\beta \times \Delta C)]$$

#### 6.2 ADVANTAGES AND LIMITATIONS OF THE HIF APPROACH

The HIF approach has the following advantages and limitations.

# Advantages:

- Simplicity: The HIF methodology is transparent, easy to understand, and straightforward to apply.
- Reproducibility: The use of clearly defined inputs enables consistent application across different populations and geographic areas.

# Limitations:

- *Uncertainty:* Estimates can vary because of uncertainty in input parameters, data availability, data attribution accuracy, and assumptions around exposure levels.
- Extrapolation: CRFs are often derived from studies conducted in specific regions or populations. Applying these estimates to other settings can introduce bias, especially if demographic or environmental conditions differ.
- Temporal and spatial sensitivity: Models calibrated on past populations may not accurately reflect future risk levels, particularly as public health interventions, population sensitivity, and pollution sources evolve. Geographic variability in exposure, medical access, and population vulnerability also adds complexity.
- Interaction with other climate-related factors: Air pollution may interact with other climate-related risks—such as extreme heat—which are not captured in the standalone HIF model.

Despite these limitations, the HIF remains a practical tool for initial estimates of pollution-attributable health outcomes and is particularly useful in scenario-based modeling.

#### 6.3 RESULTS

The AirQ+ methodology was applied to two pollutants: ozone  $(O_3)$  and PM<sub>2.5</sub>, with a focus on estimating excess mortality among individuals aged 65 and older in California for the year 2021. Values for the Risk Ratios associated with these two pollutants come from the AirQ+ tool.

# 6.3.1 PROJECTED IMPACT OF OZONE ON MORTALITY (AGED 65+)

This case study modeled the effect of rising temperatures on ozone concentrations and the corresponding mortality impact. It assumes that each one degree C increase in temperature leads to a  $2.8 \,\mu\text{g/m}^3$  increase in ozone concentration.  $^{47}$ 

To clarify the analytical approach, two key concepts are defined:

- *SOMO35:* This metric captures cumulative exposure to ozone concentrations exceeding 35 parts per billion over a defined period. It serves as a proxy for the health burden associated with elevated ozone levels.
- Additional mortality rate: This is calculated by comparing the number of excess deaths observed under elevated pollution conditions to a baseline scenario, expressed relative to the at-risk population.

The analysis begins with a baseline scenario in which ozone concentrations are minimal. In this scenario, the SOMO35 value is set at 6,000, a level representative of observed conditions in California. At this concentration, approximately 5,418 premature deaths are estimated among the elderly population. See Tables 5 and 6.

As temperatures rise, ozone concentrations increase accordingly, driving a clear upward trend in mortality. For instance, a two degrees C increase in temperature results in an estimated absolute increase in the mortality rate of 0.20% among individuals aged 65 and older.

Table 5
RETAINED HYPOTHESIS FOR THE MODELING: CALIFORNIA (AGED 65+)

Population		RR per 10 µg/m³	
at Risk <sup>a</sup> (65+)	Deaths per 1.000 <sup>b</sup>	All Causes of Mortality	SOMO35°
5,964,526	40.2	1,014	6,000

a. The Population 65 Years and Older: 2021, United States Census Bureau,

https://www.census.gov/library/visualizations/interactive/population-65-and-older-2021.html.

**c.** Fleming, Z. L., Doherty, R. M., von Schneidemesser, E., Malley, C. S., Cooper, O. R., Pinto, J. P., Colette, A., Xu, X., Simpson, D., Schultz, M. G., Lefohn, A. S., Hamad, S., Moolla, R., Solberg, S., & Feng, Z. (2018). "Tropospheric Ozone Assessment Report: Present-day ozone distribution and trends relevant to human health." *Elementa: Science of the Anthropocene*, 6. <a href="https://doi.org/10.1525/elementa.273">https://doi.org/10.1525/elementa.273</a>.

b. CDC WONDER, https://wonder.cdc.gov/deaths-by-underlying-cause.html.

<sup>&</sup>lt;sup>47</sup> https://acp.copernicus.org/articles/19/13367/2019/acp-19-13367-2019-discussion.html.

Table 6
RESULTS OF THE HIF APPROACH: ALL CAUSES OF MORTALITY

Temperature (C)	Baseline Situation	1	1.5	2	3	4
Additional $O_3$ concentratio $n (\mu g/m^3)$	0	2.8	4.2	5.6	8.4	11.2
SOMO35	6,000	7,022	7,533	8,044	9,066	10,088
Premature deaths	5,418	9,103	12,288	15,428	21,581	27,564
Excess of deaths		3,685	6,870	10,011	16,163	22,146
Additional mortality rate for 65+ age class		0.06178%	0.11518%	0.16784%	0.27098%	0.37130%

The results show that even modest temperature increases can result in significant increases in premature deaths. Estimated premature deaths rise from approximately 5,400 in the baseline scenario to more than 27,000 in a four degrees C warming scenario.

# 6.3.2 PROJECTED IMPACT OF PM<sub>2.5</sub> ON MORTALITY (AGED 65+)

The relationship between temperature and  $PM_{2.5}$  is more complex than with ozone and varies by region.  $PM_{2.5}$  levels are influenced by a variety of factors, including emissions, chemical reactions, and meteorological conditions such as humidity, wind, and temperature.

A comprehensive review by Tai et al. concluded that, in general, higher temperatures can increase  $PM_{2.5}$  concentrations, but the magnitude of this effect varies by region and is also influenced by factors such as humidity and precursor emissions.<sup>48</sup> In some cases, higher temperatures can enhance atmospheric mixing and reduce  $PM_{2.5}$ , especially in arid regions.

In Southeastern and Western U.S.,  $^{49}$  studies suggest that a one degree C temperature increase corresponds to a 0.3 µg/m³ increase in the annual PM<sub>2.5</sub> concentration. In the summer, this rise in temperature can lead to a 1 µg/m³ rise in the concentration of pollutants. In particular, the article shows that in Los Angeles, the impact varies between a 0.25 and a 0.8 µg/m³ increase in annual PM<sub>2.5</sub> concentration. Therefore, it has been assumed that in California, a one degree C temperature increase corresponds to a 0.5 µg/m³ increase in the annual PM<sub>2.5</sub> concentration.

<sup>&</sup>lt;sup>48</sup> A. P. K. Tai et al., "Correlations Between Fine Particulate Matter (PM<sub>2.5</sub>) and Meteorological Variables in the United States: Implications for the Sensitivity of PM<sub>2.5</sub> to Climate Change," *Atmospheric Environment* 44, no. 32 (2010): 3976–3984, <a href="https://doi.org/10.1016/j.atmosenv.2010.06.060">https://doi.org/10.1016/j.atmosenv.2010.06.060</a>.

<sup>&</sup>lt;sup>49</sup> Yin, L., Bai, B., Zhang, B. et al. « Regional-specific trends of PM<sub>2.5</sub> and O<sub>3</sub> temperature sensitivity in the United States." *npj Clim Atmos Sci* 8, 12 (2025). https://doi.org/10.1038/s41612-024-00862-4.

# 6.3.3 PROJECTED IMPACT OF PM<sub>2.5</sub> LEVELS ON MORTALITY AMONG THE ELDERLY (AGED 65+) IN CALIFORNIA, 2021 BASELINE SCENARIO AND TEMPERATURE VARIATIONS

Analogous to the methodology employed for ozone, the following tables present projections of the impact of fine particulate matter ( $PM_{2.5}$ ) on mortality under various temperature scenarios.

Table 7
RETAINED HYPOTHESIS FOR THE MODELING: CALIFORNIA (AGED 65+)

Population at risk <sup>a</sup> (65+)	Deaths per 1,000b	RR per 10 µg/m³ All Natural Causes of Mortality
5,964,526	40.2	1,08

a. The Population 65 Years and Older: 2021, United States Census Bureau,

https://www.census.gov/library/visualizations/interactive/population-65-and-older-2021.html.

b. CDC WONDER, https://wonder.cdc.gov/deaths-by-underlying-cause.html.

Table 8
RESULTS OF THE HIF APPROACH: ALL (NATURAL) CAUSES OF MORTALITY

Temperature (C)	Baseline Situation	1	1.5	2	3	4
PM <sub>2.5</sub> concentratio n ( $\mu$ g/m <sup>3</sup> )	12.7	13.2	13.5	13.7	14.2	14.7
Premature deaths	1,838	2,759	3,218	3,676	4,590	5,501
Excess of deaths		921	1,380	1,838	2,752	3,662
Additional mortality rate for 65+ age class		0.0154%	0.0231%	0.0308%	0.0461%	0.0614%

Applying these assumptions, projected excess deaths due to PM<sub>2.5</sub> exposure among individuals aged 65+ increase steadily with temperature. For example, a four degrees C rise could lead to more than 5,500 premature deaths—roughly triple the baseline scenario.

Because the ozone and  $PM_{2.5}$  scenarios use different assumptions about how each pollutant responds to temperature in California, the results are not directly comparable and do not indicate which pollutant is inherently more harmful.

# **⚠** Important Note on Comparing Ozone and PM<sub>2.5</sub> Results

The ozone and  $PM_{2.5}$  estimates in this section are based on **different assumptions about how each pollutant responds to temperature changes** in California. Ozone was modeled with a stronger and more consistent link to temperature, which produced a larger increase in concentrations in the scenarios shown.  $PM_{2.5}$ , in contrast, was modeled with a smaller and more complex temperature response that varies by region and conditions.

Because of these differences, the two results **are not directly comparable** as a measure of which pollutant is more harmful overall. In most epidemiological studies,  $PM_{2.5}$  is associated with higher per-unit health risks than ozone. The larger ozone numbers here reflect the scenario setup—not a general conclusion that ozone is the greater hazard.

In these scenarios, as ozone has a stronger relationship with temperature than  $PM_{2.5}$ , projected excess deaths are higher, which might seem contradictory as  $PM_{2.5}$  are more harmful. However, as previously reported, the relationship between temperature and  $PM_{2.5}$  is complex, and the magnitude depends on region. Consequently, a deeper model could be used to project the future excess deaths due to future increases in  $PM_{2.5}$ .

#### 6.3.4 CHALLENGES IN ASSESSING AIR POLLUTION'S IMPACT ON MORTALITY

Several challenges must be considered when interpreting results from the HIF approach:

- Multiple pollutants and combined effects: Health impacts often arise from cumulative exposure to multiple pollutants, which are not always modeled together.
- *Pollutant prioritization and transboundary effects:* Identifying the most harmful pollutants and accounting for pollution crossing regional or national borders complicates attribution.
- Spatial resolution and exposure heterogeneity: Coarse resolution of spatial data may obscure significant local variation in pollution exposure and associated health outcomes.
- Selection of concentration-response functions: Selecting a concentration-response function that aligns with the data is critical. Although linear and log-linear models offer simplicity, some scenarios may require more nuanced nonlinear models, such as logistic functions, to capture complex relationships accurately.
- Demographic and climate dynamics: Incorporating projected changes in population size, age structure, and pollution control measures can improve the relevance of future impact assessments.

To enhance model accuracy and usefulness, it is recommended that projections incorporate the following:

- Future demographic trends to yield a more accurate assessment of exposure levels. By estimating the population size potentially subject to elevated ozone concentrations, a clearer picture of health risks can be gained.
- Alternative pollution scenarios to enable the evaluation of a range of possible outcomes.
- Refined CRFs based on local epidemiological studies, reflecting local contexts and improving their specificity.

# Section 7: Conclusion

The models presented in this report illustrate a range of ways to estimate the mortality impact of air pollution, each with distinct data requirements and use cases. This concluding section summarizes key insights, modeling challenges, and opportunities for future application by insurers.

Although wildfires can lead to direct mortality, most of their impact on population health occurs indirectly—through increased air pollution and its associated long-term health outcomes. This report focuses on understanding and modeling the mortality attributable to air pollution, recognizing that wildfires are one of several contributing sources.

The analysis demonstrates that multiple modeling approaches can be used to estimate the mortality burden of air pollution, each with distinct advantages and limitations:

- The Climate Lee-Carter model introduces air pollution as a climate-sensitive factor within a well-established mortality framework. Although the pollution-attributable mortality signal is modest, this approach allows for integration with climate scenarios and offers a structured path for projecting pollution-related mortality.
- The *prevalence scenario approach* is the most intuitive and aligns closely with morbidity modeling practices. However, it requires robust health data and disease-specific projections, which can be resource-intensive to develop.
- The AirQ+ methodology, based on WHO standards, provides a practical and transparent framework for estimating excess mortality due to pollution. Although easier to implement, it involves several assumptions—particularly regarding relative risks—that may limit precision and transferability.

Among these, only the prevalence scenario and AirQ+ approaches attempt to address long-term effects. The prevalence scenario method offers the greatest flexibility and specificity but comes with significant data demands. AirQ+ is more readily deployable and may serve as a useful approximation when granular data are unavailable.

A key modeling challenge is the need for detailed and locally specific climate inputs. Although many climate scenarios include projected temperature trends, comprehensive projections of pollution variables—such as particulate concentrations and wildfire emissions—are less commonly available. Moreover, modeling the transport and dispersion of pollutants across geographies would require additional input from atmospheric scientists, especially when estimating health impacts beyond the source region.

This report applies the described models to the U.S. context; however, all the models presented can be adapted and applied to other regions, considering any geographical specificities (existence of other pollutants harmful to health, for example).

Although projections were not performed in this study, the models presented here can be adapted for scenario analysis. Insurers may apply these frameworks to assess *climate mortality shocks* in stress testing, evaluate the potential benefits of mitigation policies, or incorporate region-specific pollution risks into pricing. For example, applying a pollution-adjusted shock to existing mortality tables could enhance long-term pricing accuracy in wildfire-prone areas. Over time, this could support the development of pollution-specific zoning strategies for insurance risk assessment.

In conclusion, modeling the impact of air pollution on mortality is inherently complex, requiring interdisciplinary data and assumptions. Although existing tools can support first-order estimates for internal use, advancing this work will require further investment in data infrastructure, epidemiological

research, and climate-health integration. For actuaries, these models represent an important step toward incorporating environmental risk into long-term mortality forecasting and product design.







# Section 8: Acknowledgments

The researchers' deepest gratitude goes to those without whose efforts this project could not have come to fruition: the Project Oversight Group for their diligent work overseeing, reviewing, and editing this report for accuracy and relevance.

Project Oversight Group members:

Sam Gutterman, FSA, CERA, MAAA, FCAS, FCA, HonFIA

Charlie Mathews

Donna Megregian, FSA, MAAA

Rebecca Owen, FSA, MAAA, FCA

Sandra Said

Aadit Sheth, FSA, CERA, FCIA

Cirhan Truswell, BSc, MSc

Georgiana Willwerth, MD

At the Society of Actuaries Research Institute:

Kara Clark, FSA, MAAA, Senior Research Actuary

Rob Montgomery, ASA, MAAA, FLMI Consultant-Research Project Manager

Ronora Stryker, ASA, MAAA, Senior Research Actuary

Barbara Scott, Senior Research Administrator

# Appendix A: Comparison Between CDC and GBD Death Rates

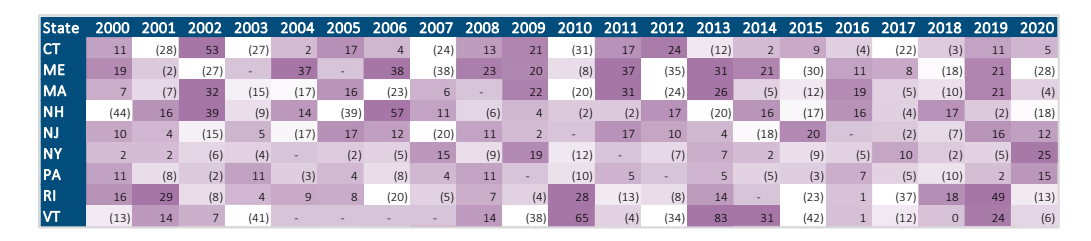
This appendix compares cause-of-death mortality rates from the Centers for Disease Control and Prevention (CDC) and the Global Burden of Disease (GBD) databases, with a focus on respiratory conditions potentially influenced by air pollution. The objective is to assess consistency between these two sources to validate their suitability for modeling mortality attributable to pollution-related risks. The CDC data, which reflect raw mortality records, contrast with the GBD's statistically smoothed estimates to evaluate alignment in trends, magnitudes, and temporal patterns.

#### A.1 CDC RATES

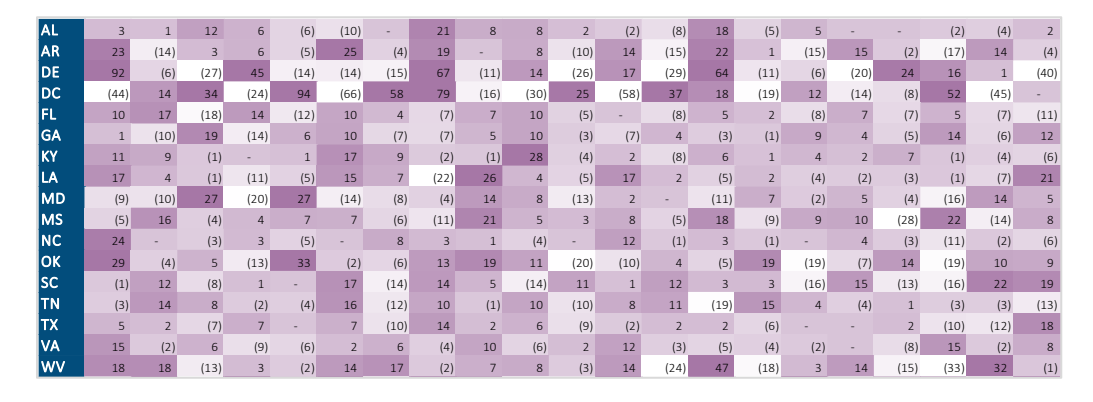
Figures A.1 and A.2 present the evolution of CDC-reported mortality rates for two age groups: 20–54 and 55+, with a focus on respiratory causes of death. Grey cells represent unavailable or missing data.

Figure A.1 shows considerable year-over-year variability in CDC mortality rates for individuals aged 20–54. Data gaps are especially frequent in this age range because of low event counts for many respiratory causes.

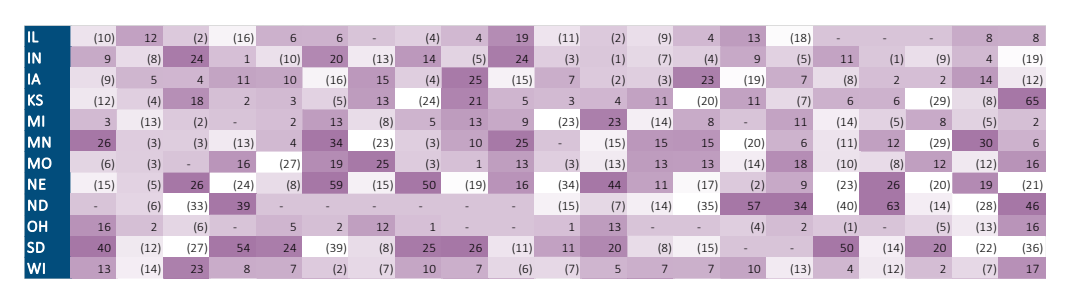
Figure A.1
HEAT MAP OF CDC MORTALITY RATES EVOLUTION FOR 20–54 AGE GROUP



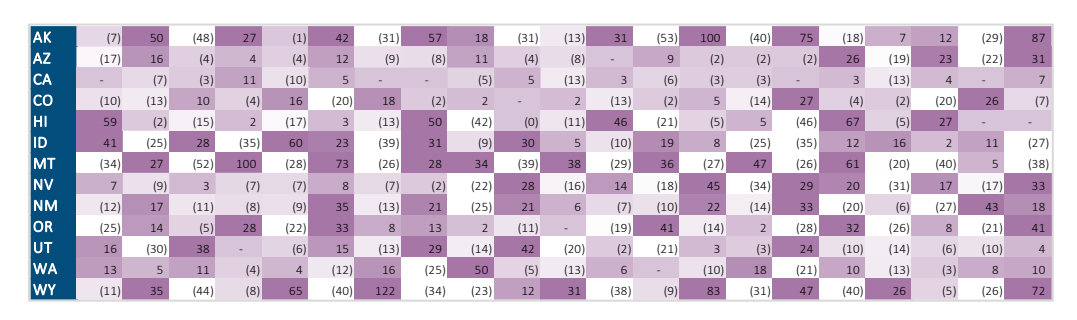
#### South



## Midwest



# West

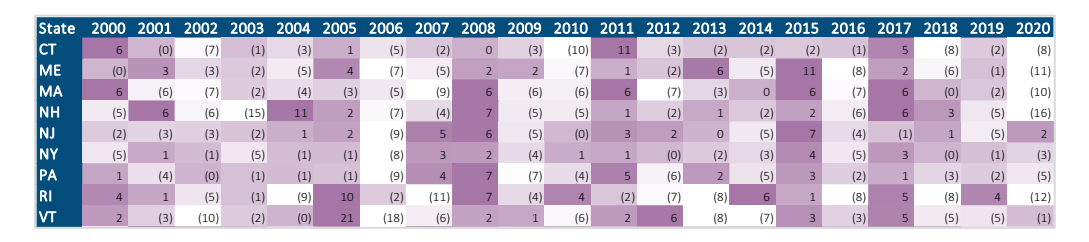


Data source: CDC Wonder. Gray blocks are not available.

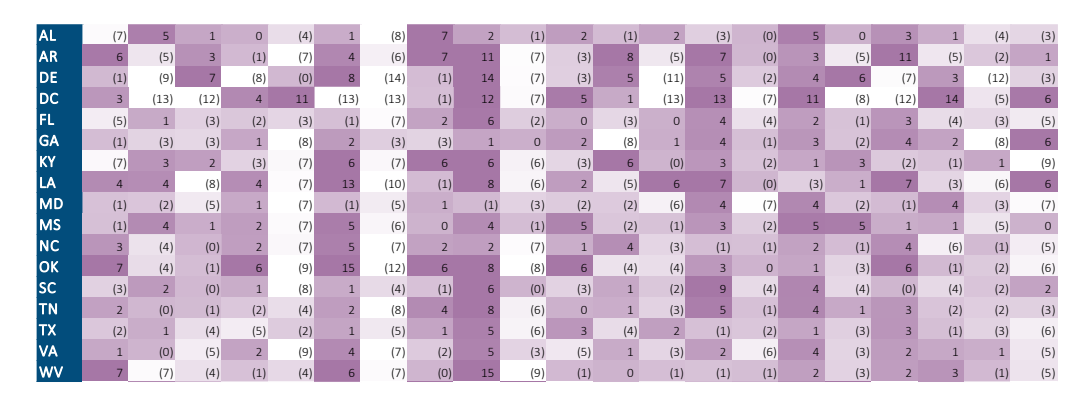
Figure A.2 highlights mortality rates for individuals aged 55 and older. Although trends are somewhat more stable in this cohort, notable fluctuations persist. A pronounced peak is observed in 2008 across many states, which aligns with findings in GBD data (see Figure A.2).

Figure A.2
HEAT MAP OF CDC MORTALITY RATES EVOLUTION FOR 55+ AGE GROUP

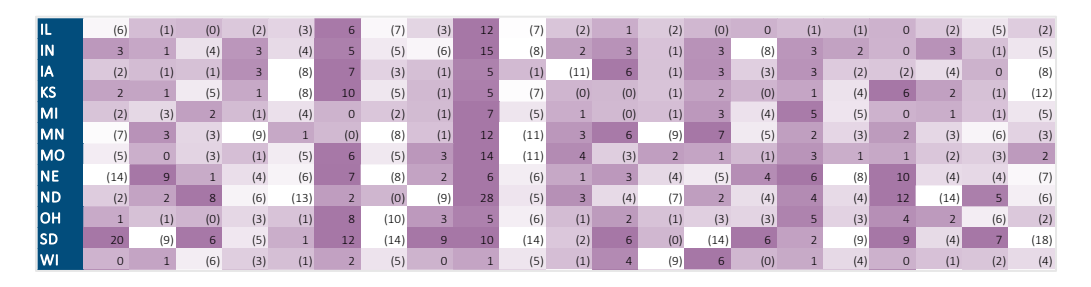
#### Northeast

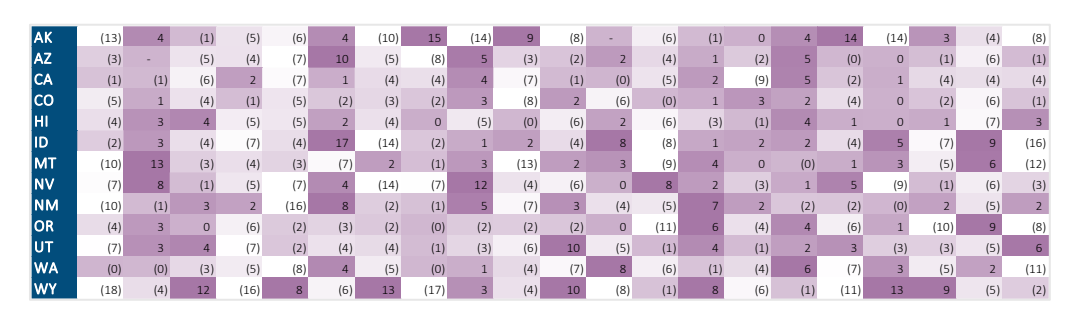


#### South



# Midwest





This observed volatility in the CDC data underscores several limitations for modeling applications. Because the CDC relies solely on death certificate data—often subject to inconsistent cause-of-death reporting, regional disparities, and classification challenges—year-to-year comparability may be compromised. These data are valuable for analyzing absolute mortality counts and cause-specific distributions but may benefit from smoothing or supplementary context when used for longitudinal modeling.

#### **A.2 GBD RATES**

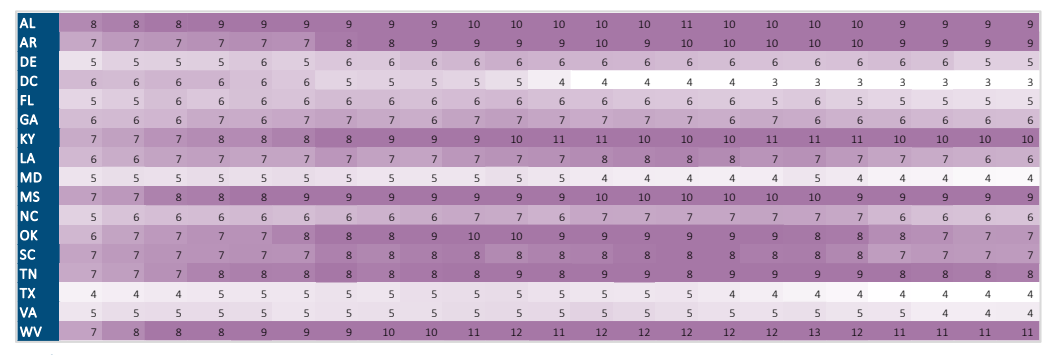
Figures A.3 and A.4 present GBD-reported mortality rates for respiratory causes across states, by year, for the same two age groups: 20–54 and 55+. These data are derived from modeled estimates that incorporate multiple sources—such as epidemiological studies, health surveys, and registry data—and apply statistical techniques to correct for underreporting and missing values.

Figure A.3 displays GBD mortality rates for adults aged 20–54. Unlike the CDC data, these rates exhibit smoother temporal patterns with fewer missing observations. Although some interannual variation is present, the underlying trends are more discernible, facilitating clearer interpretation for modeling purposes.

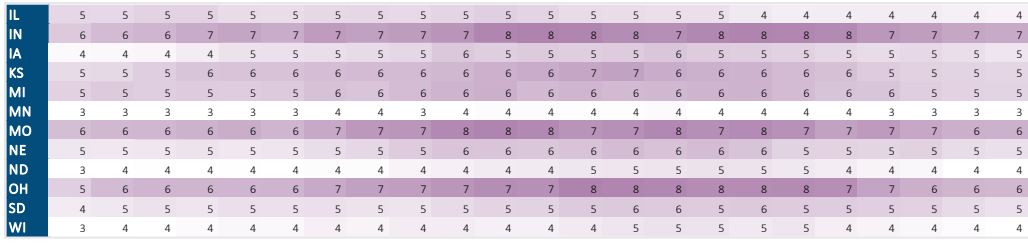
Figure A.3
HEAT MAP OF GBD MORTALITY RATES FOR 20–54 AGE GROUP

State	1999	2000	2001	2002	2003	2004	2005	2006	2007	2008	2009	2010	2011	2012	2013	2014	2015	2016	2017	2018	2019	2020	2021
ст	4	4	4	4	4	4	4	4	4	4	4	4	4	4	4	4	4	4	4	4	4	4	3
ME	5	5	5	5	5	6	6	6	6	6	6	6	6	6	7	7	7	7	7	7	7	7	7
MA	4	4	4	4	4	4	4	4	4	4	4	4	4	4	4	4	4	4	4	4	4	3	3
NH	4	4	4	4	4	5	5	5	5	5	5	5	5	5	5	5	5	6	6	5	5	5	5
NJ	4	4	4	4	4	4	4	4	4	4	4	4	4	4	4	4	4	4	4	4	4	3	3
NY	4	4	5	5	4	4	4	4	4	4	4	4	4	4	4	4	4	4	4	4	3	3	3
PA	5	5	5	5	5	5	5	5	5	6	6	5	6	5	5	5	5	5	5	5	5	4	4
RI	4	4	4	4	4	4	4	4	4	4	4	4	4	4	4	4	4	4	4	4	4	3	3
VT	5	5	5	5	5	5	5	5	5	5	5	5	5	5	5	5	5	5	5	5	5	5	5

# South



# Midwest



# West

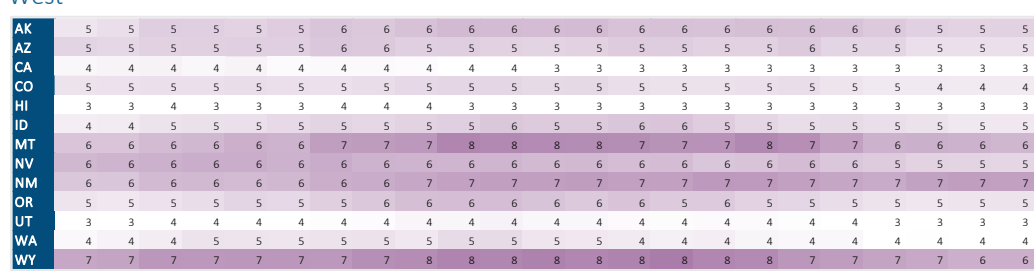
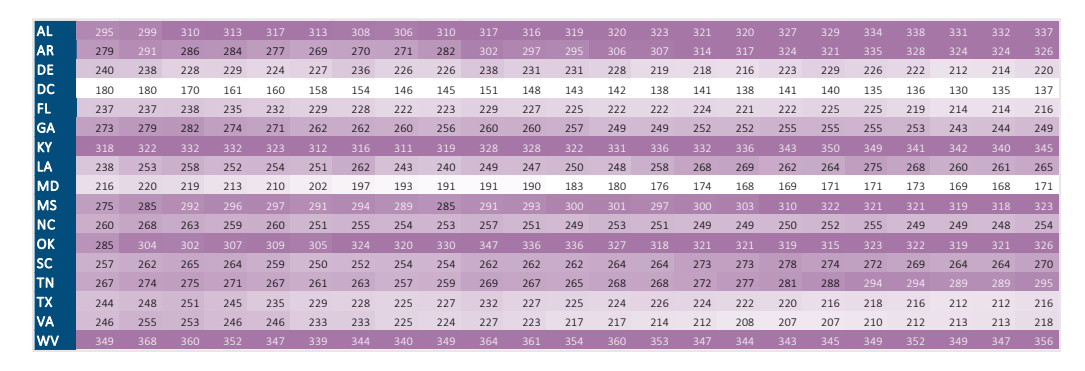


Figure A.4 shows GBD mortality rates for the 55+ population. These rates suggest a general decline in respiratory mortality over the early part of the time series, with an uptick beginning around 2016 in several states. This pattern does not appear in the CDC data for the same cohort, likely because of the higher volatility in raw reporting.

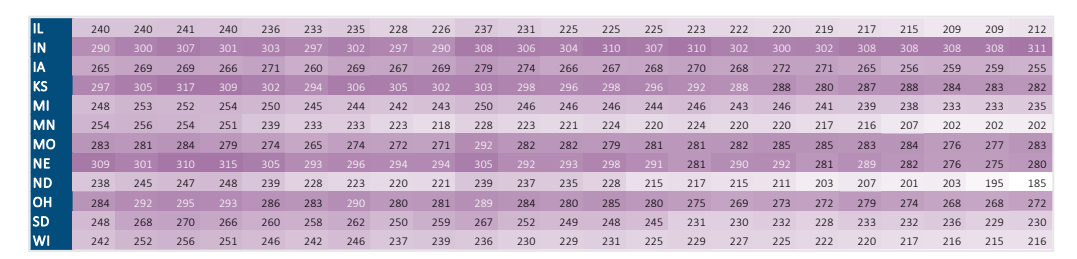
Figure A.4
HEAT MAP OF GBD MORTALITY RATES FOR 55+ AGE GROUP

State	1999	2000	2001	2002	2003	2004	2005	2006	2007	2008	2009	2010	2011	2012	2013	2014	2015	2016	2017	2018	2019	2020	2021
ст	225	241	242	235	232	228	225	223	216	221	212	203	206	205	202	196	194	195	195	190	187	183	180
ME								286	276	275	273	271	269	266	268	269	278	267	268	264	266	261	269
MA	259	273	272	262	254	243	237	227	217	217	217	210	213	205	203	205	207	203	205	203	200	193	187
NH	268	267	269	255	242	244	253	246	243	248	241	232	231	228	225	226	225	225	227	230	223	221	223
NJ	203	205	203	199	197	198	198	194	193	199	194	192	193	191	188	182	180	180	180	178	172	171	168
NY	191	192	194	191	186	184	179	171	171	171	169	168	170	169	167	163	162	160	159	158	156	156	157
PA	258	265	265	263	258	256	255	247	248	256	248	242	246	241	238	231	233	232	233	225	221	221	221
RI	233	241	247	247	240	233	237	234	223	230	231	231	228	221	213	215	214	202	205	194	196	185	183
VT	272	275	270	259	256	256	265	243	235	240	244	238	236	235	225	217	220	213	214	209	206	201	209

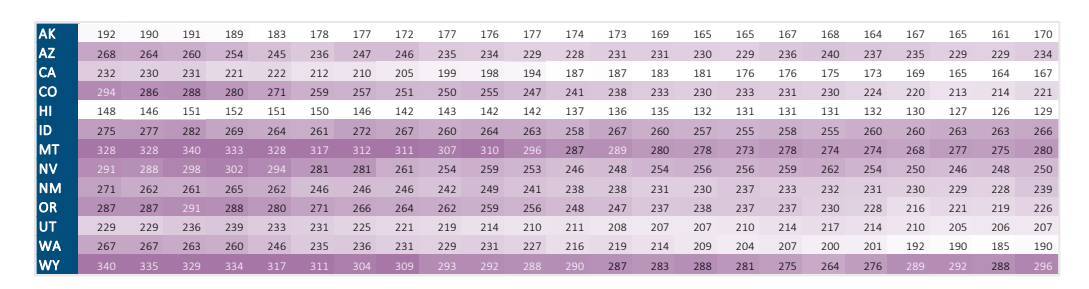
#### South



#### Midwest

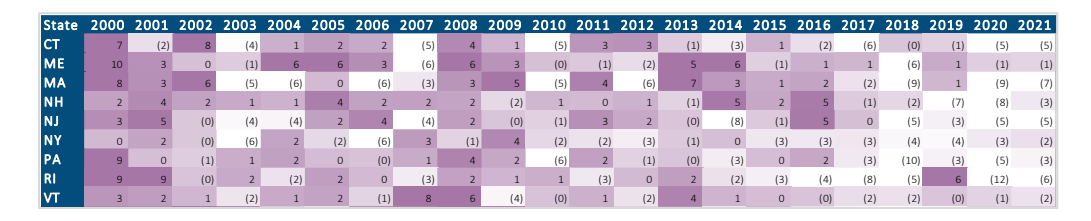


# West

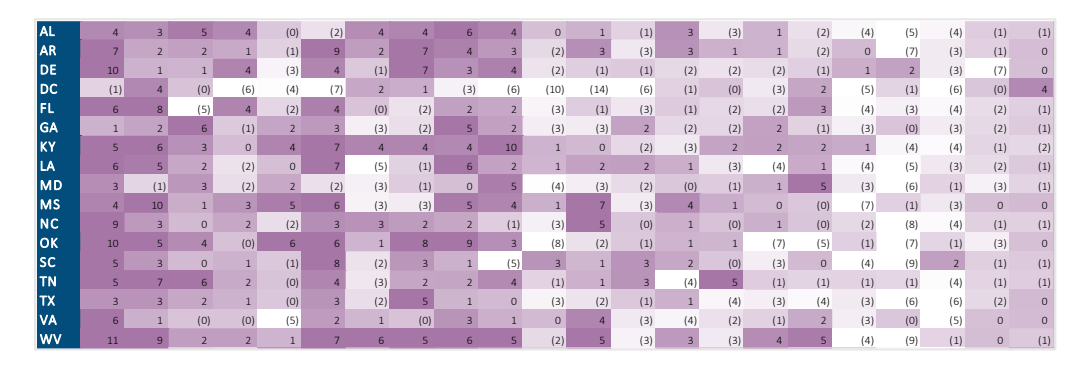


Figures A.5 and A.6 illustrate the year-over-year percentage changes in GBD mortality rates for both age groups, offering additional insight into the direction and magnitude of trends. These increases may reflect cumulative exposure to air pollution, aligning with wildfire activity and air quality deterioration during that period.

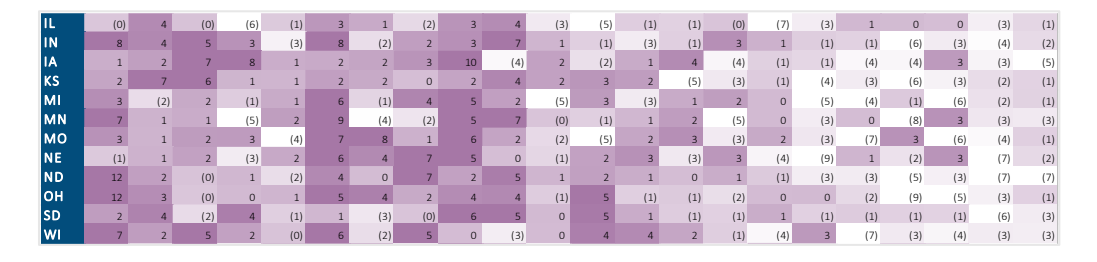
Figure A.5
HEAT MAP OF GBD MORTALITY RATES EVOLUTION FOR 20–54 AGE GROUP



#### South



#### Midwest



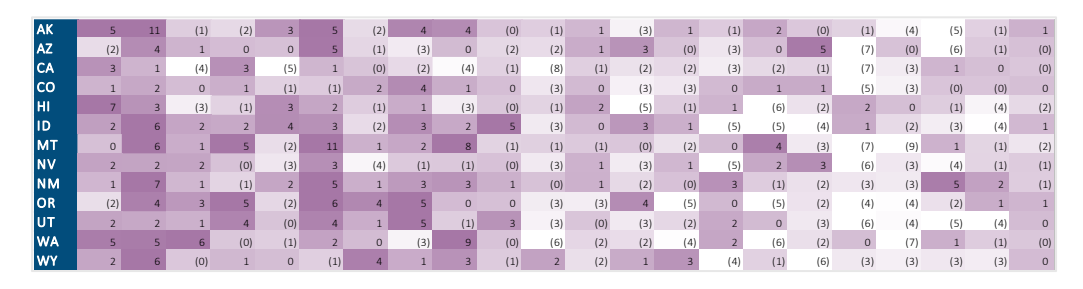
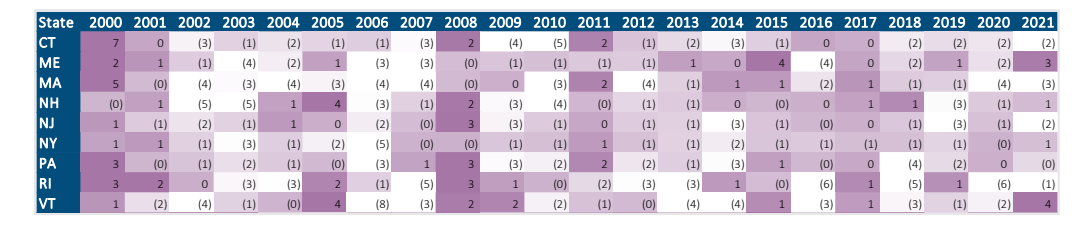
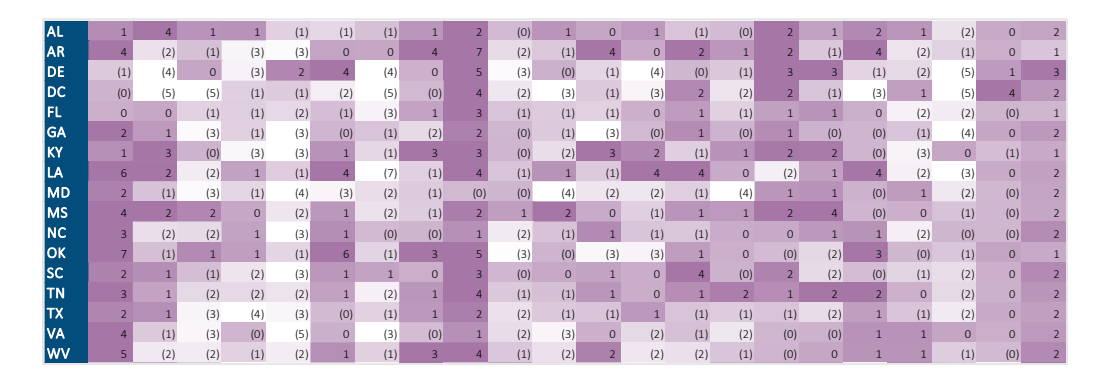


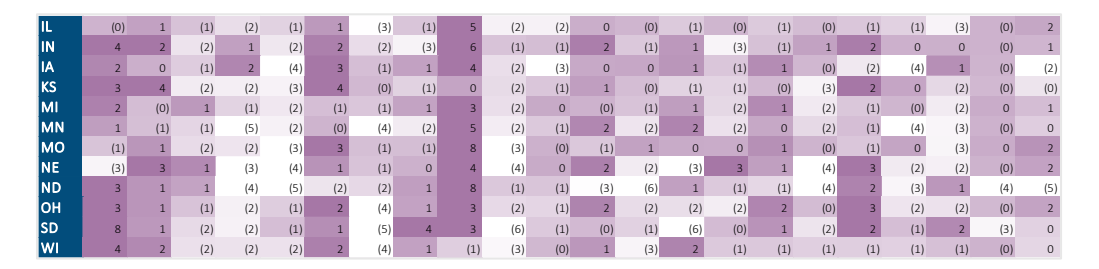
Figure A.6
HEAT MAP OF GBD MORTALITY RATES EVOLUTION FOR THE 55+ AGE GROUP



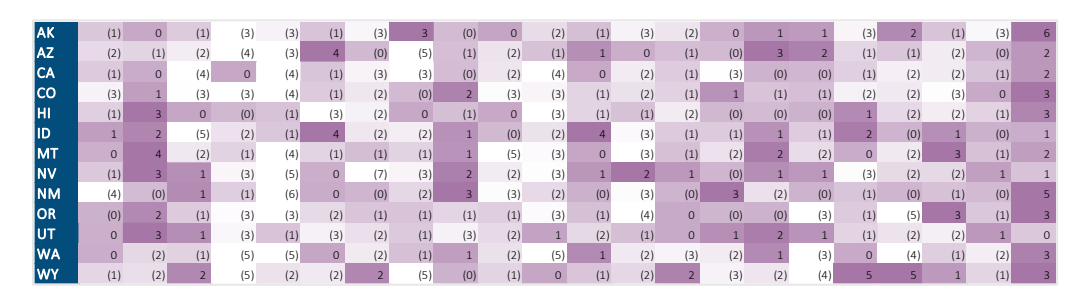
# South



### Midwest



#### West



In contrast to the CDC dataset, GBD data offer greater stability and geographic completeness, making them more suitable for time series analysis and mortality risk modeling. The observed rise in GBD mortality rates among older populations in key western states further supports the use of GBD data for studies assessing climate- and pollution-related mortality impacts.

#### A.3 COMPARISON OF CDC AND GBD BY STATE

To evaluate consistency between the CDC and GBD mortality datasets, a direct comparison was conducted for selected states using mortality rates from both sources for individuals aged 55 and older. The comparison focuses on respiratory causes of death associated with air pollution exposure, using the ICD-10 code groupings and GBD cause categories outlined in Table 1 (Section 2.2.2).

Figures A.7 through A.9 present time series plots for three representative states—California, Idaho, and Missouri—highlighting mortality rates from both databases.

- Figure A.7 (California): Both CDC and GBD datasets follow similar trends, including a notable peak in 2008. However, the CDC data show greater year-to-year volatility, whereas the GBD curve is smoother, reflecting its statistical adjustment process.
- Figure A.8 (Idaho): GBD mortality rates indicate a gradual increase from 2016 onward, consistent with broader pollution exposure patterns in the Pacific Northwest. In contrast, CDC data show substantial annual variability, with limited alignment to GBD trends in later years.
- Figure A.9 (Missouri): The two datasets generally agree on overall magnitude but again differ in their temporal profiles. The GBD curve captures gradual trend shifts, whereas the CDC series shows larger fluctuations, likely because of smaller population size or inconsistencies in cause-of-death attribution.

These comparisons confirm that although both data sources are directionally aligned, the CDC mortality rates exhibit higher volatility, particularly in smaller states or less populous age groups. The GBD rates provide more stable input for longitudinal modeling and are better suited for analyzing trends attributable to environmental factors such as air pollution.

For actuarial modeling purposes—especially when estimating mortality attributable to pollution exposure—the GBD database offers a more reliable basis because of its methodological consistency and completeness across geography and time. Nonetheless, CDC data remain valuable for validating absolute counts and exploring demographic breakdowns where granularity is needed.

Figure A.7
COMPARISON OF CDC AND GBD DEATH RATES: CALIFORNIA, AGED >55 YEARS



Rates: Deaths per 100,000 population

Figure A.8

COMPARISON OF CDC AND GBD DEATH RATES: IDAHO, AGED >55 YEARS



Rates: Deaths per 100,000 population

Figure A.9
COMPARISON OF CDC AND GBD DEATH RATES: MISSOURI, AGED >55 YEARS



Rates: Deaths per 100,000 population

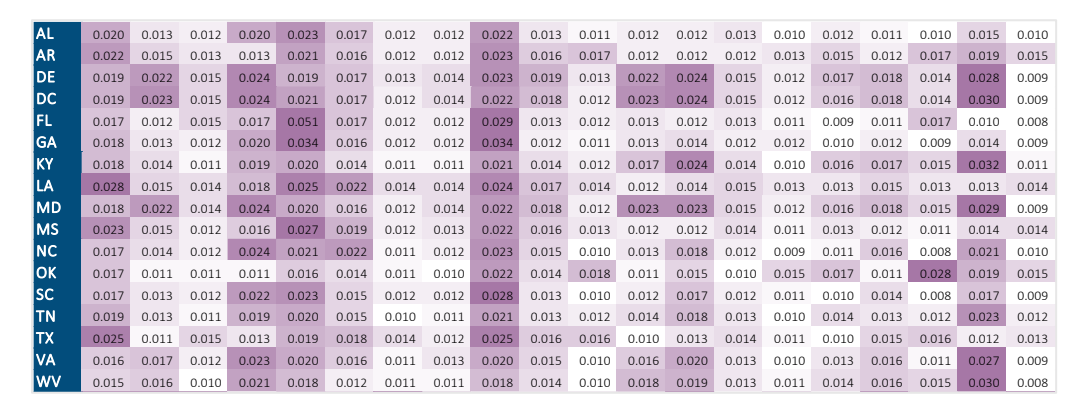
# Appendix B: Evolution of Air Pollution Variables

This appendix presents historical trends in air pollution indicators used throughout the report, with a focus on fine particulate matter (PM<sub>2.5</sub> and PM<sub>10</sub>) and aerosol optical depth variables linked to wildfire emissions. These data, derived from the Copernicus Atmospheric Monitoring Service (CAMS), provide context for evaluating the temporal dynamics of pollutant concentrations across states from 2003 to 2022. Understanding these trends is essential for interpreting modeled mortality impacts, particularly when projecting long-term exposure or calibrating climate-sensitive mortality models. The figures that follow illustrate both average and peak pollutant levels by year and geography, supporting the correlation analyses and model inputs discussed in Section 2 and Section 4.

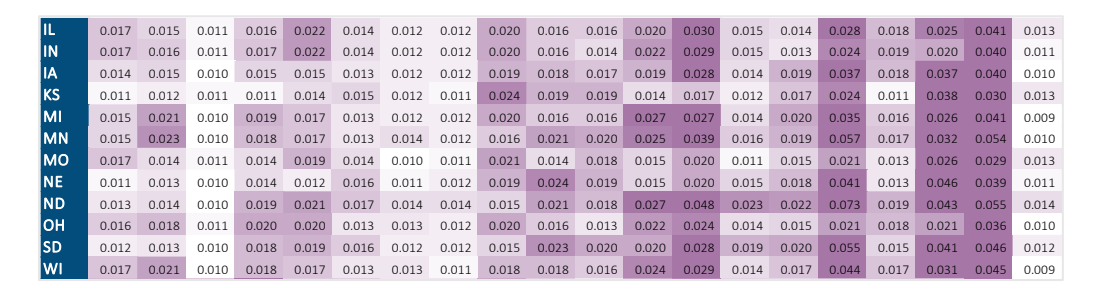
Figure B.1 MAX BCA

State	2003	2004	2005	2006	2007	2008	2009	2010	2011	2012	2013	2014	2015	2016	2017	2018	2019	2020	2021	2022
СТ	0.018	0.021	0.016	0.026	0.016	0.017	0.013	0.013	0.020	0.016	0.013	0.020	0.024	0.015	0.015	0.019	0.017	0.018	0.030	0.008
ME	0.019	0.021	0.016	0.023	0.016	0.011	0.011	0.015	0.016	0.014	0.014	0.022	0.026	0.015	0.015	0.019	0.016	0.017	0.024	0.008
MA	0.017	0.020	0.014	0.025	0.015	0.015	0.012	0.012	0.018	0.015	0.012	0.020	0.023	0.014	0.015	0.018	0.016	0.018	0.027	0.007
NH	0.017	0.019	0.013	0.024	0.013	0.013	0.011	0.014	0.016	0.013	0.011	0.020	0.023	0.013	0.016	0.018	0.014	0.018	0.025	0.007
NJ	0.020	0.022	0.016	0.025	0.019	0.018	0.013	0.013	0.023	0.018	0.014	0.020	0.024	0.016	0.014	0.019	0.018	0.017	0.031	0.009
NY	0.017	0.019	0.014	0.023	0.014	0.014	0.012	0.011	0.018	0.015	0.012	0.021	0.023	0.014	0.018	0.020	0.015	0.018	0.030	0.007
PA	0.016	0.019	0.012	0.023	0.017	0.015	0.012	0.011	0.019	0.016	0.012	0.022	0.021	0.013	0.015	0.018	0.016	0.019	0.032	0.008
RI	0.017	0.021	0.015	0.026	0.015	0.016	0.012	0.013	0.018	0.015	0.012	0.019	0.023	0.015	0.014	0.019	0.016	0.019	0.028	0.008
VT	0.017	0.018	0.013	0.024	0.013	0.012	0.011	0.014	0.017	0.014	0.011	0.021	0.023	0.014	0.017	0.019	0.015	0.018	0.026	0.007

#### South



### Midwest



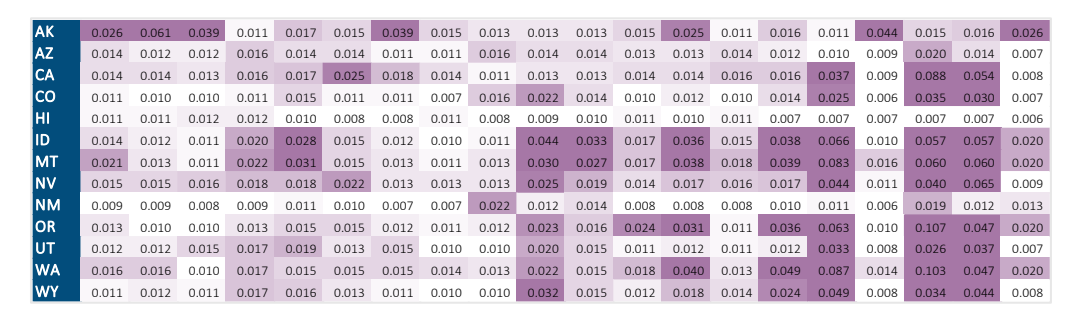
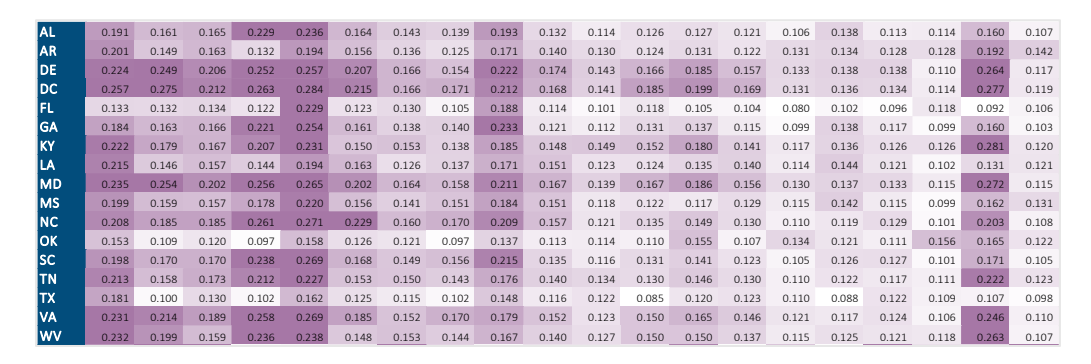


Figure B.2 MAX\_OMA

State	2003	2004	2005	2006	2007	2008	2009	2010	2011	2012	2013	2014	2015	2016	2017	2018	2019	2020	2021	2022
СТ	0.207	0.216	0.182	0.256	0.186	0.211	0.154	0.144	0.184	0.154	0.129	0.174	0.176	0.135	0.135	0.155	0.146	0.120	0.280	0.094
ME	0.176	0.201	0.180	0.216	0.152	0.148	0.147	0.143	0.139	0.135	0.121	0.172	0.180	0.116	0.142	0.142	0.162	0.124	0.238	0.095
MA	0.193	0.204	0.171	0.240	0.180	0.198	0.142	0.140	0.162	0.151	0.124	0.169	0.176	0.129	0.131	0.148	0.146	0.120	0.266	0.090
NH	0.175	0.193	0.172	0.217	0.166	0.169	0.135	0.132	0.144	0.148	0.119	0.166	0.173	0.118	0.133	0.144	0.152	0.123	0.256	0.091
NJ	0.230	0.239	0.200	0.256	0.234	0.216	0.170	0.154	0.216	0.172	0.144	0.176	0.182	0.149	0.138	0.152	0.140	0.118	0.279	0.108
NY	0.180	0.199	0.167	0.221	0.166	0.177	0.152	0.134	0.160	0.143	0.123	0.166	0.171	0.119	0.149	0.155	0.148	0.133	0.289	0.091
PA	0.199	0.220	0.171	0.238	0.218	0.184	0.161	0.136	0.181	0.153	0.130	0.165	0.163	0.131	0.140	0.151	0.138	0.130	0.290	0.099
RI	0.198	0.210	0.173	0.250	0.182	0.202	0.147	0.144	0.173	0.151	0.127	0.170	0.175	0.134	0.133	0.149	0.145	0.121	0.271	0.094
VT	0.169	0.192	0.171	0.217	0.163	0.162	0.143	0.131	0.148	0.140	0.121	0.167	0.176	0.115	0.140	0.147	0.150	0.125	0.264	0.096

#### South



#### Midwest

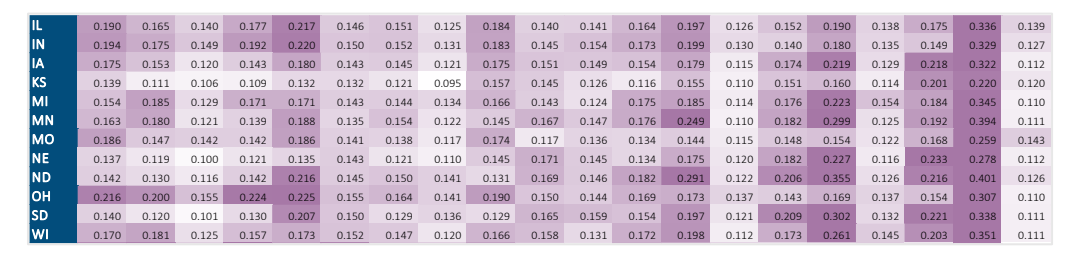
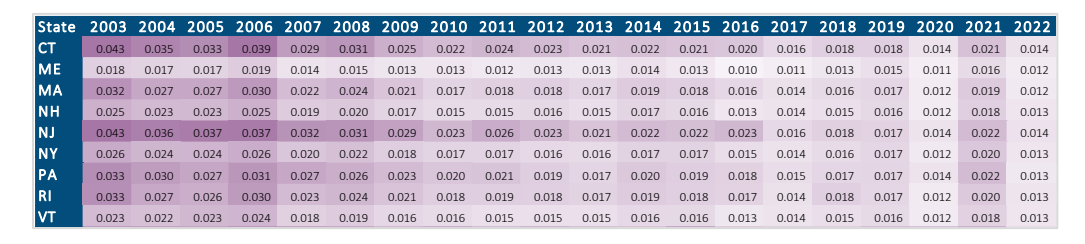
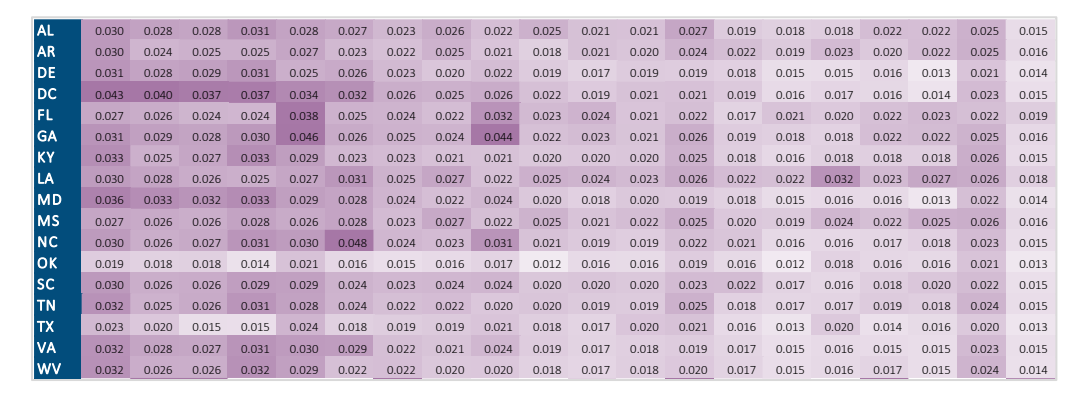




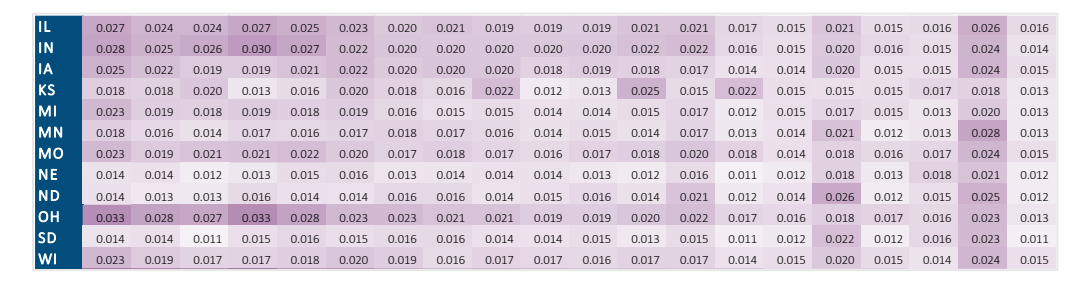
Figure B.3 MAX\_PM<sub>2.5</sub>, SCALED (MULTIPLIED BY 1M)



#### South



#### Midwest



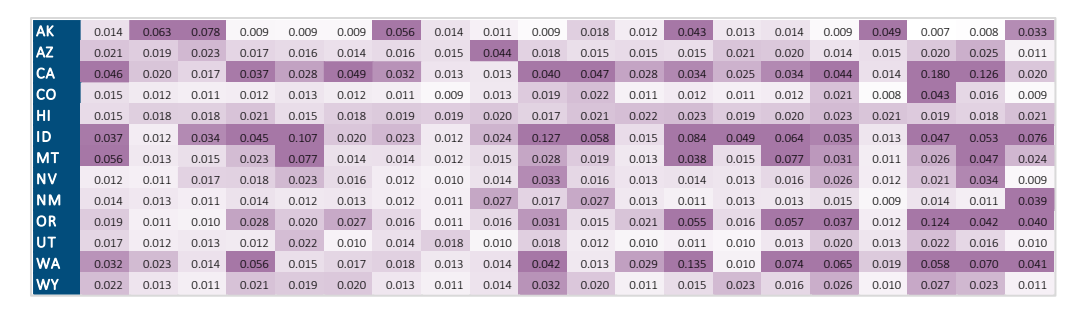
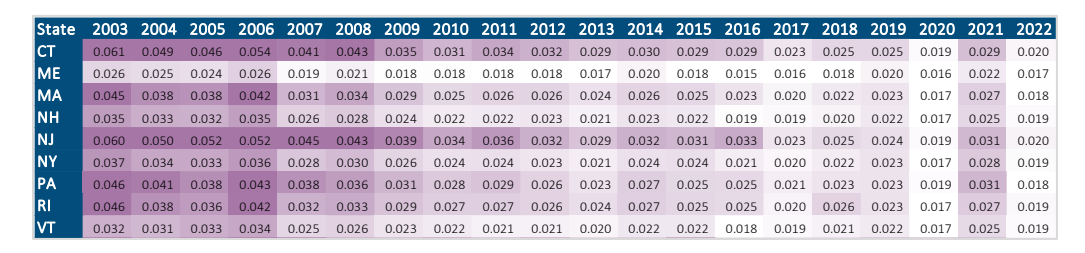
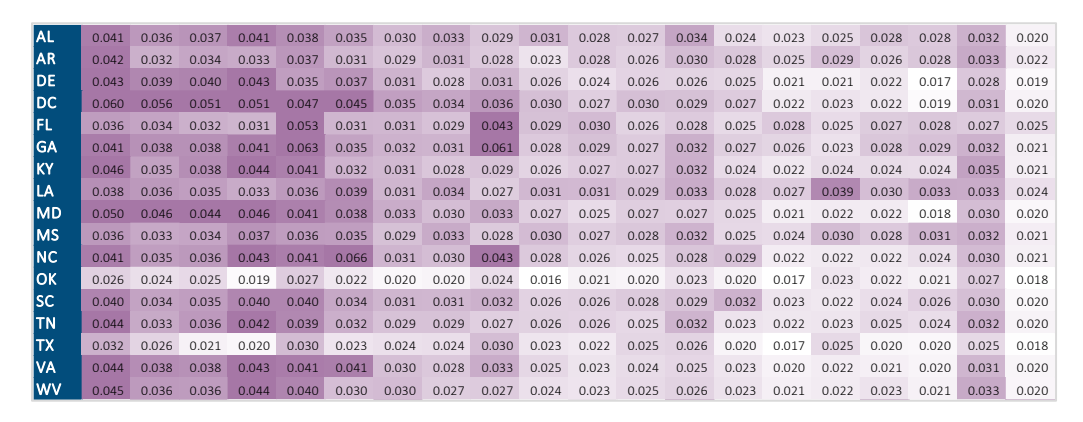


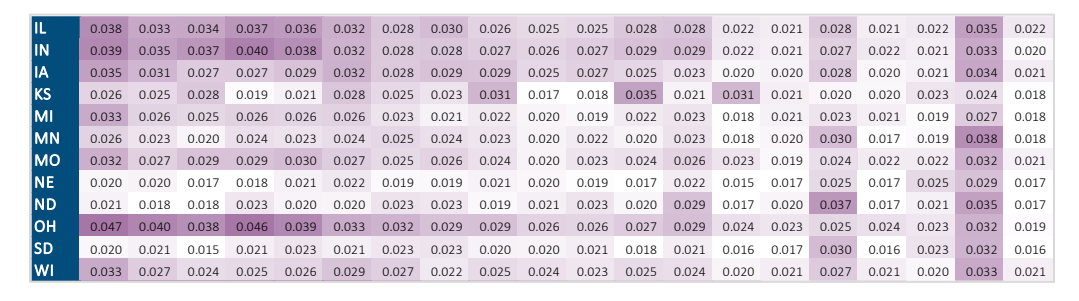
Figure B.4 MAX\_PM<sub>10</sub>, SCALED (MULTIPLIED BY 1M)



#### South



## Midwest



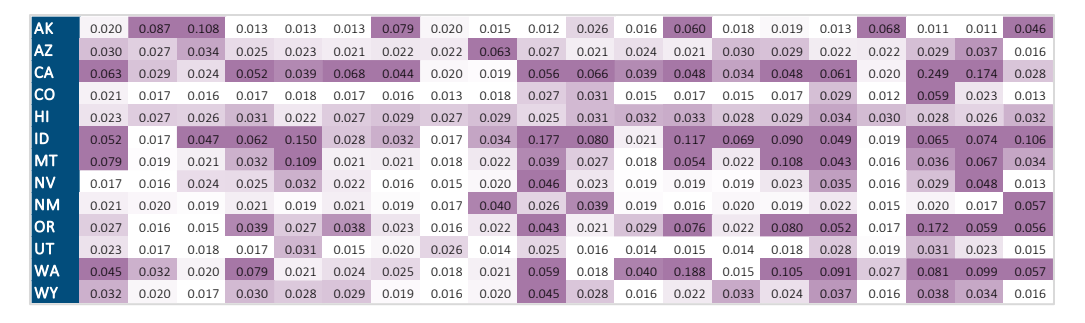
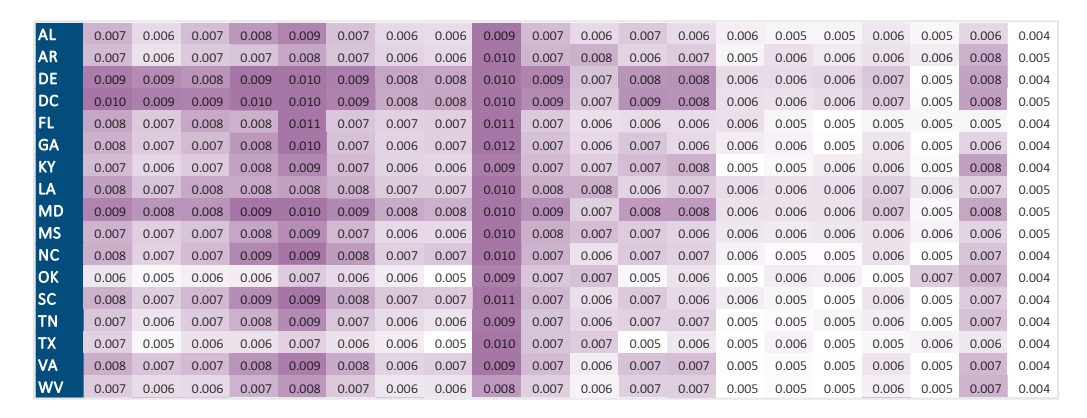


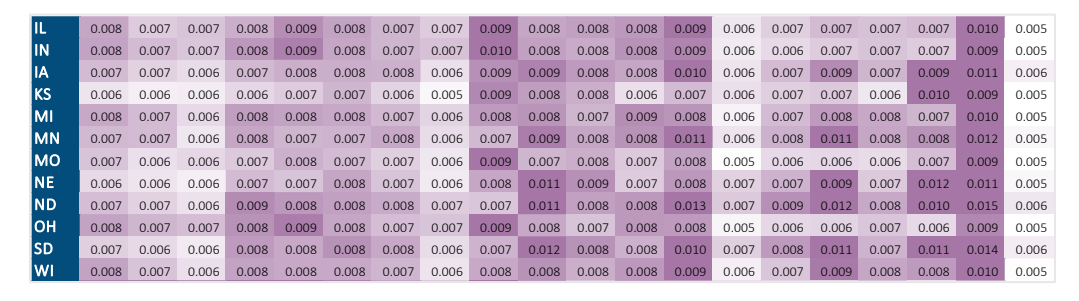
Figure B.5 MEAN BCA

State	2003	2004	2005	2006	2007	2008	2009	2010	2011	2012	2013	2014	2015	2016	2017	2018	2019	2020	2021	2022
СТ	0.009	0.009	0.008	0.009	0.009	0.009	0.008	0.007	0.009	0.008	0.007	0.008	0.008	0.006	0.006	0.006	0.007	0.006	0.008	0.004
ME	0.007	0.007	0.006	0.008	0.007	0.007	0.006	0.007	0.008	0.007	0.006	0.007	0.008	0.006	0.006	0.006	0.007	0.006	0.007	0.004
MA	0.008	0.008	0.007	0.009	0.009	0.008	0.007	0.007	0.009	0.008	0.007	0.008	0.008	0.006	0.006	0.006	0.007	0.006	0.007	0.004
NH	0.007	0.007	0.006	0.008	0.007	0.007	0.007	0.007	0.008	0.007	0.006	0.007	0.007	0.005	0.006	0.006	0.007	0.006	0.007	0.004
NJ	0.010	0.010	0.009	0.010	0.011	0.010	0.008	0.008	0.010	0.009	0.007	0.008	0.009	0.006	0.007	0.007	0.007	0.006	0.008	0.005
NY	0.008	0.007	0.007	0.008	0.008	0.008	0.007	0.007	0.008	0.008	0.006	0.008	0.008	0.005	0.007	0.006	0.007	0.006	0.008	0.004
PA	0.008	0.008	0.007	0.008	0.009	0.008	0.007	0.007	0.009	0.008	0.006	0.008	0.007	0.005	0.006	0.006	0.006	0.006	0.008	0.004
RI	0.008	0.008	0.008	0.009	0.009	0.008	0.008	0.007	0.009	0.008	0.007	0.008	0.008	0.006	0.006	0.006	0.007	0.006	0.008	0.004
VT	0.007	0.007	0.007	0.008	0.007	0.007	0.007	0.007	0.008	0.007	0.006	0.007	0.007	0.005	0.006	0.006	0.007	0.006	0.007	0.004

#### South



## Midwest



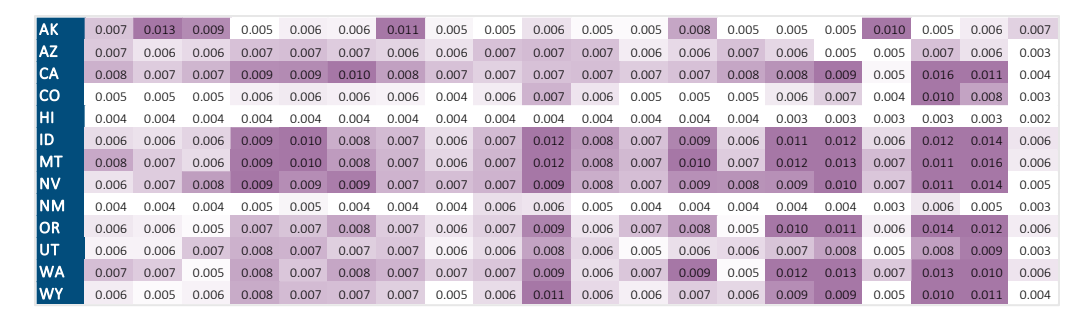
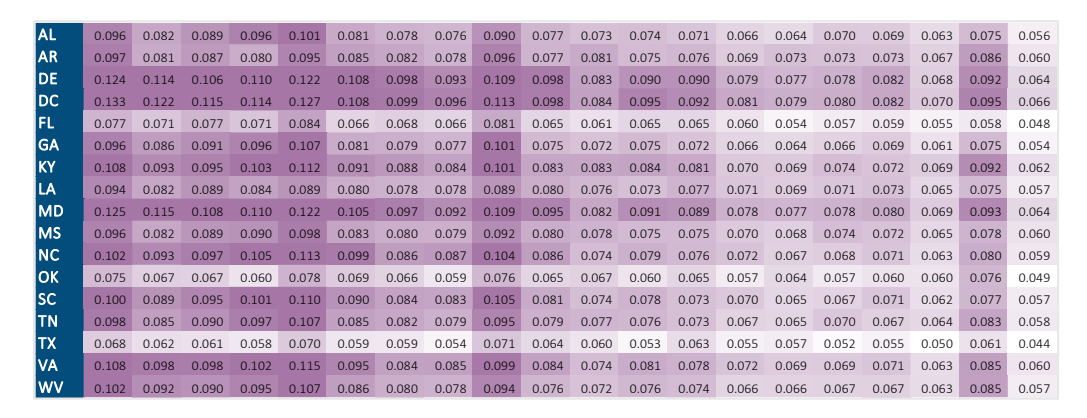


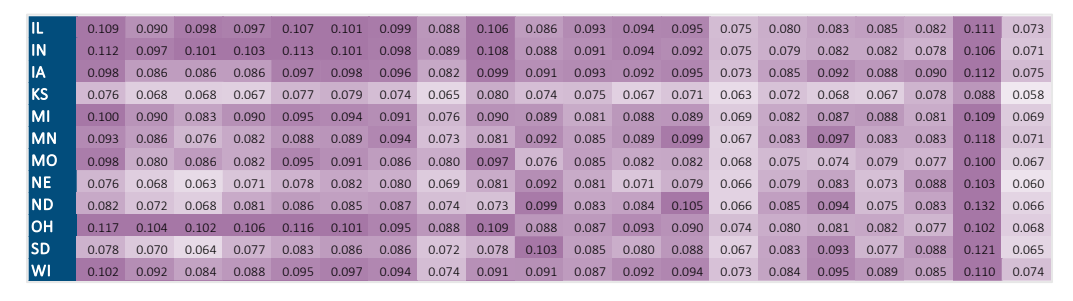
Figure B.6 MEAN OMA

State	2003	2004	2005	2006	2007	2008	2009	2010	2011	2012	2013	2014	2015	2016	2017	2018	2019	2020	2021	2022
СТ	0.115	0.110	0.097	0.103	0.108	0.103	0.093	0.082	0.099	0.092	0.080	0.085	0.085	0.072	0.076	0.076	0.081	0.069	0.091	0.060
ME	0.087	0.081	0.075	0.085	0.082	0.084	0.078	0.072	0.081	0.076	0.070	0.074	0.077	0.064	0.071	0.069	0.079	0.067	0.084	0.058
MA	0.105	0.100	0.091	0.097	0.100	0.097	0.088	0.079	0.094	0.086	0.076	0.081	0.082	0.069	0.074	0.073	0.079	0.068	0.089	0.059
NH	0.095	0.089	0.083	0.088	0.089	0.089	0.081	0.075	0.087	0.079	0.071	0.076	0.078	0.065	0.073	0.070	0.078	0.068	0.088	0.059
NJ	0.131	0.122	0.107	0.112	0.123	0.111	0.102	0.091	0.108	0.101	0.086	0.091	0.091	0.078	0.079	0.080	0.084	0.070	0.094	0.063
NY	0.105	0.097	0.090	0.094	0.096	0.093	0.089	0.079	0.093	0.085	0.075	0.082	0.083	0.066	0.079	0.074	0.083	0.072	0.095	0.063
PA	0.114	0.106	0.097	0.100	0.108	0.096	0.092	0.082	0.100	0.087	0.078	0.085	0.085	0.070	0.078	0.076	0.079	0.070	0.094	0.062
RI	0.107	0.104	0.092	0.100	0.102	0.100	0.090	0.081	0.096	0.089	0.079	0.082	0.083	0.071	0.073	0.075	0.079	0.069	0.090	0.059
VT	0.095	0.088	0.083	0.088	0.089	0.088	0.082	0.076	0.087	0.078	0.071	0.077	0.079	0.065	0.075	0.070	0.080	0.069	0.090	0.062

#### South



## Midwest



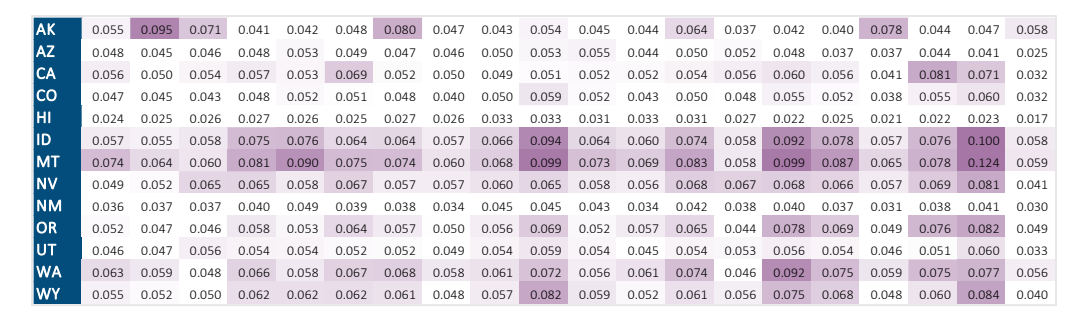
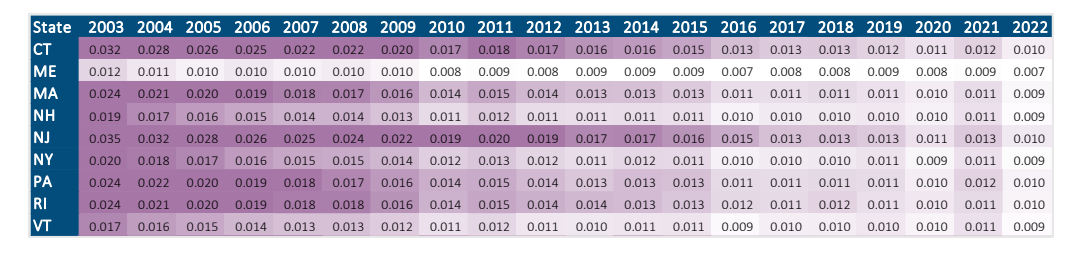
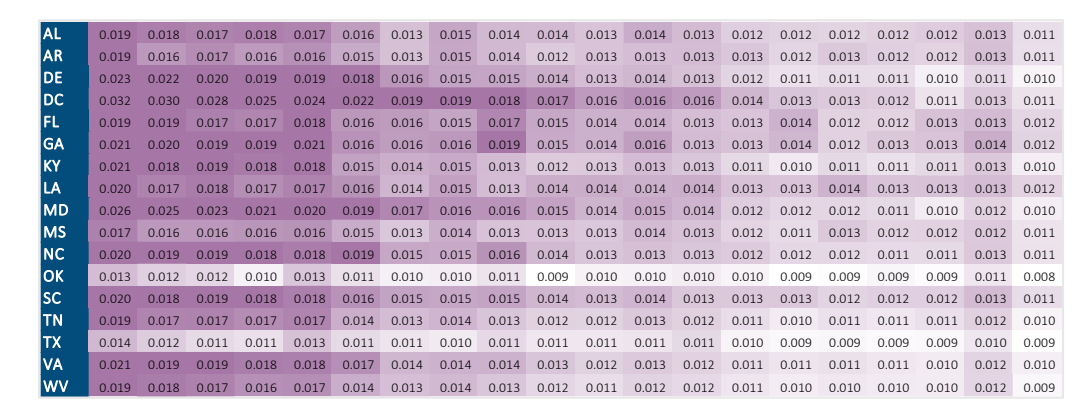


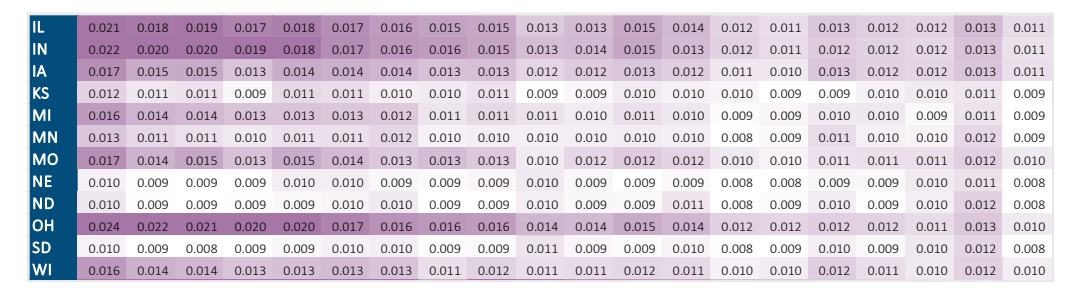
Figure B.7
MEAN\_PM<sub>2.5</sub>, SCALED (MULTIPLIED BY 1M)



#### South



## Midwest



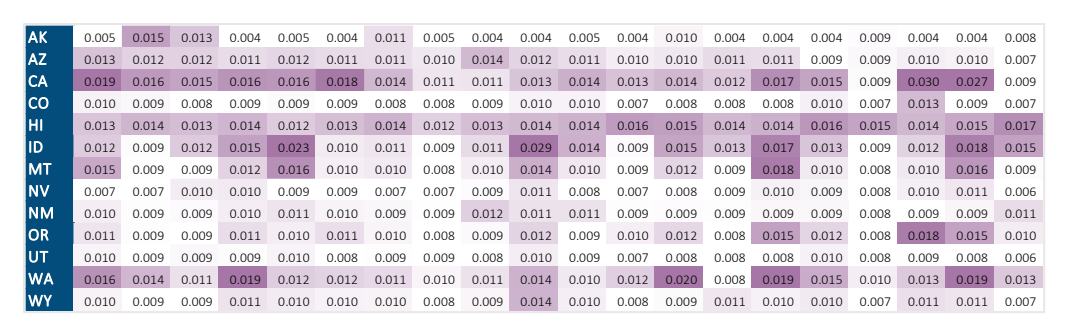
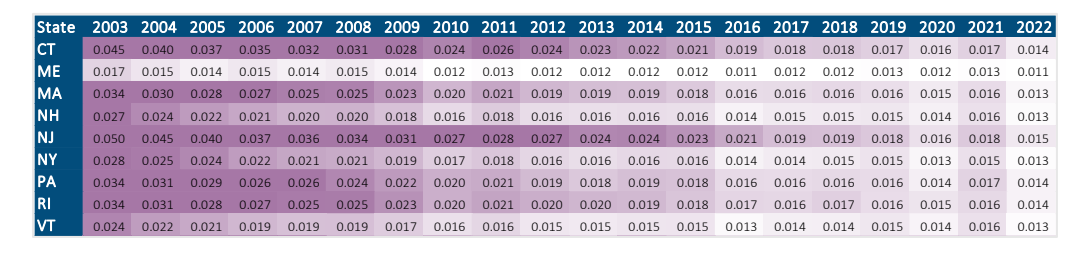
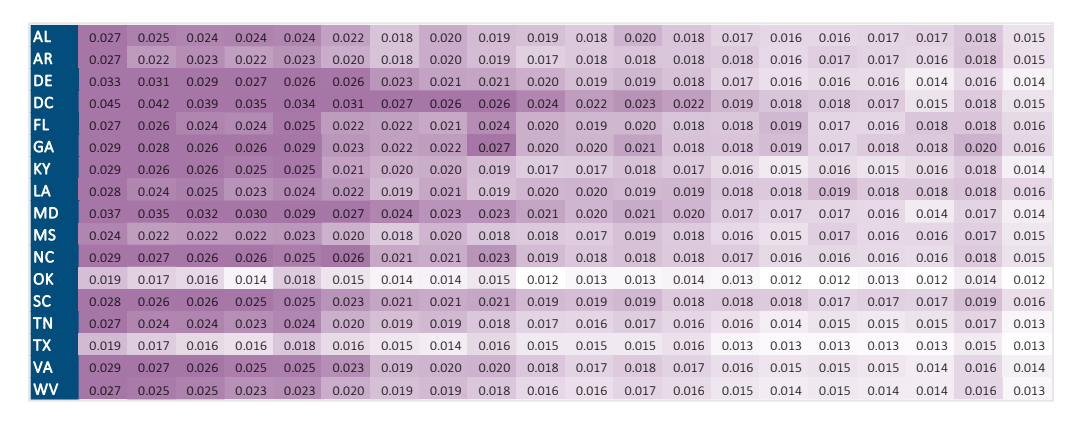


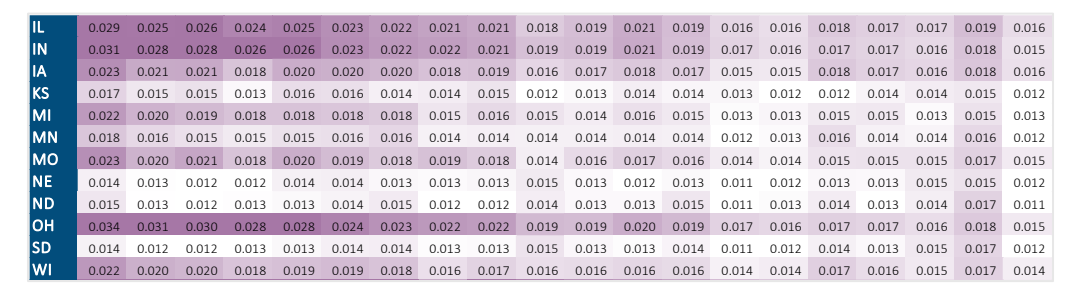
Figure B.8 MEAN\_PM<sub>10</sub>, SCALED (MULTIPLIED BY 1M)

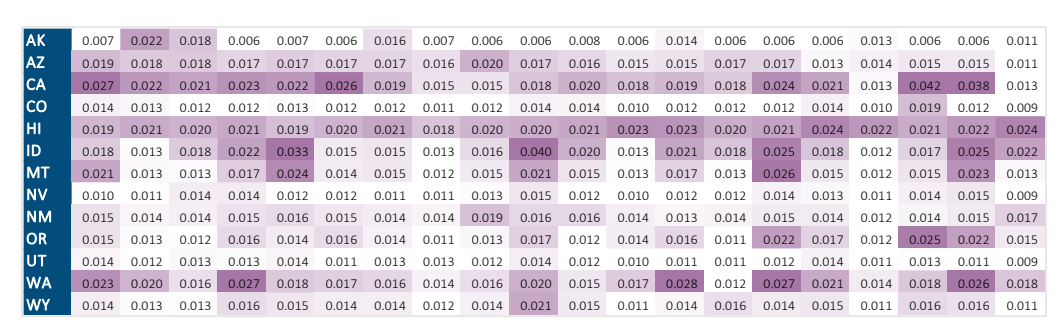


#### South



## Midwest





# Appendix C: GBD Death Rates by Risk Factor Methodology

The Global Burden of Disease (GBD) study provides mortality estimates not only by cause of death but also by associated risk factors, including air pollution. This appendix outlines the general methodology used by the GBD framework to produce mortality rates attributable to specific risk exposures. These estimates play a key role in this report's modeling approaches—particularly in Sections 2, 5, and 6—by enabling the quantification of deaths attributable to environmental factors rather than underlying medical conditions alone.

The GBD estimation process consists of the following steps:

- 1. *Data collection:* The GBD integrates data from a wide range of sources, including national health surveys, death registries, epidemiological studies, hospital discharge records and environmental monitoring systems.
- 2. Risk factor prevalence estimation: Using survey and observational data, the GBD estimates the prevalence of various risk factors within the population (e.g., exposure to PM<sub>2.5</sub>, secondhand smoke, or occupational pollutants). These exposure levels are modeled over time and across geographic units.
- 3. Attribution of mortality to risk factors: Statistical models are applied to link risk factors with specific causes of death, based on established exposure-response relationships. These models rely on meta-analyses and cohort studies that quantify the relative risk of mortality associated with a given level of exposure to a particular risk factor.
- 4. Calculation of risk-attributable mortality rates: Once the share of mortality attributable to a risk factor is estimated, that fraction is applied to the total number of deaths by cause, age, and geography. The result is a set of mortality rates that isolate the portion of deaths attributable to each specific risk factor.
- 5. Comparison with cause-specific mortality: The last step involves validating the consistency between risk-attributable and cause-specific mortality rates. This cross-check helps ensure the plausibility of attribution estimates and informs any necessary model adjustments.

These risk-attributable mortality rates—such as those for ambient air pollution—are central to assessing the health impacts of environmental exposures. Although the methodology enables comparability across regions and over time, it is important to note that the outputs are modeled estimates, not direct observations. As such, they should be interpreted with an understanding of the underlying assumptions and potential sources of uncertainty, especially when used in scenario modeling or actuarial projections.

Copyright © 2025 Society of Actuaries Research Institute

<sup>&</sup>lt;sup>50</sup> https://www.thelancet.com/journals/lancet/article/PIIS0140-6736(24)02840-X/fulltext.

# Appendix D: A Stepwise Description of the Clustering Process

This appendix outlines the clustering methodology used in the report to group states based on similarities in air pollution levels, wildfire activity, and pollution-attributable mortality rates. Clustering is a useful tool in identifying patterns across geographies that share similar environmental risk profiles, which can enhance the interpretation of results and support the development of targeted modeling strategies.

The process involved three key steps, combining hierarchical clustering and principal component analysis (PCA) to reduce dimensionality and improve interpretability.

# Step 1: Hierarchical Clustering and Dendrogram Construction

The first step employed an ascending hierarchical classification (AHC) algorithm. This technique calculates pairwise dissimilarities between observations—in this case, states—based on selected input variables (e.g., mortality rates, wildfire metrics, or pollutant concentrations). States are then grouped iteratively into clusters that minimize intragroup variance. The output is a dendrogram, which visually represents how states are joined at each step and helps determine the optimal number of clusters based on the height at which branches merge.

### Step 2: Principal Component Analysis (PCA) for Cluster Visualization

To aid interpretation, a PCA was performed on the same input variables used in the clustering. PCA reduces the multidimensional dataset into a smaller number of uncorrelated principal components that capture the majority of the variance. Each state is then plotted in the space defined by the first two principal components, with clusters color coded to show group membership. This visualization enables clear differentiation between clusters and highlights the dominant variables influencing each grouping.

# Step 3: Interpretation of Cluster Characteristics

Finally, the relationships between input variables and principal components were analyzed to characterize each cluster. By examining which variables align most strongly with each PCA axis, the key environmental or mortality attributes that define each group of states were identified. This step provided insight into the underlying drivers of cluster formation—for example, whether states grouped together because of consistently high pollution levels, frequent wildfire events, or elevated pollution-attributable mortality in older populations.

Figure D.1
RESULTS OF THE PRINCIPAL COMPONENT ANALYSIS

(Displays the relationship between input variables and principal components.)

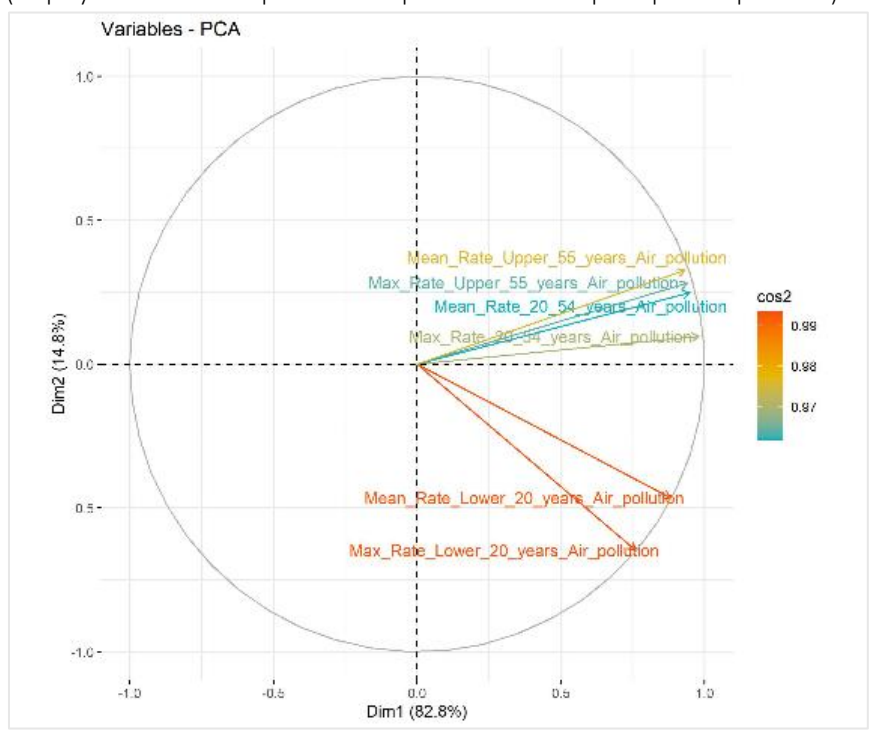
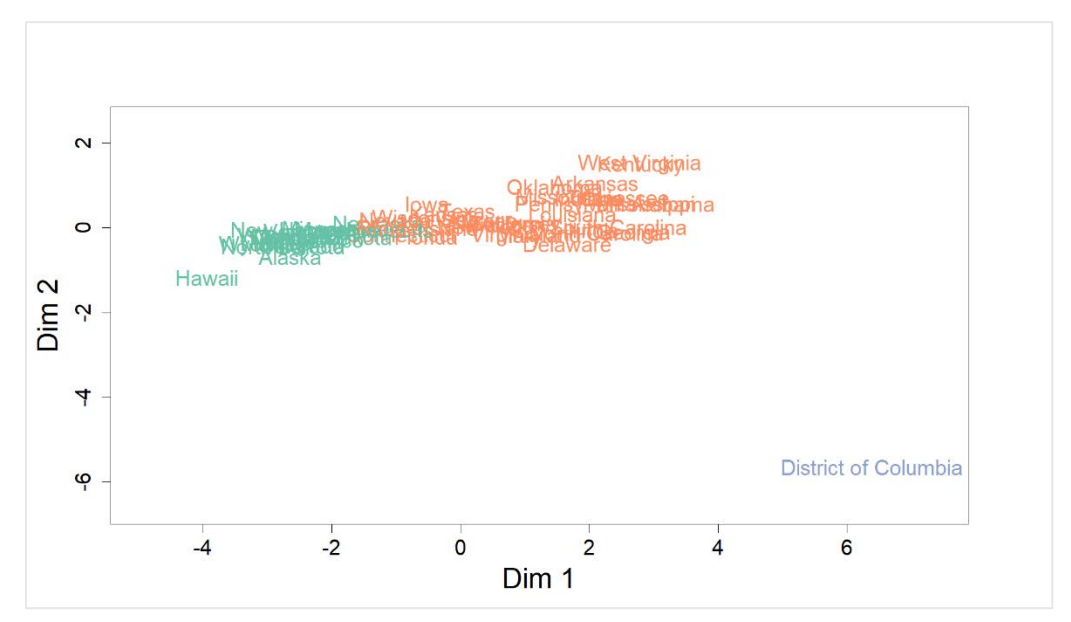


Figure D.2
PROJECTION OF STATES ONTO THE FIRST TWO PRINCIPAL COMPONENTS



Note: Shows state locations and assigned clusters in reduced-dimensional space.

These clustering results support the analysis presented in Sections 2 and 4, enabling more targeted insights into geographic heterogeneity in pollution exposure and mortality impacts. They also provide a framework for state-level differentiation in future actuarial modeling or climate risk segmentation.

# About The Society of Actuaries Research Institute

Serving as the research arm of the Society of Actuaries (SOA), the SOA Research Institute provides objective, data-driven research bringing together tried and true practices and future-focused approaches to address societal challenges and your business needs. The Institute provides trusted knowledge, extensive experience, and new technologies to help effectively identify, predict, and manage risks.

Representing the thousands of actuaries who help conduct critical research, the SOA Research Institute provides clarity and solutions on risks and societal challenges. The Institute connects actuaries, academics, employers, the insurance industry, regulators, research partners, foundations and research institutions, sponsors, and non-governmental organizations, building an effective network that provides support, knowledge, and expertise regarding the management of risk to benefit the industry and the public.

Managed by experienced actuaries and research experts from a broad range of industries, the SOA Research Institute creates, funds, develops, and distributes research to elevate actuaries as leaders in measuring and managing risk. These efforts include studies, essay collections, webcasts, research papers, survey reports, and original research on topics impacting society.

Harnessing its peer-reviewed research, leading-edge technologies, new data tools, and innovative practices, the Institute seeks to understand the underlying causes of risk and the possible outcomes. The Institute develops objective research spanning a variety of topics with its <a href="strategic research programs">strategic research programs</a>: aging and retirement; actuarial innovation and technology; mortality and longevity; diversity, equity and inclusion; health care cost trends; and catastrophe and climate risk. The Institute has a large volume of <a href="topical research available">topical research available</a>, including an expanding collection of international and market-specific research, experience studies, models and timely research.

Society of Actuaries Research Institute 8770 W Bryn Mawr Ave, Suite 1000 Chicago, IL 60631 www.SOA.org